UNITED STATES
DEPARTMENT OF THE INTERIOR
BUREAU OF RECLAMATION

BOULDER CANYON PROJECT
FINAL REPORTS

PART VI—HYDRAULIC INVESTIGATIONS

Bulletin 2

MODEL STUDIES OF PENSTOCKS AND OUTLET WORKS

UNITED STATES
DEPARTMENT OF THE INTERIOR
HAROLD L. ICKES, Secretary

BUREAU OF RECLAMATION
JOHN C. PAGE, Commissioner
R. F. WALTER, Chief Engineer

BOULDER CANYON PROJECT
FINAL REPORTS

PART VI—HYDRAULIC INVESTIGATIONS

Bulletin 2

MODEL STUDIES OF PENSTOCKS AND OUTLET WORKS

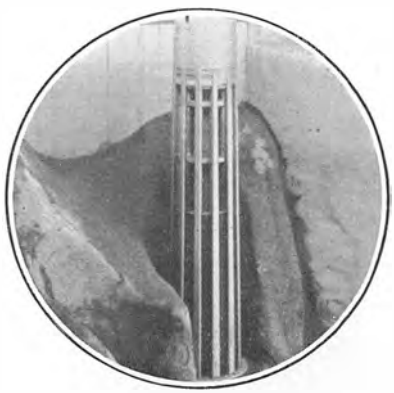

DENVER, COLORADO
1938

This bulletin is one of a series prepared to record the history of the Boulder Canyon Project, the results of technical studies and experimental investigations, and the more unusual features of design and construction. A list of the bulletins available and tentatively proposed for publication is given at the back of this report.

FRONTISPIECE—BOULDER DAM FROM NEVADA SIDE SHOWING INTAKE TOWERS AND SPILLWAYS

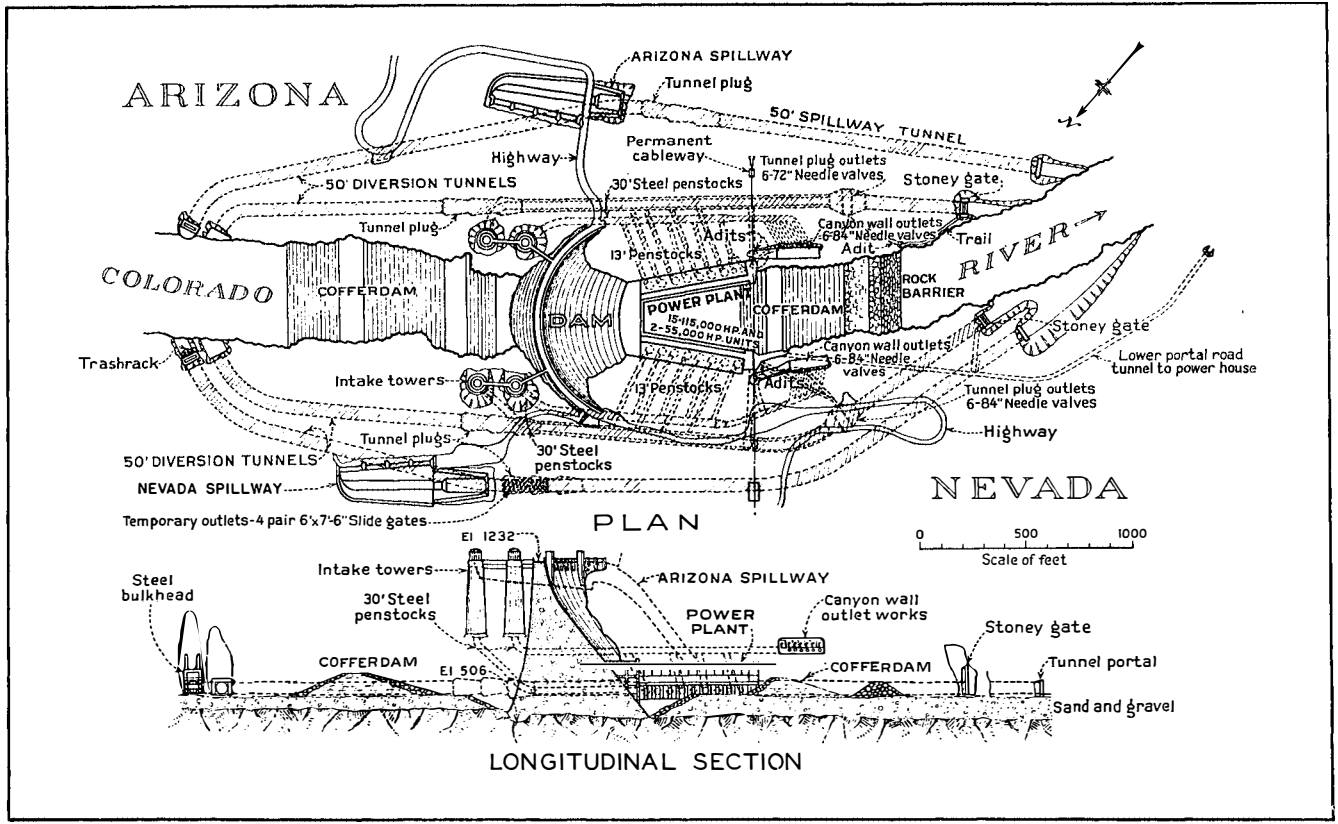

BOULDER DAM AND APPURTENANT WORKS

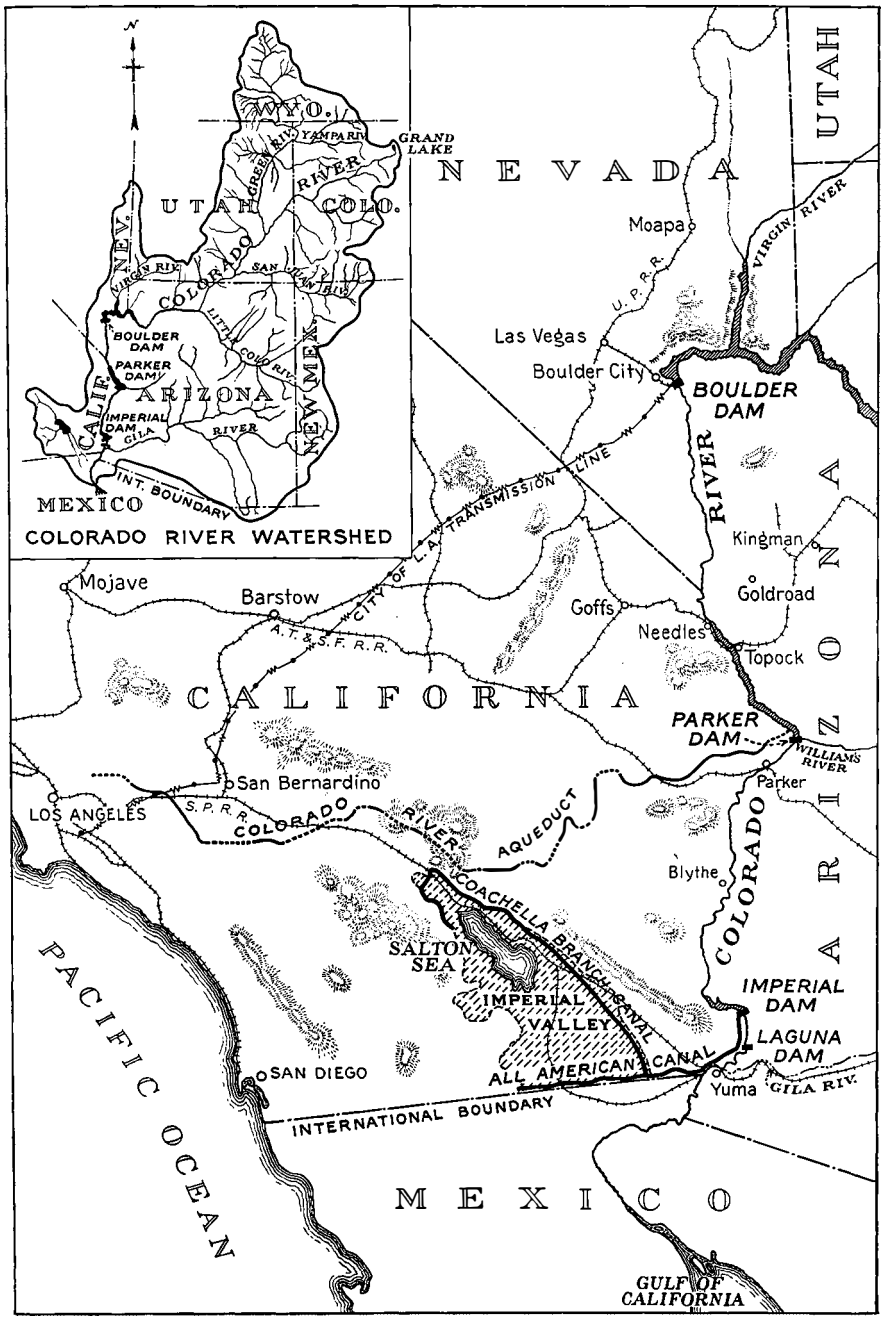

BOULDER CANYON PROJECT—LOCATION MAP

BOULDER CANYON PROJECT

ENGINEERING ORGANIZATION DURING CONSTRUCTION

ADMINISTRATIVE OFFICE, WASHINGTON, D. C.

Elwood Mead* — Commissioner of Reclamation

ENGINEERING AND EXECUTIVE OFFICE, DENVER, COLORADO

Raymond F. Walter — Chief Engineer
Sinclair O. Harper — Assistant Chief Engineer
John L. Savage — Chief Designing Engineer
Leslie N. McClellan — Chief Electrical Engineer
William H. Nalder — Assistant Chief Designing Engineer
Byram W. Steele — Civil Engineer-Dams
Erdman B. Debler — Hydraulic Engineer
Charles M. Day* — Mechanical Engineer
Ivan E. Houk — Senior Engineer-Technical Studies
Harry R. McBirney — Civil Engineer-Canals
Kenneth B. Keener — Assistant Civil Engineer-Dams
Harvey F. McPhail — Electrical Engineer
Robert A. Monroe — Structural Engineer
Porter J. Preston — Senior Engineer-Investigations
Howard C. Stetson — Senior Engineer-Specifications

PROJECT OFFICE, BOULDER CITY, NEVADA

Walker R. Young — Construction Engineer
Ralph Lowry — Field Engineer
John C. Page — Office Engineer

CONSULTANTS

Colorado River Board: — William L. Sibert,* Chairman
Charles P. Berkey — Warren J. Mead
Daniel W. Mead — Robert Ridgway

Boulder Dam Board: — Andrew J. Wiley,* Chairman
William F. Durand — Arthur P. Davis*
David C. Henny* — Louis C. Hill

Concrete Research Board: — Phaon H. Bates, Chairman
Franklin R. McMillan — Raymond E. Davis
Herbert J. Gilkey — William K. Hatt

Special Consultants:
Harald M. Westergaard — Mechanics
Frederick L. Ransome* — Geology
Gordon B. Kaufmann — Architectural Features

PRINCIPAL CONTRACTORS

General Contractors — Six Companies, Inc., San Francisco
Penstock & Outlet Pipe — The Babcock & Wilcox Co., New York

* Deceased.

FOREWORD

Colorado River, originating in the melting snows of the Wyoming and Colorado Rockies and augmented by rapid run-off from spasmodic rains and cloudbursts over a vast arid region, has menaced life and property in its descent to the Gulf of California since the days of the first covered wagon.

With increased population along the lower reaches of the river the problem of controlling the Colorado became more important. During recent years millions of dollars have been spent in mitigating the evils of silt deposition and in protecting the highly cultivated Imperial Valley lands from annual threats of inundation.

The need for a comprehensive plan of development to check the ravages of Colorado River, to regulate its flow, and to utilize a part of its enormous energy led, first, to investigations by the Reclamation Service of all water storage possibilities; next, to the Colorado River Compact, a mutual agreement for the protection of the seven basin states; and, finally, to the adoption of the Boulder Canyon Project, as the initial development.

The Boulder Canyon Project Act, approved December 21, 1928, authorized a total appropriation of $165,000,000 for the various features involved. These include Boulder Dam and appurtenant works, the power plant, the reservoir, and the All-American Canal System. The purposes of the project are: (1) flood and silt control for protection of lands along the lower river; (2) improvement of navigation; (3) river regulation and storage of water for irrigation and municipal use; and (4) development of electric power for domestic and industrial purposes. The project is self-liquidating, largely through contracts for disposal of electrical energy. It was constructed and is being operated under the supervision of the Bureau of Reclamation, United States Department of the Interior.

Boulder Dam is located on the Nevada-Arizona boundary near Las Vegas, Nevada, at a place where Colorado River has carved a deep gorge between towering rock cliffs, known as Black Canyon. The dam is a concrete arch gravity structure with a maximum height of 726 feet above foundation rock, a maximum base thickness of 660 feet, and a crest length of 1,244 feet. The dam and appurtenant works contain 4,400,000 cubic yards of concrete, of which 3,250,000 cubic yards were required in the dam.

During construction the river was diverted through four 50-

foot diameter, concrete-lined tunnels, two on each side of the river. These tunnels were subsequently plugged near the upstream ends. The spillways, each of 200,000 second-feet capacity, are connected through inclined shafts to the two outer tunnels. A 30-foot diameter steel power penstock is installed in each of the inner tunnels. Discharge from the reservoir is controlled by cylinder gates in four intake towers, founded on the canyon walls near the upstream face of the dam. Four 30-foot steel penstocks, connected to the bases of the intake towers, conduct water to the power plant and to the outlet valves for release of flood, irrigation, and domestic water supply when the power plant discharge is insufficient for such purposes. The reservoir above the dam is 115 miles long and has a capacity of 30,500,000 acre-feet, the equivalent of two years' normal river flow.

The power plant is in a U-shaped, reinforced concrete structure, over 200 feet high and 1,500 feet long, located immediately downstream from the dam. The plant is designed for an ultimate installation of fifteen 115,000 and two 55,000 horsepower units, making a total installed capacity of 1,835,000 horsepower.

The All-American Canal, located near the Mexican border, will carry water to irrigate lands in the Imperial and Coachella Valleys. The canal proper, with a diversion capacity of 15,000 second-feet, is the largest ever constructed for irrigation purposes in America.

The entire Boulder Canyon Project is characterized by the extraordinary. The height and base thickness of the dam, the size of the power units, the dimensions of the fusion-welded, plate-steel pipes, the novel system of artificially cooling the concrete, the speed and coordination of construction, and other major features of the project are without precedent. The magnitude of the undertaking introduced many new problems and intensified many usual ones, requiring investigations of an extensive and diversified character to insure structures representing the utmost in efficiency, safety, and economy of construction and operation.

The major credit for the conception of the project and the initiation of investigations leading to its adoption must be given to the late Arthur P. Davis, former Director of the Reclamation Service. Dr. Elwood Mead, Commissioner of Reclamation during the greater part of the construction period, passed away January 26, 1936, four months after the dedication of Boulder Dam. In commemoration of his untiring services on the Boulder Canyon Project, the reservoir created by the construction of the dam has been officially named "Lake Mead".

CONTENTS

CONTENTS (Continued)

ACCURACY OF RESULTS

CHAPTER III—INTAKE TOWER AND PENSTOCK ASSEMBLY

INTAKE TOWER MODEL

PENSTOCK ASSEMBLY

INTAKE TOWER ELECTRIC-ANALOGY STUDIES

CHAPTER IV—TESTS ON TUNNEL-PLUG OUTLET

TUNNEL-PLUG OUTLET MODEL

CONTENTS (Continued)

TUNNEL-PLUG NEEDLE VALVES

CHAPTER V—CHANNEL CONDITIONS BELOW BOULDER DAM

RIVER MODEL

LIST OF FIGURES

LIST OF FIGURES (Continued)

LIST OF TABLES

CHAPTER I—INTRODUCTION AND SUMMARY

INTRODUCTION

1. Scope of Bulletin.—The Boulder Dam structures, in general, were of far greater magnitude than any similar structures built in the past. Careful investigation was made of the validity of existing formulae and design methods before proceeding to final designs. Early hydraulic model tests of side-channel spillways for Boulder Dam, described in Part VI, Bulletin 1, gave results of such great value that it was decided to test other major features by model experiments. This bulletin describes the following hydraulic model tests:

1. Studies of junctions between the 13-foot penstocks and the 30-foot headers.
2. Hydraulic losses and pressure conditions in intake towers.
3. Flow characteristics of needle valves in tunnel-plug outlets.
4. Hydraulic conditions in the river downstream from the powerhouse.

This bulletin presents a description of the laboratory and laboratory procedure, and an analysis of the results obtained. The relationship between the dam and the penstocks is shown in figure 1. This figure shows the preliminary design used as a basis for the experiments. Final designs are shown in Part IV, Bulletin 6, "Penstocks and Outlet Pipes".

2. Laboratory and General Equipment.—With the exception of the tests on the 1:20 model of the tunnel-plug outlet, made at the Montrose laboratory, all studies described in this bulletin were conducted in the hydraulic laboratory of the Colorado Agricultural Experiment Station at Fort Collins, Colorado. A general layout of the laboratory showing locations of models is given in figure 2. Water for the experiments was supplied from a reservoir, with a capacity of 30,000 cubic feet, located on a hill adjacent to the laboratory. Flow from the reservoir, controlled by three 12-inch hand-operated gates, passed through a diverging flume into a

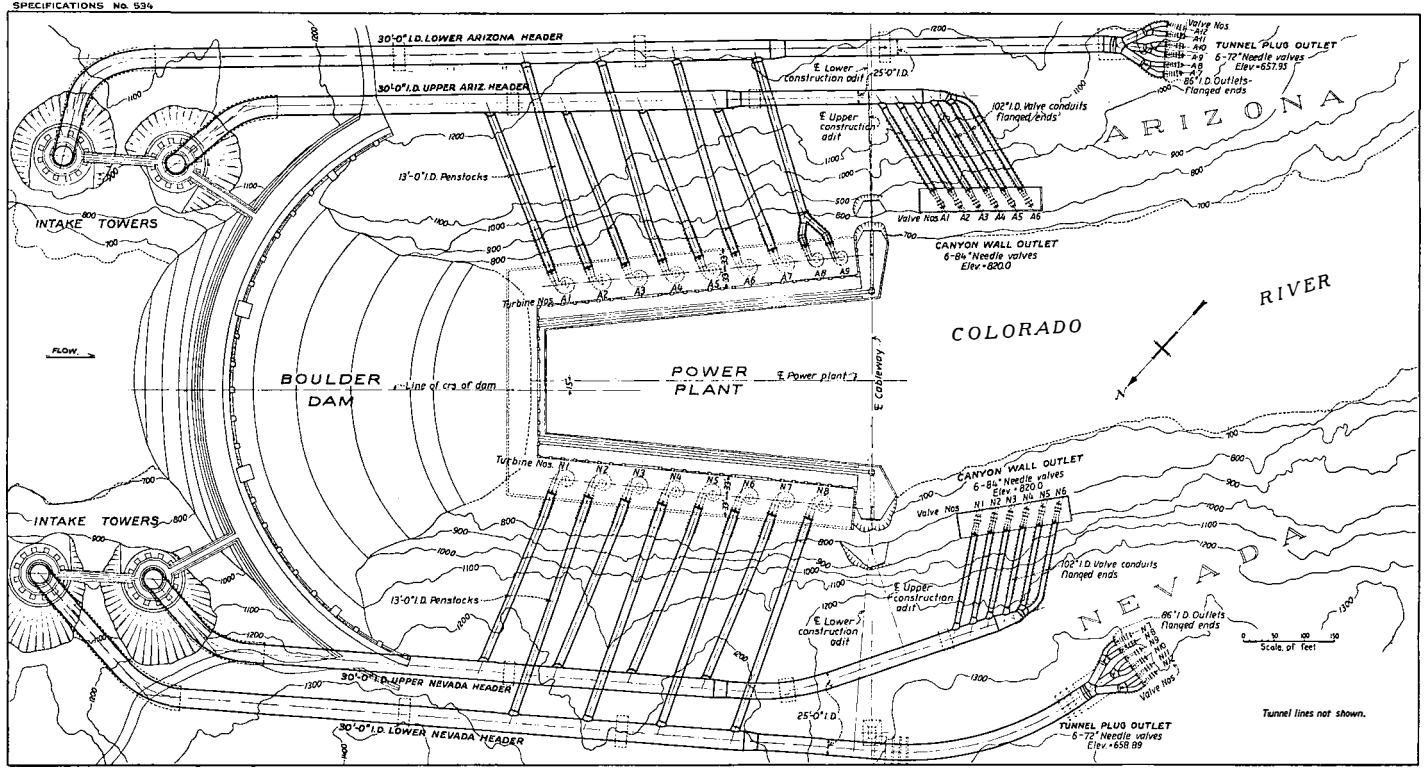

FIGURE 1—BOULDER DAM PLATE-STEEL OUTLET PIPES—PRELIMINARY LAYOUT

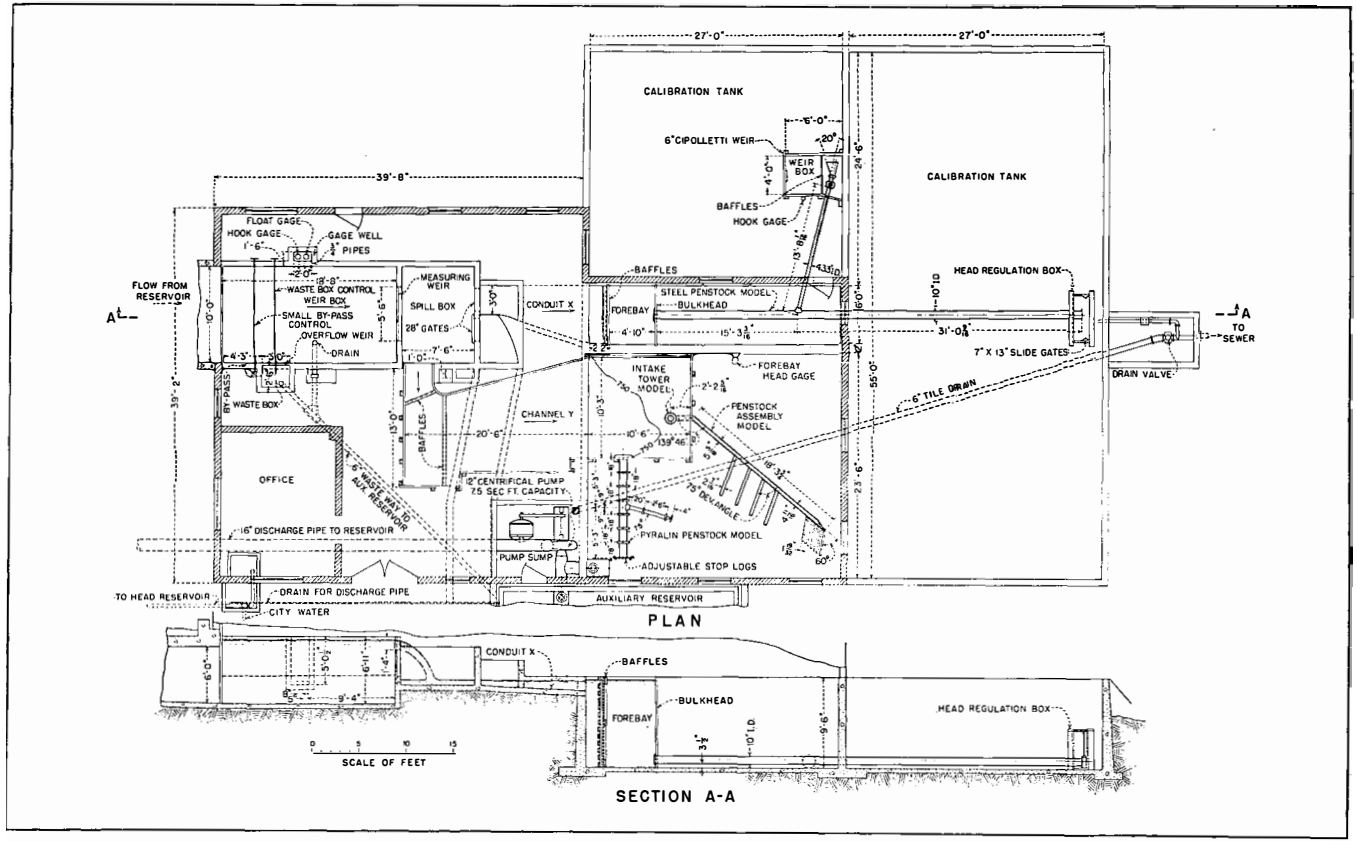

FIGURE 2—LOCATION OF MODELS IN LABORATORY

concrete weir-channel, 19.5 feet long, 10 feet wide, and 7.25 feet deep. A by-pass gate and a 4-inch by-pass valve were located in one side of the weir channel, 13 feet upstream from the weir. Small adjustments of the discharge passing over the weir were made by varying the flow through the by-passes. The head on the weir was measured by a hook gage and a float gage, both operating in a stilling well connected to the weir channel. During the experiments two weir plates were used, a 90-degree V-notch for discharges up to 2 second-feet, and a 2-foot Cipolletti for flows of 2 to 8 second-feet. Both weirs were calibrated by the Irrigation Division of the United States Department of Agriculture and were checked by the laboratory staff of the Bureau of Reclamation prior to the model testing.

Equipment thus far described was common to all experimental work; but from this point, the equipment varied for each model. When operating either the visual penstock junction model, the intake tower model, or the penstock assembly model, shown in figure 2, the 28-inch gates were closed, thus diverting water into a flume on the laboratory floor which served as a reservoir as well as a channel. Adjustable baffles were installed in the flume to eliminate undesirable cross-currents produced by the bend at the upper end. A tank, 10.5 feet by 10.25 feet by 12 feet deep at the downstream end of the channel, served as a forebay for the models.

When operating the quantitative penstock junction model, one diverter gate was opened, allowing water from the measuring weir to flow straight ahead through a conduit beneath the floor of the laboratory into the forebay.

A one-inch rod, extending from the ceiling to the floor of the laboratory, in a central location, served as a mounting for a forebay head gage. The rod contained 3/8-inch holes, drilled at 2-foot intervals. By means of a pin and clamp, a hook gage with a range of 2 feet could be mounted at any hole. A stilling well in which the hook operated, was held in position on the rod by a friction clamp. A rubber hose made it possible to connect either forebay to the well. The water surface elevations in the forebay, which varied over a wide range, were obtained from this gage.

3. Personnel.—The hydraulic research program was begun under the general supervision of E. W. Lane, former research engineer, and completed under the direction of Jacob E. Warnock, present research engineer. Experiments on the tunnel-plug outlet,

conducted at Montrose, Colorado, were supervised by W. M. Borland, associate engineer. Tests described in chapters II and III were conducted by J. N. Bradley, who also prepared these portions of the bulletin, with the exceptions of sections 22 to 29.

As this report was made possible by the cooperative efforts of a number of individuals, it is desired to acknowledge the help of W. H. Price, C. W. Thomas, J. W. Ball, A. N. Smith, W. J. Colson, and W. O. Parker, who assisted in the model construction work and laboratory testing. H. W. Brewer and J. D. McCrum assisted in the preparation of this report. Special acknowledgment is made to S. P. Wing, engineer, who prepared sections 22 to 29 and cooperated in the analysis of results.

It is further desired to acknowledge the cooperation of the Colorado State Board of Agriculture, governing board of the Colorado State College of Agricultural and Mechanical Arts, and the staff of the United States Bureau of Agricultural Engineering. These agencies permitted the use of the hydraulic laboratory of the Colorado Agricultural Experiment Station for conducting the model experiments.

4. Penstock Symbols.—

Q_a = Total discharge, second-feet.

Q_s = Discharge through branch, second-feet.

Q_b = Discharge in main pipe below junction, second-feet.

A_a = Area of main pipe above junction, square feet.

A_s = Area of branch, square feet.

A_b = Area of main pipe below junction, square feet.

$V_a = Q_a/A_a$ = Mean velocity in main pipe upstream from junction, feet per second.

V_s = Mean velocity in branch, feet per second.

V_b = Mean velocity in main pipe below junction, feet per second.

D_a = Average diameter of main pipe above junction, feet.

D_s = Average diameter of branch, feet.

D_b = Average diameter of main pipe below junction, feet.

Q_s/Q_a = Ratio of branch discharge to total discharge.

h_v = Velocity head, feet.

P_1 = Pressure head at piezometer 1, feet.

P_2 = Pressure head at piezometer 2, feet, etc.

P_x = Average of pressure heads at piezometers 2, 3, 4, and 5, feet.

S = Friction loss per foot of straight pipe, feet of water.

$h_{f(x\text{-}7)}$ = Pipe friction loss from P_x to piezometer 7, feet of water.

$h_{f(6\text{-}36)}$ = Pipe friction loss from piezometer 6 to 36, etc.

J_b = Junction loss in main pipe, feet.

J_s = Junction loss in branch, feet.

$J/V^2\,2g$ = Junction loss coefficient.

$R = VD/\nu$ = Reynolds' number.

$F = V^2/gD$ = Froude's number.

ν = Kinematic viscosity $= u/\rho$, square feet per second.

u = Absolute viscosity $= \dfrac{0.00003716}{0.4712 + 0.01435T + 0.0000682T^2}$, $\dfrac{\text{lb.sec.}}{\text{ft.}^2}$

where T is the temperature in degrees Fahrenheit.

ρ = Density of water at T degrees Fahrenheit, $\dfrac{\text{lb. sec.}^2}{\text{ft.}^4}$

βV = Average velocity where

$\beta = \displaystyle\int \frac{V^2 dA}{V^2 A}$ = Coefficient of velocity, where $V = Q/A$ = mean velocity.

αH_v = True velocity head where

$\alpha = \displaystyle\int \frac{V^3 dA}{V^3 A}$ = Energy head coefficient.

5. Intake Tower Symbols.—

d_1 = Difference in elevation between the water surface outside and inside the tower, feet (model).

d_2 = Difference in elevation between the reservoir surface and the reading of piezometer 45 (model).

d_3 = Difference in elevation between the reservoir surface and the reading of any one of the five piezometer rings A, B, C, D, and E located below the tower (model).

D_1 = Difference in elevation between the water surface outside and inside the tower (prototype).

h_t = Total loss through tower, feet of water.

h_{eu} = Entrance loss through upper gate, feet of water.

h_{eb} = Entrance loss through lower gate, feet of water.

h_{pu} = Average head required inside tower to change direction of flow at upper gate (model).

h_{pb} = Average head required inside tower to change direction of flow at lower gate (model).

H_p = Average head required inside tower to change direction of flow at either gate (prototype).

$h_{f(45\text{-}u)}$ = Pipe friction from piezometer 45 to bottom of the upper gate (model).

$h_{f(c\text{-}b)}$ = Pipe friction from piezometer ring C to the bottom of the lower gate (model).

h_b = Compound bend loss in main header directly below intake tower.

SUMMARY

6. Results.—Aside from verifying hydraulic design features, the tests brought to attention considerable detailed information concerning formation of eddies, distribution of pressures, and friction losses in hydraulic structures. The results, discussed in the following chapters, are summarized as follows:

1. Eddy zones were defined, junction losses measured, and pressures recorded at the junctions of the 13-foot turbine penstocks with the main 30-foot header. It was concluded that junction losses obtained from very small models are not truly representative of losses in large junctions such as those at Boulder Dam.

2. Model tests made possible a definite analysis of the losses in the intake tower; offered a simple yet accurate method of measuring the flow through the towers; and made practical the elimination of a proposed set of air vents at the base of each tower.

3. A material improvement was obtained in the conditions of flow in the 50-foot concrete-lined tunnel below the tunnel-plug outlets; considerable piping was eliminated; and a satisfactory program of operation was formulated for the needle valves located in the tunnel-plug outlets.

4. The model of the river downstream from the dam confirmed predictions that disturbances, created by the outlet works and spillways discharging into the river, will not extend sufficiently upstream to interfere with the proper operation of the powerhouse. In addition, a program of operation is outlined for different combinations of flow from spillways and outlet works.

7. Changes in Design.—In no instance did the studies described in this report lead to drastic changes in design such as resulted from the model studies of spillways. All minor changes indicated in the penstock junction and intake tower studies were not made because the design and construction had progressed to the stage where further changes were not economically feasible. However, results of the studies gave substantial evidence that the adopted designs were satisfactory. In the case of the tunnel-plug outlets, the suggested changes were incorporated in the final design. All data are believed to be of a fundamental character and of value in future design work.

CHAPTER II—TESTS FOR PENSTOCK JUNCTION LOSSES

VISUAL TESTS

8. **Purpose.**—In analyzing the design of the 30-foot headers, turbine penstocks and outlet works, it was realized that junctions between the 30-foot headers and the 13-foot turbine penstocks were potential sources of excessive loss of head. A reduction of this loss would increase the effective head on the turbines, the potential power output, and the discharge capacity of the outlet needle valves. With long radius bends incorporated in the design of the 30-foot headers, the only possibility of decreasing head losses was to improve the efficiency of the junctions between headers and turbine penstocks. For this purpose extensive tests, both qualitative and quantitative, were made on models of one of the junctions.

As a preliminary and qualitative study, a model representing the junction between the 30-foot upper Arizona header and the 13-foot penstock leading to turbine A-1, shown in figure 1, was built of transparent pyralin. This particular junction was selected because it was possible to have a wide variation of flow, ranging from 100 percent of the total flow through the main penstock and no flow through the branch, to 100 percent through the branch

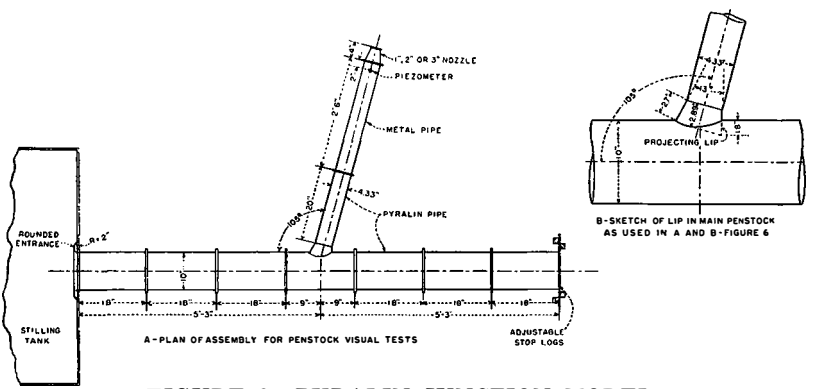

FIGURE 3—PYRALIN JUNCTION MODEL

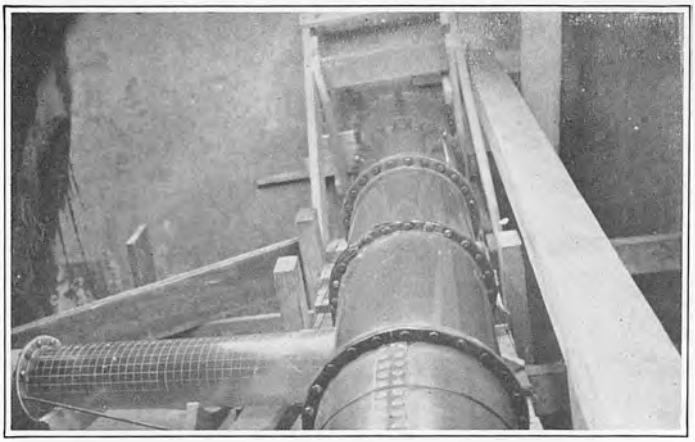

FIGURE 4—PYRALIN JUNCTION MODEL LOOKING DOWN MAIN PIPE

and no flow in the main penstock below the junction. The actual ratio of discharge in the penstock to flow in the branch depends entirely on the manner of operation downstream. It was desired to determine visually the path of the water after it entered the branch for different combinations of flow in the system, and to determine the location of eddies and disturbances in the branch for varying ratios of branch discharge to main header discharge.

9. Apparatus and Procedure.—The model for visual tests was constructed on a scale of 1:36. It consisted of a straight piece of 10-inch pipe with a 4.33-inch branch intersecting it at an angle of 105 degrees in a downstream direction, as shown in figures 3 and 4. A portion of the branch and main pipe was graduated at intervals of five-hundredths of a foot in both longitudinal and circumferential directions, as shown on figure 4. To obtain various combinations of discharge at the junction, three metering nozzles, 1, 2, and 3 inches in diameter, were used interchangeably at the end of the branch; while small stop-logs served to regulate the flow at the end of the main pipe. A piezometer was installed in the branch, two inches from the upstream end of the conical nozzle, for measuring pressures. The total discharge was measured over the laboratory weir; the discharge through the branch was computed from the observed piezometer pressure at the nozzle; and the difference was assumed to flow through the downstream portion

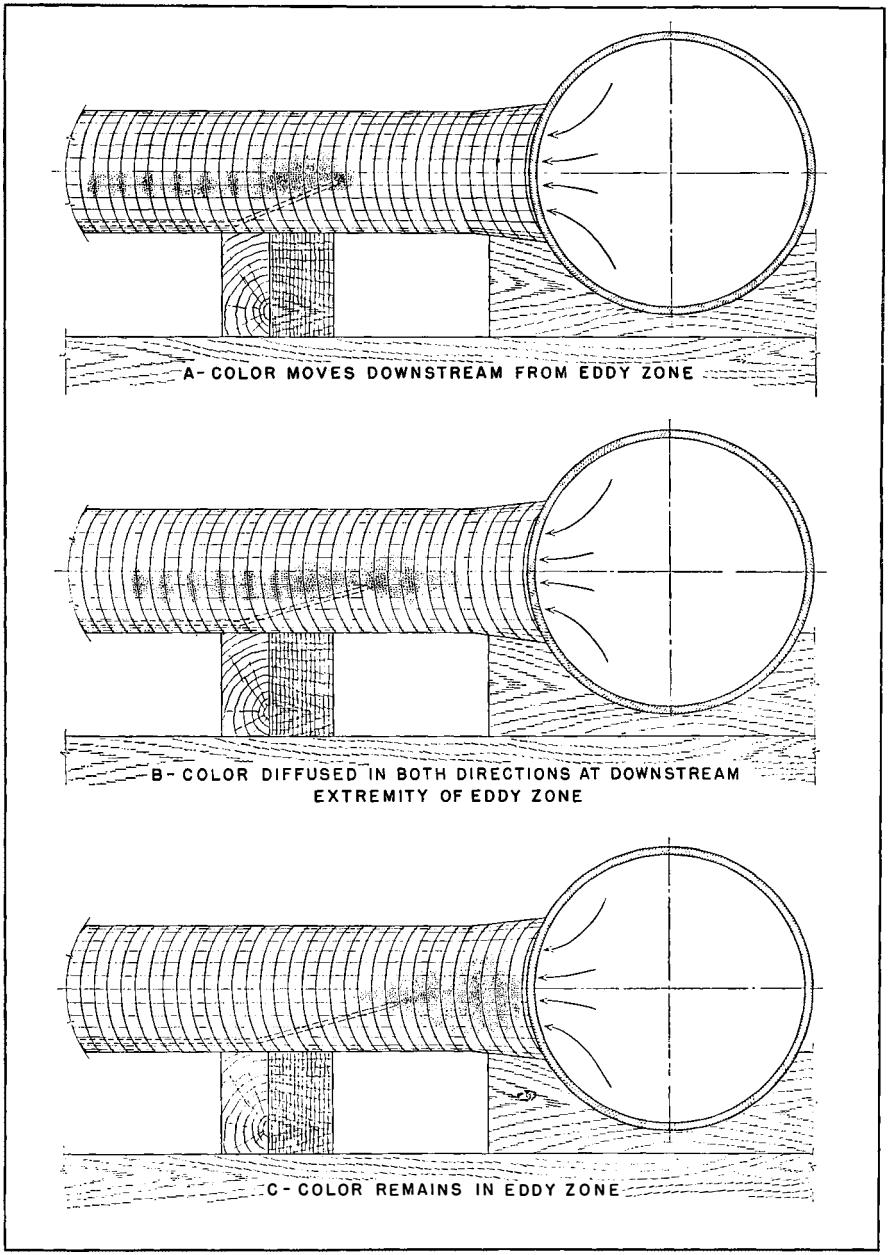

FIGURE 5—COLOR METHOD OF LOCATING EDDY ZONE

of the main pipe. It was unnecessary to calibrate the nozzles in place as the nature of the tests did not warrant such accuracy.

The path of the water as it entered the branch was traced by inserting a potassium permanganate solution, through a long copper tube which extended through the nozzle and into the branch. The tube was moved systematically in the branch and the results were recorded with respect to the coordinate lines on the pipes. The action of the water in the branch was readily detected by this method.

10. Results and Conclusions.—As water flowed from the main pipe into the branch, there was a high velocity zone on the right-hand side, looking downstream on the branch, shown in figure 3, while on the left-hand side a zone of relatively quiet water existed which was termed an "eddy zone". When color was inserted in the stream of high velocity water, it was dissipated quickly, being carried down the tube and out the nozzle, while color inserted in the eddy zone was slowly dispersed. By moving the color tube back and forth the boundary surface between the two zones was defined. Figure 5 shows diagrammatically the method used and the dispersion of the color for three positions of the color tube.

It was found that the eddy zone existed in the branch for all combinations of discharge; the dimensions of the zone decreasing as the ratio of the discharge in the branch, Q_s, to the discharge in the main pipe above the branch, Q_a, increased. Various runs plotted on figures 6 and 7 show the limits of observed eddy zones. The ratio Q_s/Q_a is referred to as the "discharge ratio."

It was thought that a lip, protruding into the main pipe on the downstream side of the branch entrance, might reduce the loss of head through the branch, although it was expected to cause an increase in loss in the main pipe. This lip, shown on figure 3-B, was installed during tests 1 to 3 inclusive. Eight runs made in these three tests are plotted on figures 6-A and 6-B. The remaining tests were performed with the lip removed and are plotted on figures 6-C and 7. Conditions under which the runs were made and results obtained are shown in table I.

Comparisons of data in table I for conditions with and without the lip show some differences in the location of the apex of the eddy zone for runs of similar discharges and similar discharge ratios. The variation is slight and occurs in both directions, indicating that the lip in the main pipe made no material difference in

TABLE I—SUMMARY OF TESTS ON VISUAL JUNCTION MODEL

WITH LIP IN MAIN PENSTOCK					WITH LIP REMOVED				
Test No.	Discharge Ratio Q_s/Q_n	Total Discharge Sec. ft.	Head on Main Penstock	Location of Apex of Eddy Zone Pipe Diam.	Test No.	Discharge Ratio Q_s/Q_n	Total Discharge Sec. ft.	Head on Main Penstock	Location of Apex of Eddy Zone Pipe Diam.
1-3	.0209	3.82	3.72	.....					
1-2	.0264	2.42	1.98	.....					
					4-8	.0409	4.84	.....	.....
1-1	.0516	1.01	1.05	1.60(B)	4-9	.0479	4.84	2.74	1.70 (B)
					4-7	.0677	2.42	0.87	1.55
2-3	.0813	3.69	3.23	1.50(A)	4-3	.0815	3.69	3.37	1.45(A)
					4-6	.0948	2.42	1.71	.....
					5-8	.0989	4.80	2.37	1.55
2-2	.1210	2.37	2.64	1.30(A)	4-2	.1241	2.30	2.63	1.40(A)(D)
					4-4	.1333	1.21	0.59	1.40(D)
2-1	.1496	1.27	0.93	1.10(B)	5-9	.1512	4.80	4.39	1.25(B)
					4-1	.1632	1.27	1.17	1.00
					4-5	.1896	1.20	1.46	0.82(C)
					5-6	.1944	2.42	1.45	0.85(C)
3-3	.2054	3.70	4.21	1.05(A)	5-3	.2041	3.70	4.18	0.83(A)(C)
3-2	.2143	2.89	2.65	0.76(A)	5-2	.2142	2.89	2.68	0.78(A)
					6-5	.2490	2.88	3.56	0.75
					5-7	.2920	2.40	3.31	0.74
					6-4	.3285	2.16	3.37	0.55
3-1	.3566	1.27	1.16	0.55(A)	5-1	.3658	1.24	1.18	0.48(A)
					5-4	.4011	1.21	2.85	0.45
					6-3	.4965	1.44	3.33	0.44
					5-12	.5464	0.73	0.81	0.35
					5-5	.5860	1.20	3.21	0.30
					5-11	.6489	0.73	1.24	0.28
					6-2	.8765	0.83	3.39	0.26
					5-10	.9959	0.73	3.43	0.24

the shape and volume of the eddy zone. The head loss through the branch was not materially different for either condition. As it was difficult to accurately determine the limits of the eddy zone, some variation was expected.

Tests 1-1 and 2-1, with the lip, as compared to tests 4-9 and 5-9, without the lip and denoted by the letter B, seem to indicate that the apex of the eddy zone moved down the branch for an increase in total discharge with the same discharge ratio. On the other hand, in tests 4-5, 5-6, and 5-3, with lip removed and denoted by the letter C, in which the discharge ratio was nearly constant, the location of the apex remained practically unchanged although the discharge varied from 1.20 to 3.70 second-feet. Tests 4-2 and 4-4, identified by the letter D, show a similar indication.

Conclusions drawn from the few runs that are comparable are,

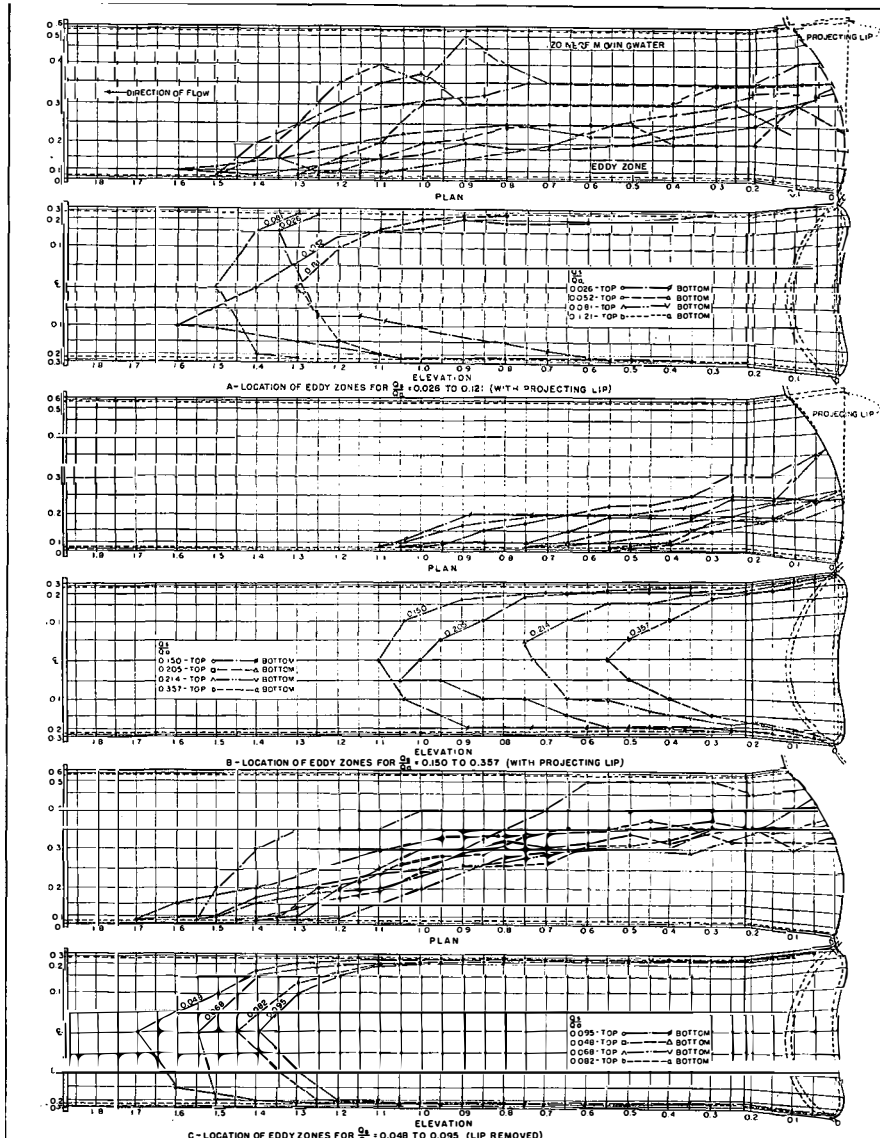

NOTE
Line and symbols indicate boundaries of eddy water zones for various ratios of discharge through branch penstock. Outside of pipe graduated in five hundredths of a foot.

FIGURE 6—VISUAL TESTS ON JUNCTION LOSSES

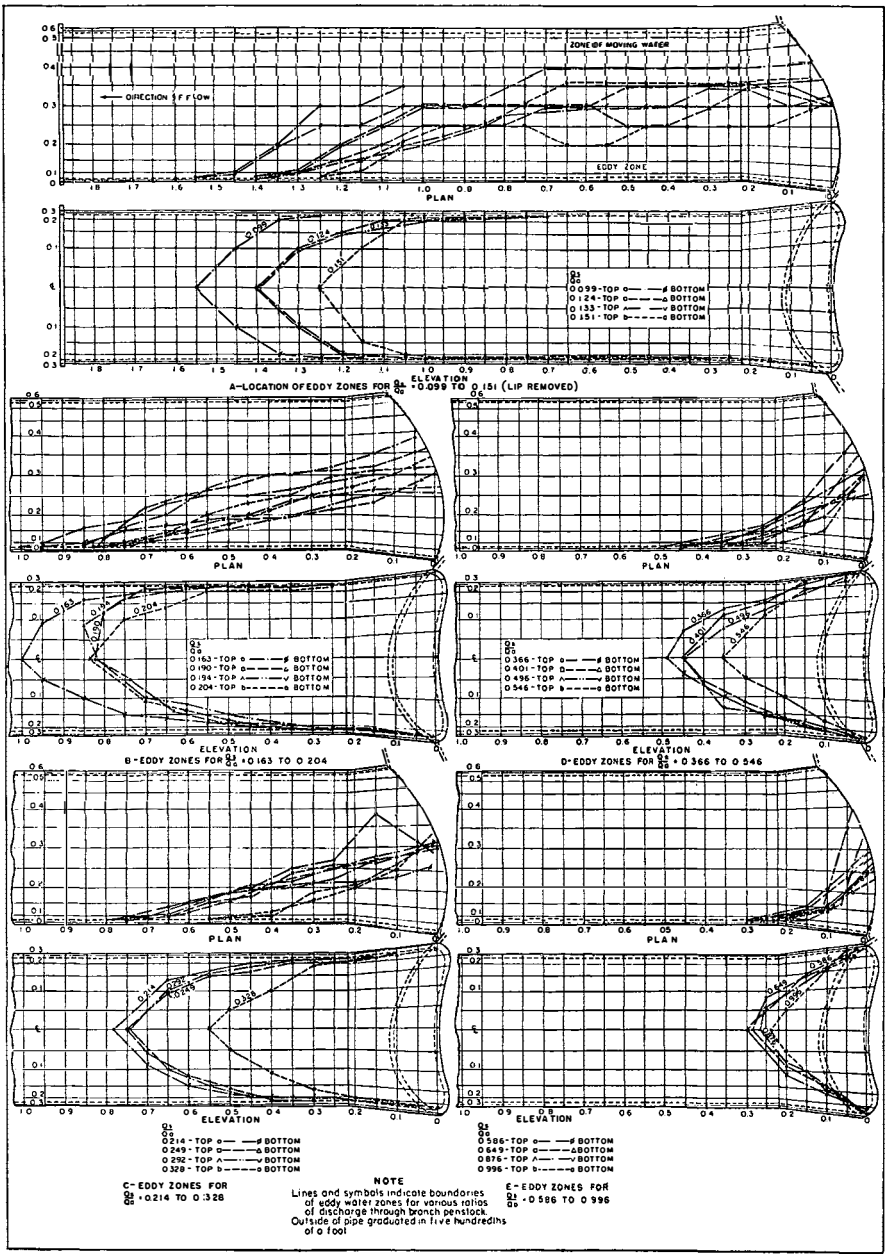

FIGURE 7—VISUAL TESTS ON JUNCTION LOSSES

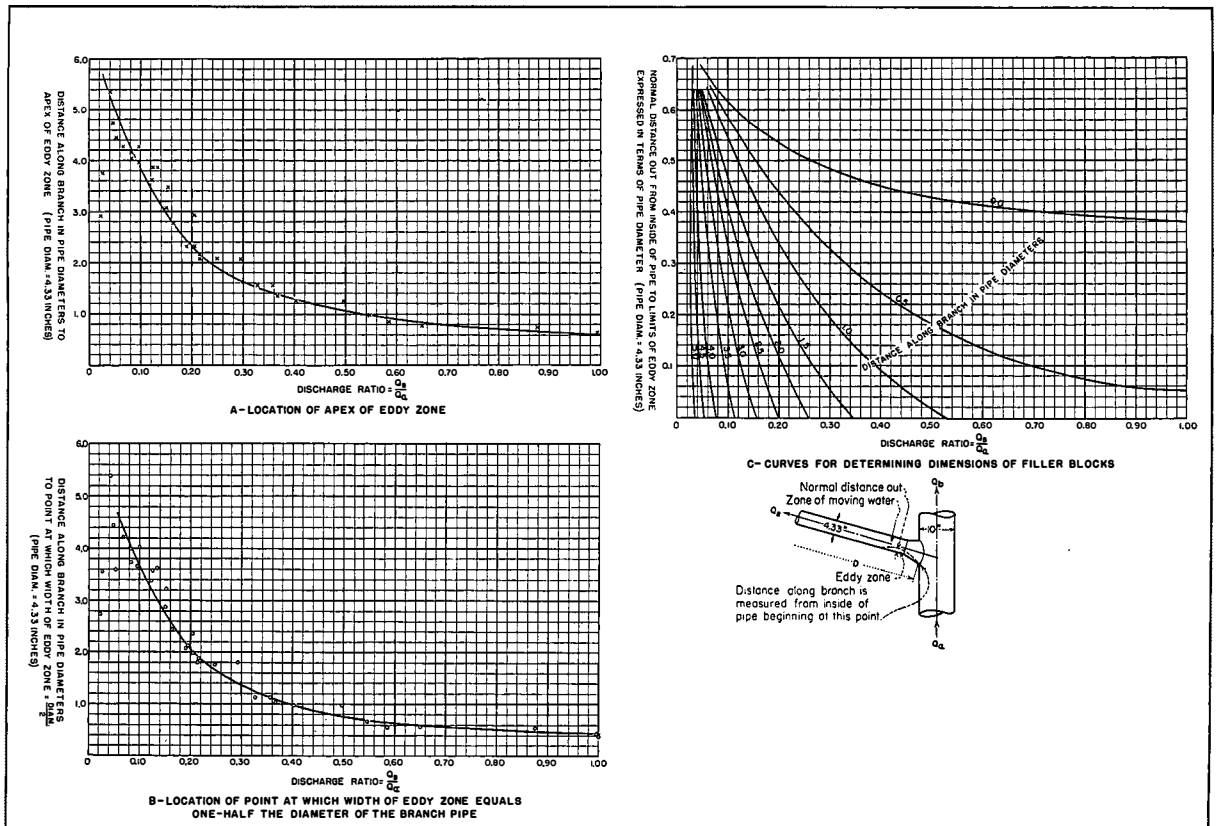

FIGURE 8—CURVES FOR DETERMINING DIMENSIONS OF FILLER BLOCKS

first, that the location and volume of the eddy zone is independent of the total discharge; and, second, that the dimensions of the zone in the branch are dependent only upon the ratio of respective discharges in the penstock and branch pipes.

Consideration was given to the possibility of filling eddy zones with blocks of the same shape as the zones to eliminate the eddies and to reduce the loss of head at the junction. Tests were made to determine the proper shape of the blocks. The results are shown on figure 8. Mean dimensions, obtained by averaging top and bottom edges of the zone, are plotted for all discharge ratios. The location of the apex for any given discharge ratio may be determined from figure 8-A; the location of the point at which the vertical width of the zone equals one-half the inside diameter of the branch may be determined from figure 8-B; and the approximate dimensions for the entire zone can be obtained from figure 8-C. For example, to obtain the dimensions of a filler block for a discharge ratio of 0.30, follow up the vertical line marked 0.30 on figure 8-C and read the normal distances out to the edge of the zone for each half-diameter measured along the branch. These values can then be plotted on a set of coordinates similar to those on the branch pipe from which a filler block may be constructed. The curves on figure 8 apply only where the ratio of pipe diameters, D_s/D_a is 0.433; the angle of the branch is 105 degrees; and the total angle of convergence of the cone is 13 degrees.

Filler blocks, designed according to figure 8, will be symmetrical, which is not always true of the eddy zone in the branch. Actual dimensions of two filler blocks for discharge ratios of 0.50 and 0.25 were obtained with the color tube on the center line quarter-points, and along the edges of the zone. These are plotted on figures 9-A and 9-B respectively. They show that the inside faces of the zones are not symmetrical. Two wooden filler blocks were built according to this data. When installed in the branch pipe, color injections showed them to be satisfactory. Elevations and sections of the two blocks are shown on figures 9-C and 9-D. The two blocks were used later in the studies made on the quantitative model of the junction of the penstock with the header.

QUANTITATIVE TESTS

11. Purpose.—The purpose of the quantitative tests was to determine accurately the loss in the junction between the first

turbine branch and the main header; and then to study effects of installing filler blocks of different dimensions, determined from the visual tests; to alter the physical shape of the junction, and reduce the disturbances and losses. Two types of blocks were used. First, a deflecting block was introduced in the main pipe in an endeavor to reduce the eddy loss in the branch at the expense of possibly increasing the loss in the main header; and, second, a solid block was used to fill the space in the branch formerly occupied by the eddy in an attempt to reduce the loss in the branch.

The quantitative model was built to the same scale as the visual model; but was carefully constructed of galvanized sheet iron and equipped with necessary instruments for measuring actual junction losses. Filler blocks could therefore be used interchangeably in either model.

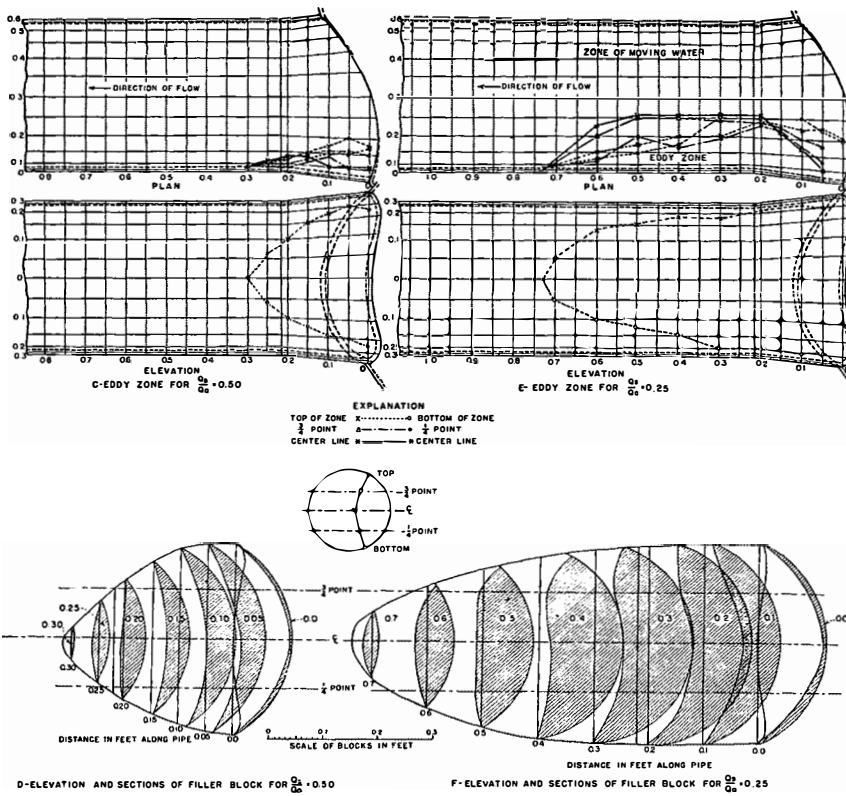

FIGURE 9—SHAPE OF FILLER BLOCKS DETERMINED FROM VISUAL TESTS

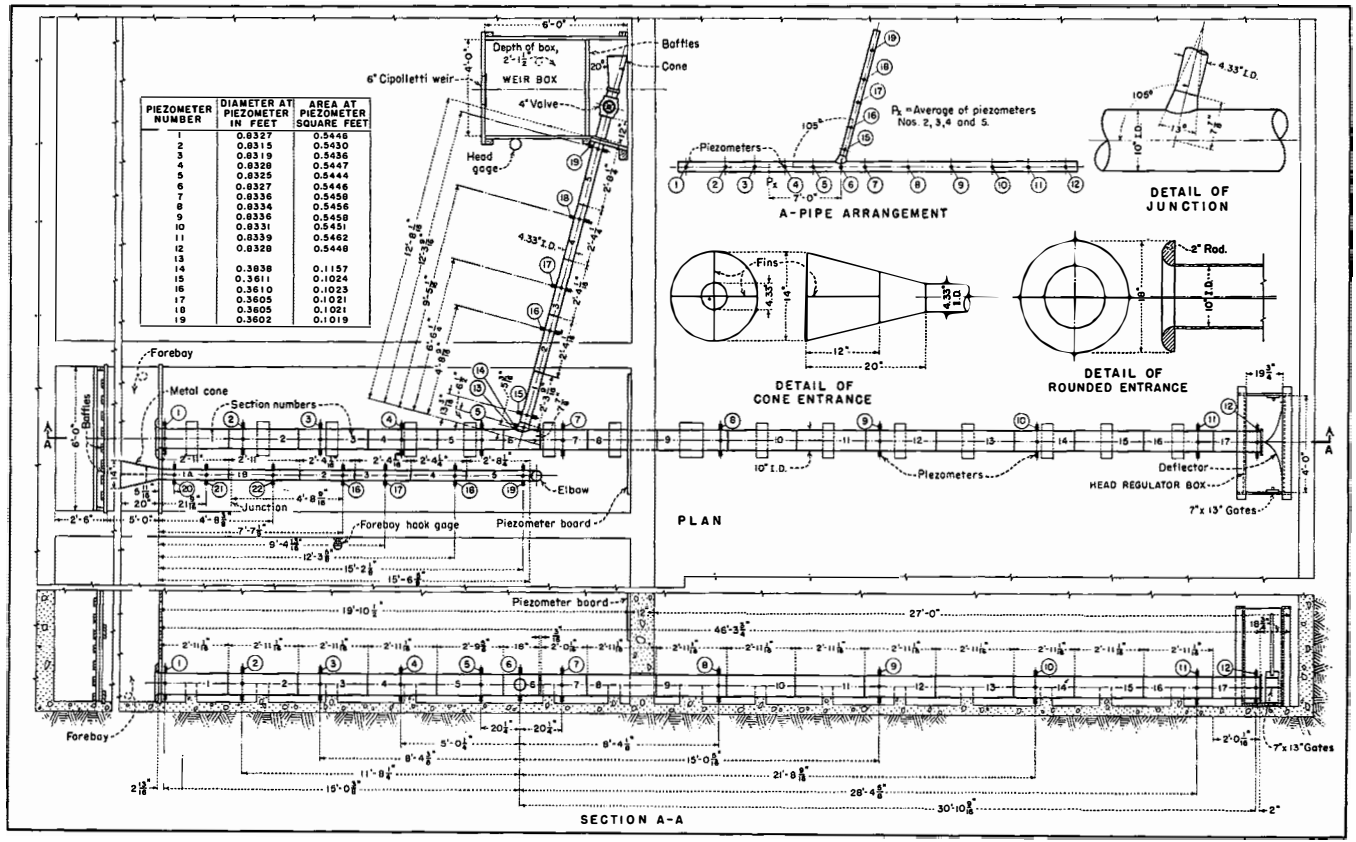

FIGURE 10—LABORATORY ASSEMBLY OF MODEL—4.33-INCH BRANCH INCLINED 105 DEGREES DOWNSTREAM

As a general experiment, a right-angle junction was tested with and without a conical connection. The layout was larger but geometrically similar to one tested by Professor D. Thoma on small brass pipe, see reference 2, section 15. The purpose of this test was to determine whether or not viscous effects in small junctions are appreciable, and if it is practical to design large pipe-line junctions from tests on small models.

12. Apparatus and Procedure.—The forebay for the quantitative penstock junction model, into which water spilled after passing over the measuring weir, was 6 feet wide, 7 feet long, and 8.5 feet deep, as shown on figure 2. It served as a stilling box, head regulator, and supply reservoir. A double set of wooden baffles was used as a stilling device. The same stilling well and hook gage were used to measure the head in the forebay as in the visual tests.

The penstock junction investigated was the same as in the visual tests. The branch, instead of being inclined downward as in the prototype, was installed horizontally and made an angle of 105 degrees in a downstream direction with the main pipe. The model, as constructed on a scale of 1:36, is shown on figure 10. It consisted of 3-foot sections of smooth galvanized sheet-iron pipe, accurately constructed and connected with butt joints. Precaution was taken to see that all inside seams and joints were smooth and free from burrs. The table on figure 10 shows the accuracy attained in constructing the pipes. These are average values obtained from a number of measurements made with an inside micrometer. The maximum deviation from the designed diameter of 0.8333 feet was 0.0018 feet, or 0.21 percent; and the maximum deviation from the designed diameter of 0.3611 feet was 0.0009 feet, or 0.25 percent.

The insides of the pipes were painted with two coats of aluminum paint before beginning the tests. A section of pipe is shown in detail on figure 11-A. The first model consisted of approximately 13 feet of 4.33-inch pipe, joined to a 46-foot section of 10-inch pipe with a downstream angle of 105 degrees. The junction was made 15 feet downstream from the entrance to the main pipe. A photograph of the pipes is shown in figure 12. As it was impossible to obtain pictures of the model in place, photographs were taken out-of-doors before installation.

An overflow box, with slide gates in the sides, was located at the downstream end of the main pipe to control the head; and a

4-inch gate valve was placed at the end of the branch pipe to regulate the discharge. A weir box, 4 feet wide, 6 feet long, and 2 feet deep, equipped with stilling baffles and a 6-inch Cipolletti weir, was located at the end of the branch to measure discharge.

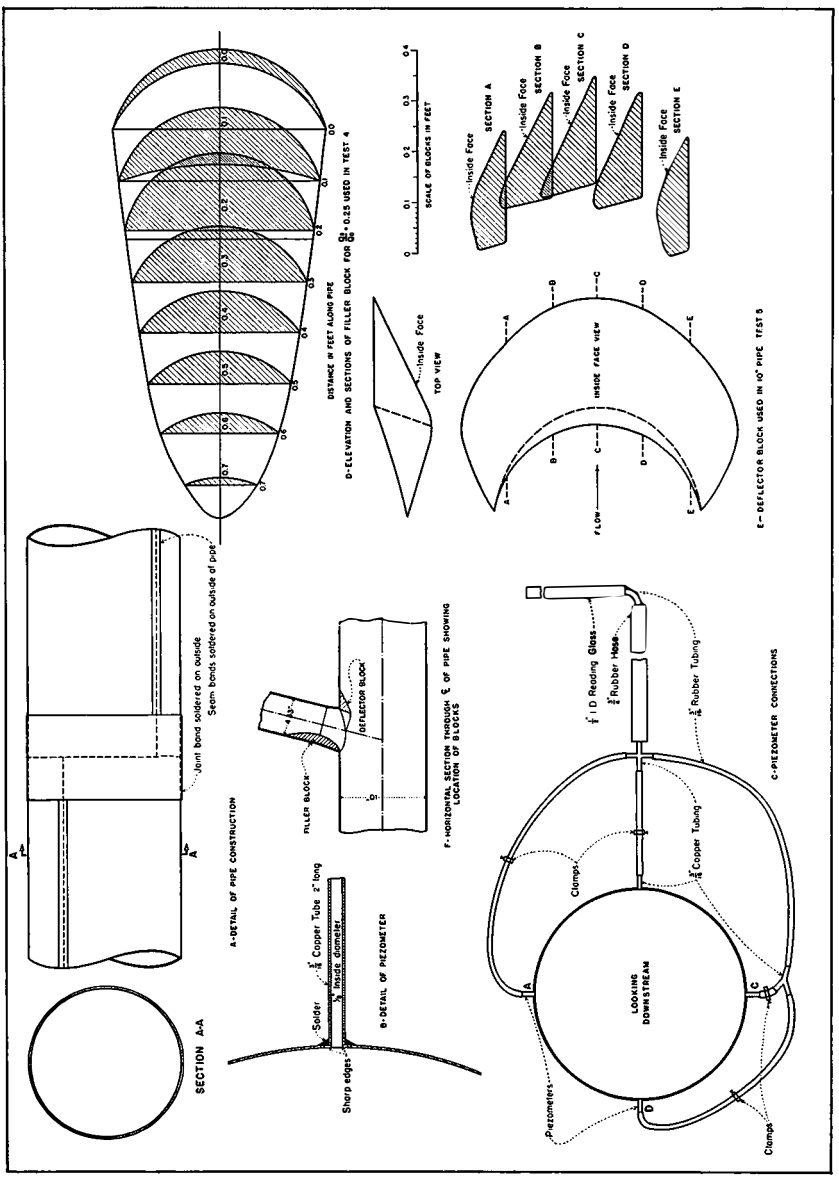

FIGURE 11—MISCELLANEOUS DETAILS OF PENSTOCK MODELS

Because the weir box was exceptionally small for the discharge, it was necessary to calibrate the 6-inch Cipolletti weir in place. This was done by completely closing the downstream end of the main pipe with a blank flange and diverting all water through the branch and over the 6-inch Cipolletti weir. The calibration was made by comparison with the 90-degree, calibrated V-notch laboratory weir. A metal cone was placed at the end of the branch pipe to recover a portion of the energy and increase the discharge.

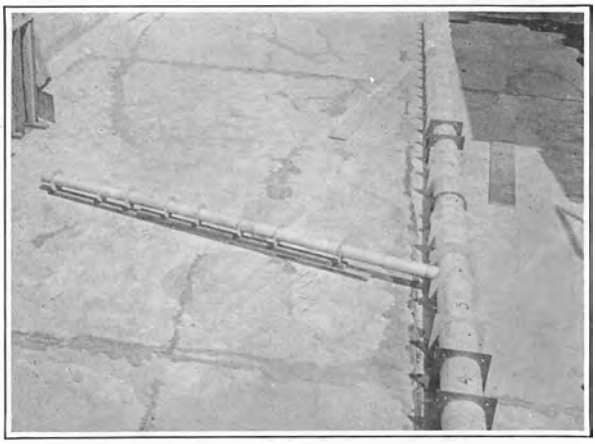

FIGURE 12—METAL PENSTOCK JUNCTION MODEL

Rings of piezometers were placed at intervals along the pipes as shown in figure 10. Four piezometers constituted a ring. Each piezometer consisted of a 3/16-inch outside diameter copper tube, 2 inches long, with a 1/8-inch bore. In construction, a 1/8-inch hole was carefully drilled in the pipe at the proper location. A copper tube was then accurately placed over the hole, normal to the pipe, and soldered in place. The inside of the tube and the hole was then reamed to remove any irregularities which might have been developed during the installation. Piezometer openings were of the sharp-corner type. Care was taken to remove all burrs and to keep the corners sharp and flush with the inside face of the pipe, as shown in figure 11-B. Piezometers installed on the cones were set normal to the surface. It was desired to read each piezometer separately, so the connections were made as shown in figure 11-C. Each ring was equipped with three screw clamps which were

alternated between the four rubber tubes, leaving one piezometer open to be read. Three-sixteenths-inch rubber tubing was used for the shorter connections, and each ring was connected to the piezometer board by a 3/4-inch rubber hose. This arrangement made it possible to use one glass tube for each ring of piezometers.

All A-piezometers were read simultaneously with all others closed; and, in rotation, all B, C, and D piezometers were read in the same manner. This procedure was repeated four times during a run, making a total of sixteen readings to a ring. Observations were made as rapidly as the board could be read; forty minutes were usually required to make a complete set.

The 3/4-inch hose, which extended from the rings to the manometer board, sloped upward to facilitate removal of entrapped air. Before each run, all piezometer clamps were loosened, and all tubes leading to the A-piezometers were disconnected to release any air. The 3/4-inch hoses were vibrated to drive air toward the board. Although this routine for eliminating air required from fifteen to twenty minutes before each run, the procedure was necessary since all the manometer tubes were located on a central board requiring hose connections as long as 30 feet.

13. 4.33-inch Branch Friction Calibration.—Friction losses in the 4.33-inch and 10-inch pipes were determined by connecting them separately to the bulkhead and making calibration runs, tests 1 and 2. In test 1, the branch pipe was connected as shown on figure 10, and two extra joints of pipe on the upstream end were added to give additional length for reducing irregularities of flow caused by entrance conditions. A conical entrance, shown in figure 10, with a vertical and horizontal fin extending from the large end to a distance two-thirds the length of the cone, to prevent vortex action, was used on the upstream end of the 4.33-inch pipe. An elbow was connected in a vertical plane to the downstream end of the pipe, to keep the pipe flowing full at all times. For the smaller discharges it was necessary to retard the flow by loosely bolting a blank flange to the end of the elbow. This increased the pressure in the pipe sufficiently to register on the manometer board.

Eleven runs were made on test 1, with discharges ranging from 0.55 to 1.70 second-feet. The two head gages on the 90-degree V-notch weir were read simultaneously with the forebay head gage at two-minute intervals during each run. The temperature of the water was recorded once during a run. Sixteen readings from each

piezometer ring were averaged and added to the respective computed mean velocity heads. These values of pressure head plus velocity head were plotted with respect to the length of the pipe. The method is illustrated on figure 13. Because the entrance loss effect extended some 40 diameters downstream, the lines drawn through the points have a slight curvature; but these would eventually terminate in straight lines were the pipe sufficiently long. As the length of the pipe was not sufficient to allow these lines to completely straighten out, it was necessary to draw a tangent to each curve near its downstream extremity. These tangents are shown on figure 13. The slope of each tangent represents the straight pipe friction per foot for a particular discharge and water temper-

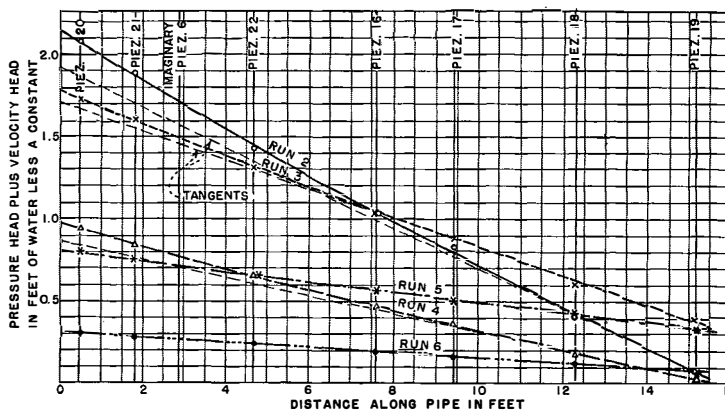

FIGURE 13—STRAIGHT PIPE FRICTION SLOPES, 4.33-INCH BRANCH

ature. A constant has been consistently subtracted in some of the runs to condense the data for comparison. The subtraction of constants in no way affects the slope of the lines. With the friction loss, discharge and temperature known, the friction factor, f, in the formula $S = \frac{fLV^2}{2gD}$, where S is the friction slope and L is unity, was computed for each run and plotted with respect to Reynolds' number on figure 14.

It has been customary in recent years to design closed conduits from curves obtained from experimental results of this type. To use these curves it is only necessary to know the range of Reynolds' numbers that will be encountered in the field and the

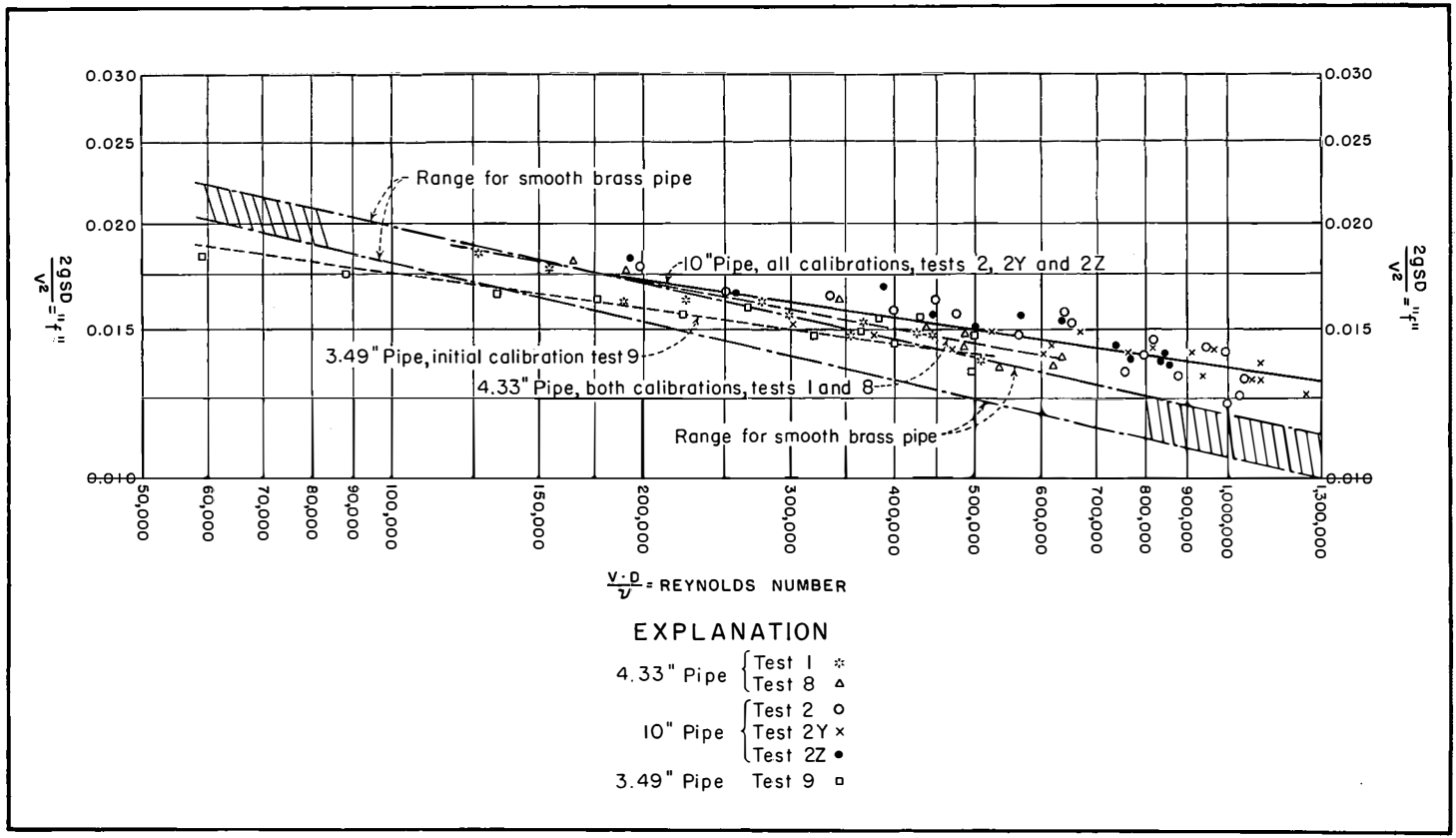

FIGURE 14—LOSSES DUE TO PIPE FRICTION ONLY

type of pipe to be used. With this information, the factor, f, can be obtained from a curve similar to those plotted on figure 14 for a pipe having comparable roughness.[1]

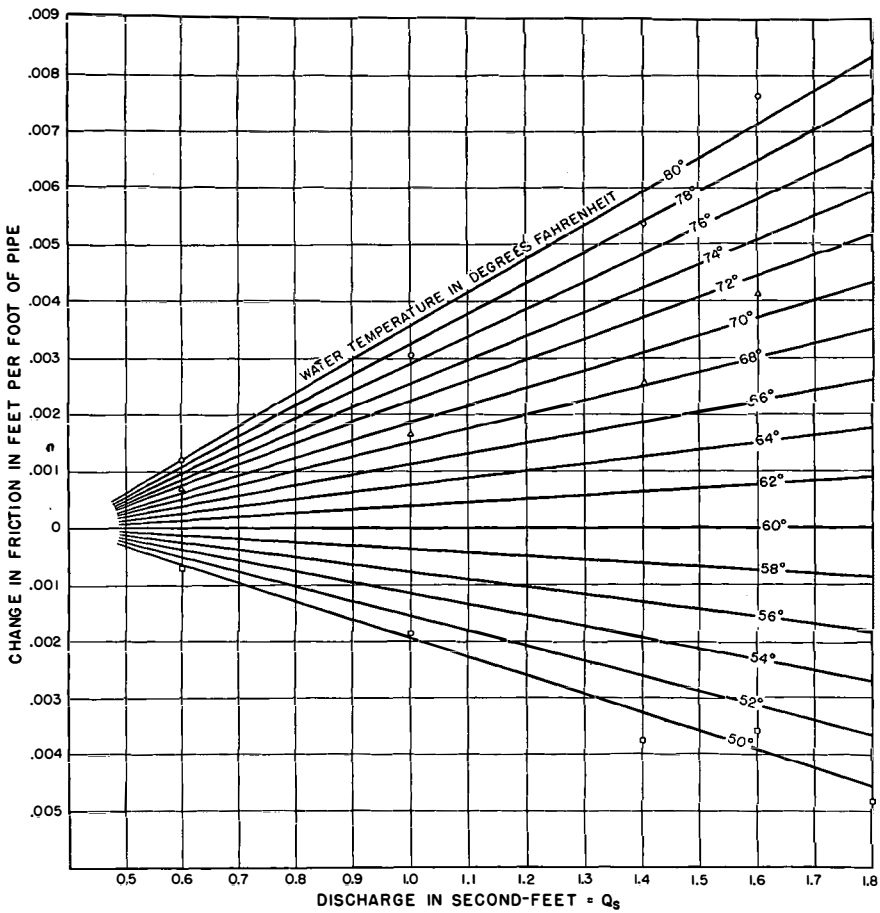

FIGURE 15—TEMPERATURE CORRECTION CURVES FOR 4.33-INCH BRANCH

As the temperature varied considerably throughout the series of tests, each run was corrected to a base temperature of 60 degrees Fahrenheit by use of the curves on figure 15. The temperature

[1]Pigott, R. J. S., The Flow of Fluids in Closed Conduits, Mechanical Engineering, August, 1933.

correction graph was constructed by choosing a number of discharges at various temperatures for the 4.33-inch pipe and computing the value of Reynolds' number for each. From figure 14, the friction loss factors were obtained for various conditions and the friction loss per foot of pipe computed. With this information, the temperature correction curves for the 4.33-inch pipe, which show the variation in friction loss due to temperature, were constructed. For example, with a discharge of 1.6 second-feet, water temperature of 70 degrees, and a pipe friction of 0.0200 feet per foot of pipe, the friction loss at a temperature of 60 degrees, see figure 15, would be $0.0200+0.0037 = 0.0237$ feet per foot of pipe.

Up to this point, the 10-inch and 4.33-inch pipes have been considered as separate entities and the main problem has been the measurement of straight pipe friction. In designing the model, piezometers were located at regular intervals in both pipes, and piezometer 6 was purposely located in the plane of the intersection of the center lines of the 4.33-inch branch and 10-inch pipe. This intersection has been considered as the "theoretical junction" of the two pipes, and, for brevity, shall be referred to as the "junction."

To evaluate losses other than those chargeable to straight pipe friction, it was necessary to isolate friction losses above and below the junction in the 10-inch pipe and below the junction in the 4.33-inch branch. A set of curves was plotted to represent friction losses from the junction to any piezometer in the branch pipe for different discharges. These were based on a temperature of 60 degrees Fahrenheit. Typical computations showing the method used in obtaining the curves are included in table 2. From the column entitled, "Plotted Energy at Junction," giving values taken from the curved lines on figure 13, the computed energy at each piezometer was subtracted separately. These values, plus or minus a temperature correction, represent the friction loss from the junction to each piezometer for various discharges at a temperature of 60 degrees. By plotting the values in the columns marked, "Drop to Junction," with respect to discharge, the curves on figure 16 were obtained.

At the completion of the tests on the 4.33-inch pipe, which covered a period of about six weeks, a set of check runs was made. The results of the two calibrations practically coincide as shown by tests 1 and 8 on figure 14 and the same tests on figure 16.

TABLE II—FRICTION CALIBRATION FOR 4.33-INCH BRANCH PIPE

Run No.	Discharge Sec. ft.	Temp. °F	Temp. Corr. Per ft. of pipe	Plotted energy at Junction	Piezometer No. 16		17		18		19	
					Computed energy	Drop to Junction	Computed energy	Drop to Junction	Computed energy	Drop to Junction	Computed energy	Drop to Junction
1	1.7232	60.5	—.00020	2.372	—.001 1.498	.875	—.001 1.245	1.128	—.002 .627	1.747	—.002 .228	2.146
2	1.4542	60.2	—.00007	1.678	—.003 1.033	.648	—.005 .830	.853	—.007 .402	1.283	—.009 .083	1.604
3	1.2030	60.3	—.00007	1.479	—.003 1.038	.444	—.005 .892	.592	—.007 .605	.881	—.009 .387	1.101
4	.9529	59.8	+.00005	.761	.002 .469	.290	.003 .363	.395	.005 .179	.577	.006 .036	.719
5	.6570	59.5	+.00005	.710	.002 .565	.143	.003 .517	.190	.005 .423	.282	.006 .341	.363
6	.4425	59.4	0	.266	.193	.073	.173	.093	.125	.141	.082	.184
7	1.5729	57.5	+.00094	2.280	.004 1.548	.728	.006 1.302	.972	.009 .831	1.440	.012 .455	1.813
8	1.3254	57.0	+.00090	1.432	.004 .898	.530	.006 .718	.708	.008 .376	1.048	.011 .092	1.329
9	1.0721	57.1	+.00067	.991	.003 .625	.363	.004 .491	.496	.006 .271	.714	.008 .082	.901
10	.8067	57.2	+.00040	.615	.002 .402	.211	.003 .302	.310	.004 .187	.424	.005 .073	.537
11	.5504	57.5	+.00015	.477	.001 .369	.107	.001 .330	.146	.001 .266	.210	.002 .206	.269
12	1.8355	.....	.....	.....	.....	.....	.....	.....	.....	.....	.....	.....

14. Ten-inch Pipe Friction Calibration.—By a procedure similar to that in test 1, the 10-inch pipe was calibrated in test 2. The calibration was made with the pipe in place and no change was necessary except that a straight section was used to replace the junction during the calibration test. Regulation of head in the forebay was made by adjusting slide gates in the regulating box at the downstream end of the pipe, see figure 10. Water was always

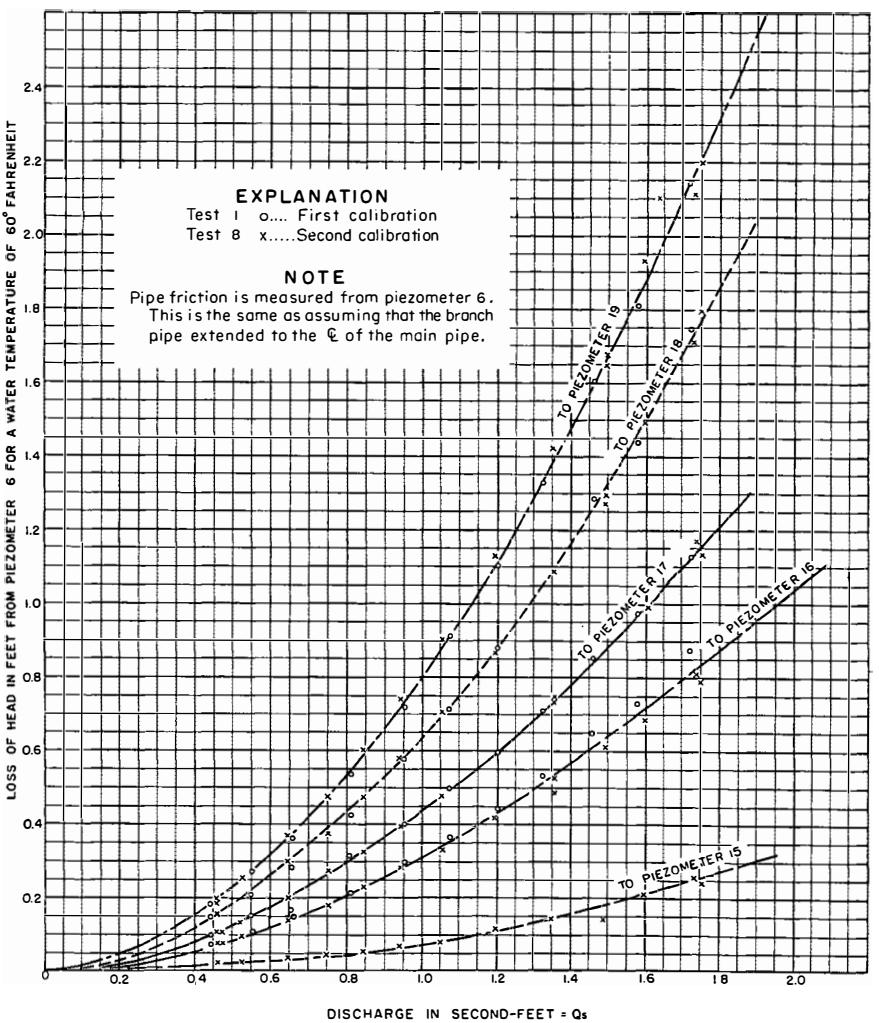

FIGURE 16—FRICTION CALIBRATION CURVES FOR 4.33-INCH BRANCH

allowed to spill over the top of the box to insure a constant head on the lower end of the pipe. The slide gates were used merely to dispose of excess flow during runs of higher discharge.

Friction slopes for the 10-inch pipe are shown for a few discharges on figure 17. Again tangents were drawn to the downstream ends of the curves and the slopes of the tangents were considered the average friction losses per foot of pipe. Temperature

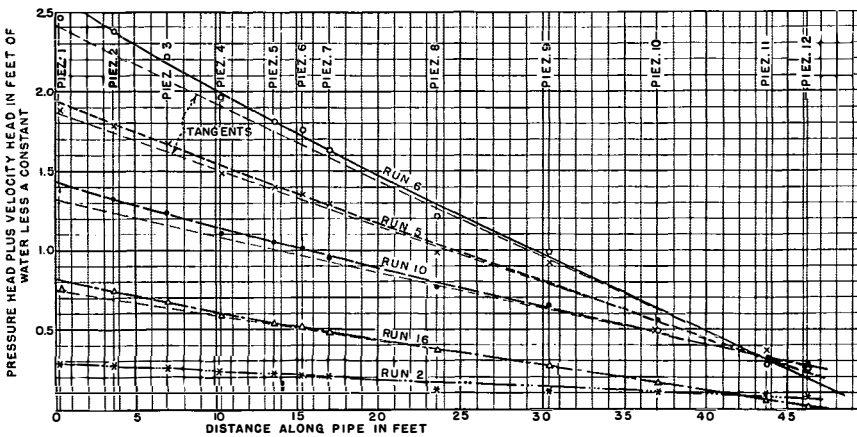

FIGURE 17—STRAIGHT PIPE FRICTION SLOPES FOR 10-INCH PIPE

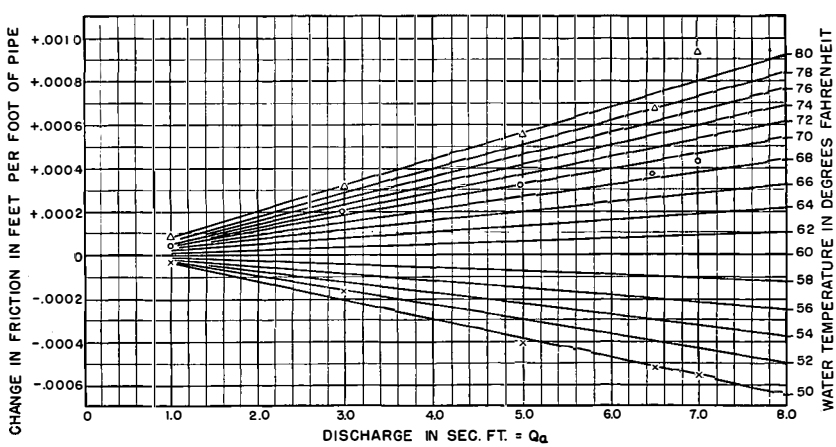

FIGURE 18—TEMPERATURE CORRECTION CURVES FOR 10-INCH PIPE

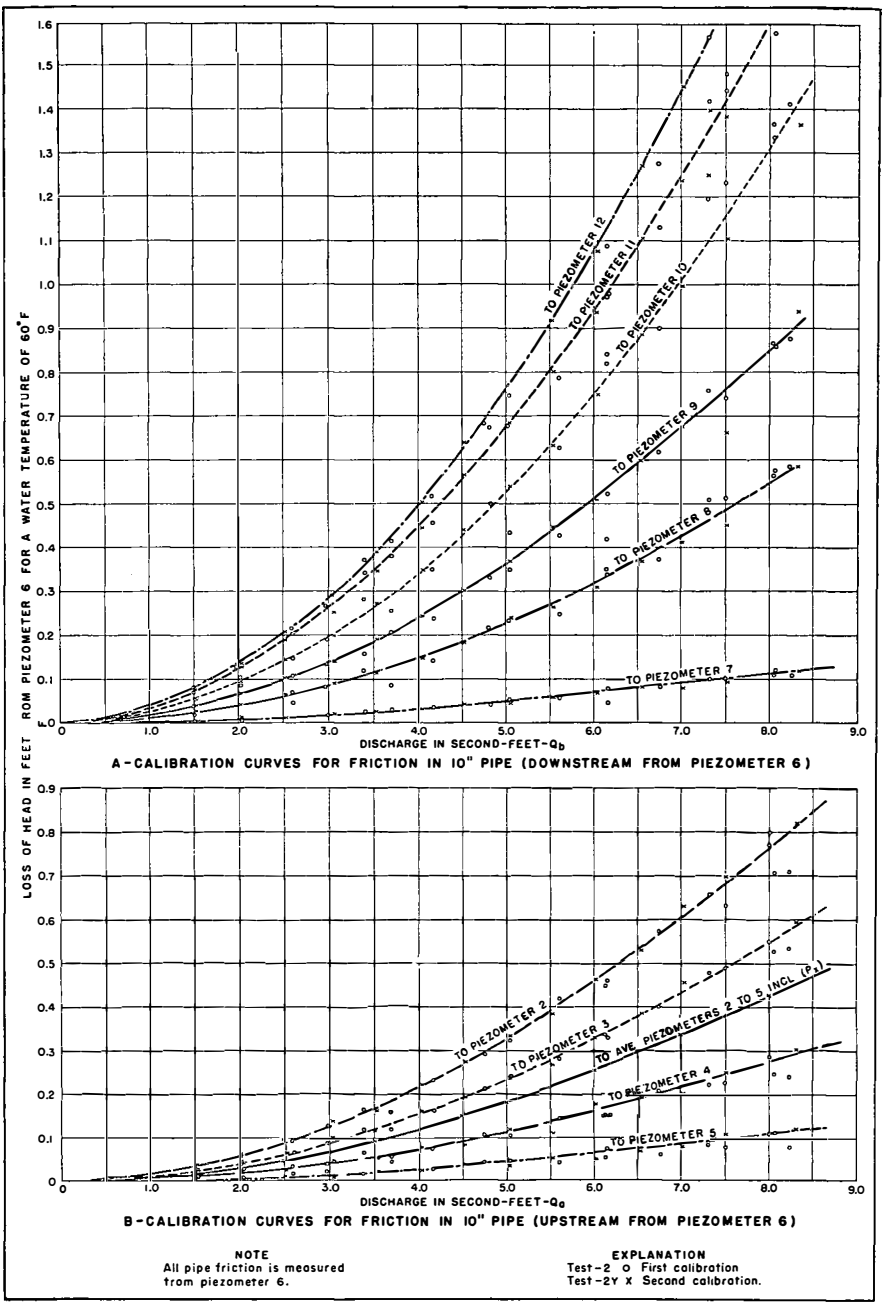

FIGURE 19—FRICTION CALIBRATION CURVES FOR 10-INCH PIPE

correction curves, used in evaluating results obtained on the 10-inch pipe, are shown on figure 18. Friction losses, measured upstream and downstream from piezometer 6, for several discharges at a temperature of 60 degrees Fahrenheit, are shown on figure 19. As in the case of the 4.33-inch pipe, piezometer 6, located at the theoretical junction, was used as a reference. Friction losses were measured upstream and downstream from this point. The friction factor, f, for the 10-inch pipe, is plotted on figure 14 with respect to Reynolds' number. A set of check runs under test 2-Y, made on the 10-inch pipe after the completion of test 2, showed a good agreement with the original set. Both sets of points are plotted on figures 14 and 19.

It is apparent from figure 14 that the 10-inch pipe had a greater surface roughness than the 4.33-inch branch for the same value of Reynolds' number, even though both were constructed in a similar manner and of the same material. Theoretically, one would expect the friction factor, f, to be smaller for the larger pipe. The explanation may lie in the fact that the 10-inch pipe had a joint to every 3.5 diameters, while the 4.33-inch pipe had a joint to about every 7.0 diameters.

15. Evaluation of Junction Losses. — After calibrating the straight pipes separately, they were connected together as shown on figure 10. Studies were then made to evaluate the loss of head in the junction. Runs were made using total discharges from 1.5 to 8.0 second-feet. By adjusting the 4-inch valve at the end of the branch in relation to the slide gates in the head-regulator box, it was possible to divert part of the total discharge through the branch. For large discharge ratios, Q_s/Q_a, total discharges were necessarily low, while for small discharge ratios, practically any total discharge could be used up to 8 second-feet. During a run, simultaneous readings were made at two-minute intervals on head gages in the large weir box, the forebay head gage, and the head gage for the 6-inch Cipolletti weir located at the end of the branch pipe. During the same period of time, each piezometer on the pipe was read four times.

For the purpose of the experiments, the junction loss is defined as the sum of the pressure drop and the drop in nominal velocity head, less the friction loss between points upstream and downstream from the junction, sufficiently remote to be free from effects caused by the junction. In determining the friction loss, pipe dis-

tances were measured to the center line of the intersection. The following equations express the above definition:

Junction loss chargeable to the main pipe:

$$J_b = P_x + V_a^2/2g - P_{10} + V_b^2/2g + h_{f(x\text{-}10)}$$

Junction loss chargeable to branch:

$$J_s = P_x + V_a^2/2g - P_{18} + V_s^2/2g + h_{f(x\text{-}18)}$$

Rather than choose a single piezometer from which to measure the pressure head above the junction, the average of piezometers 2, 3, 4, and 5, was used and is denoted as P_x. The location of P_x was approximately 7.0 feet, or 8.4 diameters, upstream from piezometer 6, shown in figure 10-A.

Energy losses determined in accordance with the above definition are subject to an error in the order of 0.05 $V^2/2g$, due to the use of the nominal velocity head instead of the velocity head integrated over the section, and due to the fact that friction losses were computed to the center of the intersection. Nevertheless, the definition seems a practical one. However, the error involved should be kept in mind in interpreting results.

Tests on the 105-degree junction were divided into two groups. In test 3 a pipe junction without modification was used, whereas in tests 4 to 7 inclusive, an attempt was made to improve the hydraulic efficiency by modifying the physical shape of the junction with filler blocks, the shapes of which were determined from the earlier visual tests.

Twenty-six runs were made on test 3, discharges through the branch ranging from 0 to 100 percent of the total. Computations for a typical run are shown in table 3. From the computed energy at P_x, the computed energy at each piezometer downstream from the junction was subtracted independently. This method tended to eliminate piezometer discrepancies. Differences in each case represent the pipe friction plus the junction loss. The pipe friction for each discharge in the main pipe, for a temperature of 60 degrees, was obtained from the curves on figure 19. The pipe friction for the branch was secured from figure 16. The temperature correction curves on figures 15 and 18 were used to correct the pipe friction for temperature. After subtracting the corrected pipe friction from the total loss, the remaining loss was charged to the junction. Junction losses in the main pipe were computed in terms of velocity head upstream from the junction. In the branch they

were computed in terms of velocity head upstream from the junction and also in terms of velocity head in the branch.

TABLE III—JUNCTION LOSS COMPUTATIONS

$Q_a = 1.9964$ $Q_s = 1.2033$ $Q_b = 0.7931$ $Q_s/Q_a = 0.6027$ Temp. 67.5°F

P_x Average of Piezometers 2-3-4 & 5 = 3.955
Average $V_a^2/2g$ at Piezometers 2-3-4 & 5 = 0.209
Energy at P_x = 4.164

	PIEZOMETER NO.									
	7	8	9	10	11	12	16	17	18	19
Ave. Piezometer Reading	4.064	4.070	4.066	4.060	4.049	4.041	1.241	1.051	.780	.519
Velocity Head	.033	.033	.033	.033	.033	.033	2.151	2.161	2.161	2.169
Pipe Friction Above Piez. 6	.029									
Temperature Correction	.001									
Corrected	.028	.028	.028	.028	.028	.028	.028	.028	.028	.028
Pipe Friction Below Piez.6	.001	.008	.012	.019	.021	.028	.434	.592	.880	1.112
Temperature Correction	0	0	0	0	.001	.001	.009	.012	.018	.023
Corrected	.001	.008	.012	.019	.020	.027	.425	.580	.862	1.089
Junction Loss	.038	.025	.025	.034	.034	.035	.319	.344	.334	.359
$J_b/V_a^2/2g$	.182	.120	.120	.163	.163	.167	1.526	1.646	1.598	1.718
$J_s/V_s^2/2g$							0.148	0.159	0.155	0.166

Average $V_s^2/2g = 2.161$

Results of junction loss determinations, chargeable to the main pipe, were plotted with respect to discharge ratios, and are shown for test 3 on figure 20. In figure 20-B, the discharge ratio is shown in relation to junction losses obtained from each of the individual downstream piezometers. Separate piezometer curves are in close agreement with the exception of piezometers 7 and 12, which, in most cases, were disregarded when drawing average curves, due to their undesirable locations. The curve for test 3 on figure 20-A was obtained from the average of the individual piezometer curves on figure 20-B.

Average results of junction loss determinations, chargeable to the branch, were plotted with respect to discharge ratios, and

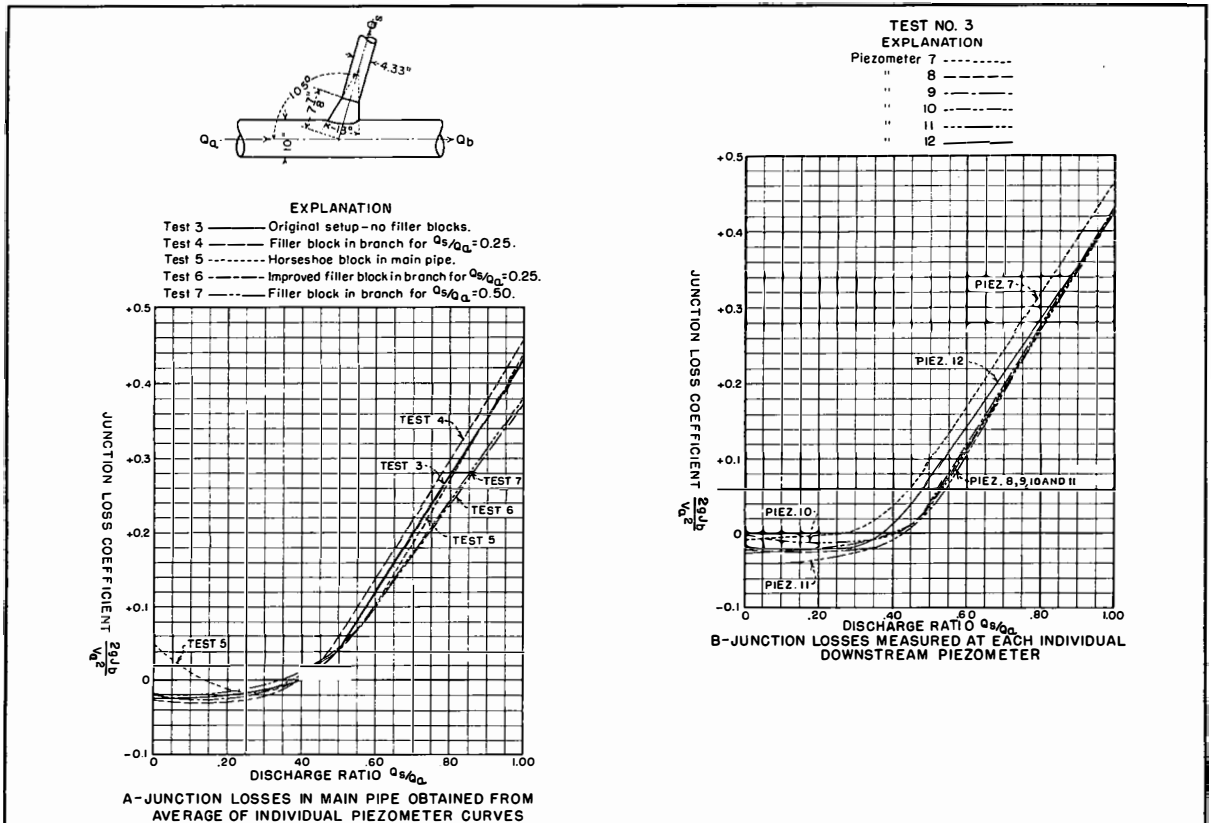

FIGURE 20—JUNCTION LOSSES IN MAIN PENSTOCK

are shown on figure 21. In figure 21-A, junction losses are in terms of velocity head in the branch. In figure 21-B they are in terms of velocity head in the main pipe upstream from the junction. Separate piezometer curves for the branch are in good agreement. The straight pipe friction charged to the branch was computed on the assumption that the branch pipe extended in to the center line of the main pipe. The reason for this assumption becomes apparent when an attempt is made to design a junction in a large pipe-line from experimental data.

For $Q_s/Q_a = 0$, all flow occurred in the main pipe, and within the limits of experimental error, the intersection of the branch with the header caused no loss, although the diameter of opening was more than half that of the main pipe. The results in figure 20 verify experiments made by Professor D. Thoma[2] on small brass pipe in that an apparent gain of head was recorded in the main pipe downstream from the junction for discharge ratios of less than 0.40. This gain in head was partly due to the manner in which the loss coefficients were determined and partly due to the pressure reaction from the water diverted into the branch. It is, of course, not a gain in energy.

It is possible to compute, within reasonable limits, the junction loss chargeable to the branch by assuming that the entrance to the branch is an ordinary, sharp-edged, conical pipe entrance. Hydraulic textbooks state that the entrance loss for a cone of this angle and type, when connected to a still reservoir, should be approximately $0.15\ V_s^2/2g$. As this entrance does not connect to a still reservoir, but to a pipe in which varying conditions of flow exist, there is an additional loss to be added, which, for the lower ratios of Q_s/Q_a, is approximately $0.4\ V_a^2/2g$. This value is not a constant for all conditions of flow, but its presence becomes negligible as the ratio of Q_s/Q_a increases. The total junction loss, computed in this manner, would be:

$$J_s = 0.15\ V_s^2/2g + 0.4\ V_a^2/2g \qquad (1)$$

---

[2]Thoma, Prof. D., Hydraulic Losses in Pipe Fittings, Transactions of the Tokyo Sectional Meeting, World Power Conference, Tokyo, 1929. For a more detailed description of these experiments see "Losses in Oblique Angled Pipe Branches" by Franz Peterman, Mitteilungen des Hydraulischen Instituts der Technischen Hochschule München, Bulletin 1, p. 75; and Bulletin 2, p. 61. These articles have been translated in the "Transactions of the Munich Hydraulic Institute" and published by the American Society of Mechanical Engineers as Bulletin No. 3.

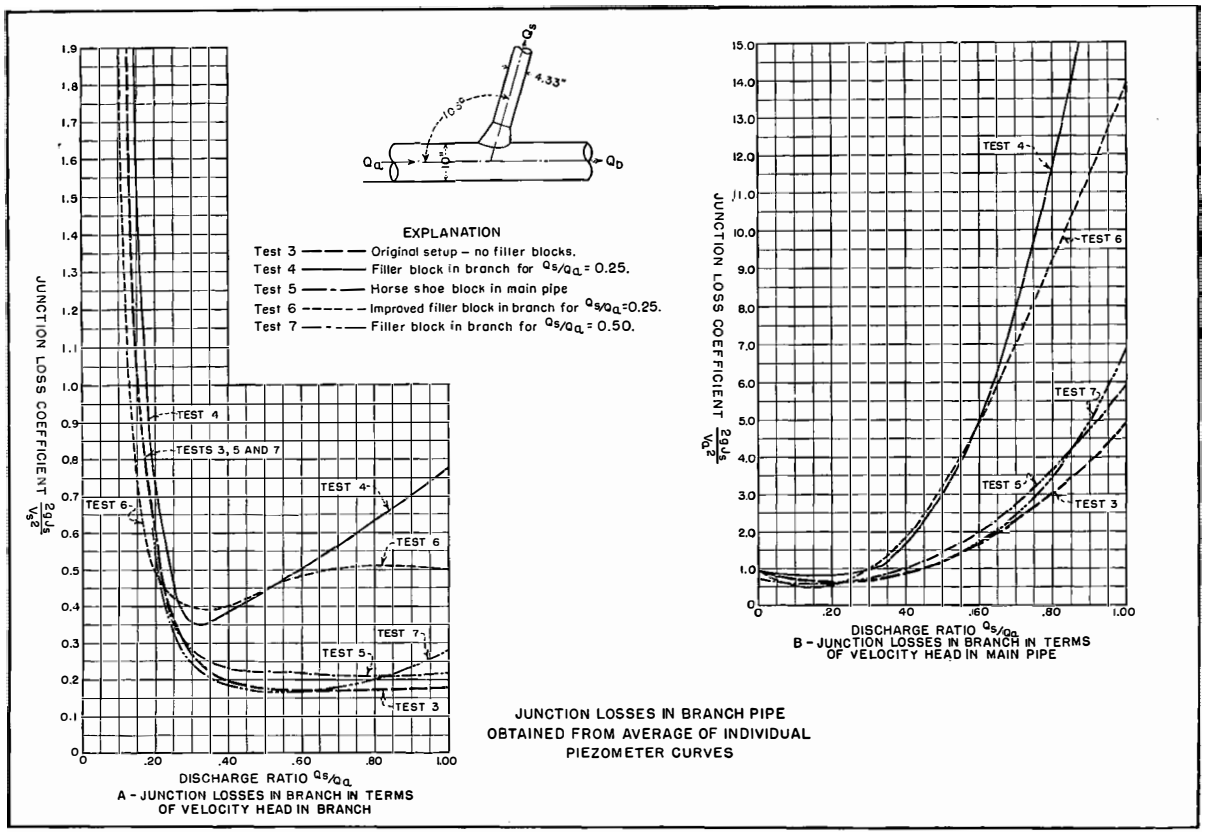

FIGURE 21—JUNCTION LOSSES IN BRANCH PENSTOCK

Expressing the entire loss in terms of velocity head in the branch, the procedure is as follows:

$$\frac{V_s^2}{V_a^2} = \frac{\left(\frac{Q_s}{A_s}\right)^2}{\left(\frac{Q_a}{A_a}\right)^2} = \frac{(Q_s A_a)^2}{(Q_a A_s)^2}$$

$$\frac{V_a^2}{2g} = \frac{V_s^2}{2g} = \frac{(Q_a A_s)^2}{(Q_s A_a)^2}$$

Substituting this value in equation 1 the junction loss coefficient

$$\frac{J_s}{V_s^2/2g} = 0.15 + 0.4\,\frac{Q_a^2 A_s^2}{Q_s A_a} \qquad (2)$$

By substituting various values of Q_a/Q_s in equation 2, a curve agreeing closely with the one for test 3 on figure 21-A is obtained. The value of A_s/A_a is equal to 0.1875 in this case.

Although comparative data are meager, the following instance is of interest. In the visual tests on the pyralin model, it was established that the volume of the eddy zone in the branch was independent of the discharge, varying only with the discharge ratio, Q_s/Q_a. Gustav Vogel, associated with Professor Thoma, makes the following statement from his experience:[3] *"The tests showed that for the same type of tee, the junction loss coefficient depends only upon the branch relation Q_s/Q_a (velocity relation V_s/V_a) and not upon the absolute value of the water quantities (velocities)."*

Variations in loss coefficients for different values of Reynolds' number are plotted on figure 22. The curves on figure 22-A show that the junction loss in the branch varies only with the discharge ratio, Q_s/Q_a, and not with the total discharge or Reynolds' number. The curves on figure 22-B show a similar indication for the junction losses in the main pipe; but the points are somewhat scattered due to the exaggerated scale of the graph. These results agree with the visual tests made with the transparent pipe and also with the quantitative tests performed on small brass pipe by Professor Thoma.

16. Reduction of Junction Losses.—Tests 4 to 7 inclusive were

[3]Vogel, Gustav, Dip. Engr., Experiments to Determine the Loss in Right Angle Pipe Tees, A Translation from German, U.S.B.R. Technical Memorandum 299, p. 12. (Unpublished)

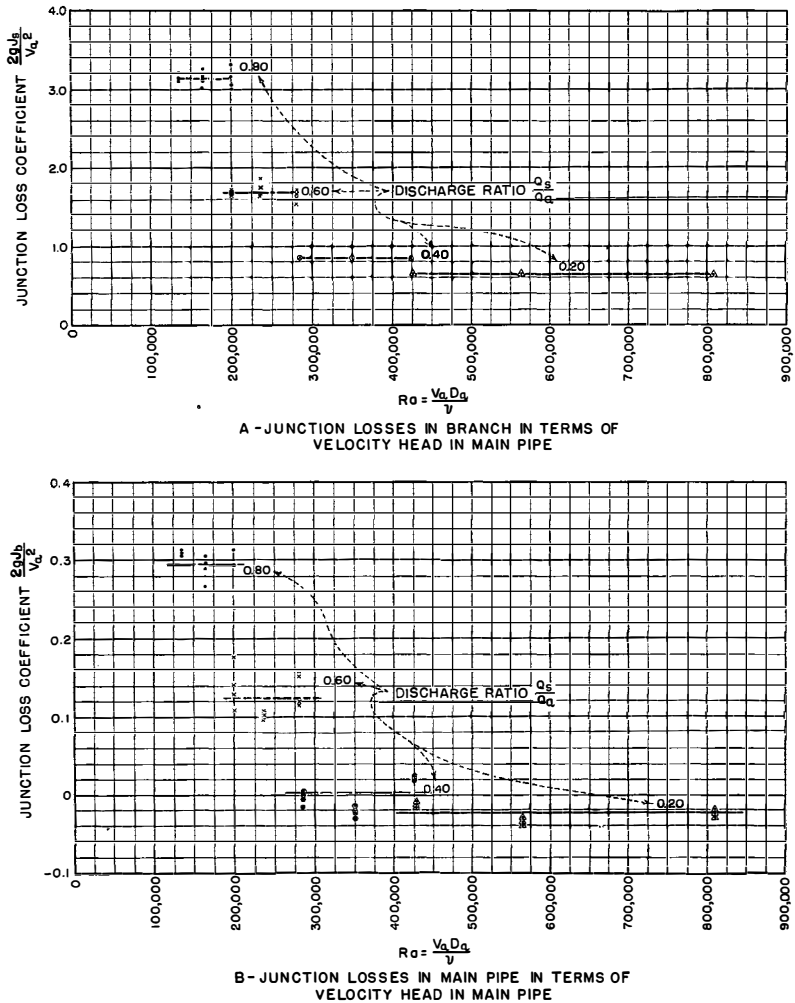

FIGURE 22—VARIATION OF JUNCTION LOSS COEFFICIENT WITH THE DISCHARGE RATIO

made in an effort to reduce junction losses at discharge ratios of 0.25 and 0.50. In test 5, a deflecting block was installed in the main pipe. In tests 4, 6, and 7, wooden filler blocks, made to the same sizes and shapes as the eddy zones in the pyralin model, were installed in the branch pipe immediately below the junction.

The deflecting block used in test 5 is shown in figure 11-E. Its position in the main pipe is shown in figure 11-F. The block was similar to the lip used in the preliminary tests on the pyralin model. Results from the six runs made in this test are plotted on figures 20-A, 21-A, and 21-B. This block produced no improvement in the junction loss coefficients in either the branch or the main pipe, nor did it appear to produce any detrimental effects for the lower discharge ratios.

The filler block shown in figure 11-D was designed from the curves on figure 8, for a discharge ratio of 0.25, and was installed in the branch pipe in the location shown on figure 11-F. Results plotted on figures 20-A, 21-A, and 21-B, for test 4, reveal that this block failed to reduce the junction loss coefficient; but instead, increased it, compared with test 3, for all discharge ratios.

Another attempt was made in test 6 to improve conditions at the junction by using a filler block for a discharge ratio of 0.25. Special care was exercised to obtain the same shape for this block as in the pyralin model shown in figure 9-D. The block was somewhat smaller and more accurate than the one used in test 4 and better results were obtained. The curves on figure 21 show a small improvement over test 3 for discharge ratios below 0.22. Due to the restriction of area that these blocks caused in the branch, junction losses chargeable to the branch were expected to increase for discharge ratios above that for which the blocks were designed.

The filler block shown in figure 9-C, for a discharge ratio of 0.50 was used in test 7. When compared with the results from test 3, shown in figure 21, little change in the junction loss coefficient is noticeable up to a discharge ratio of 0.60. In fact, this block shows a slight improvement in the coefficient, when compared with test 3, for discharge ratios of less than 0.60. Above this ratio, junction losses increase in the branch compared to the results shown in figure 21; while losses show a decrease in the main pipe, compared to the results shown in figure 20-A, for discharge ratios above 0.50.

From these tests it was concluded that the filler blocks actually did decrease the junction loss coefficients in the majority of cases for discharge ratios under that for which they were de-

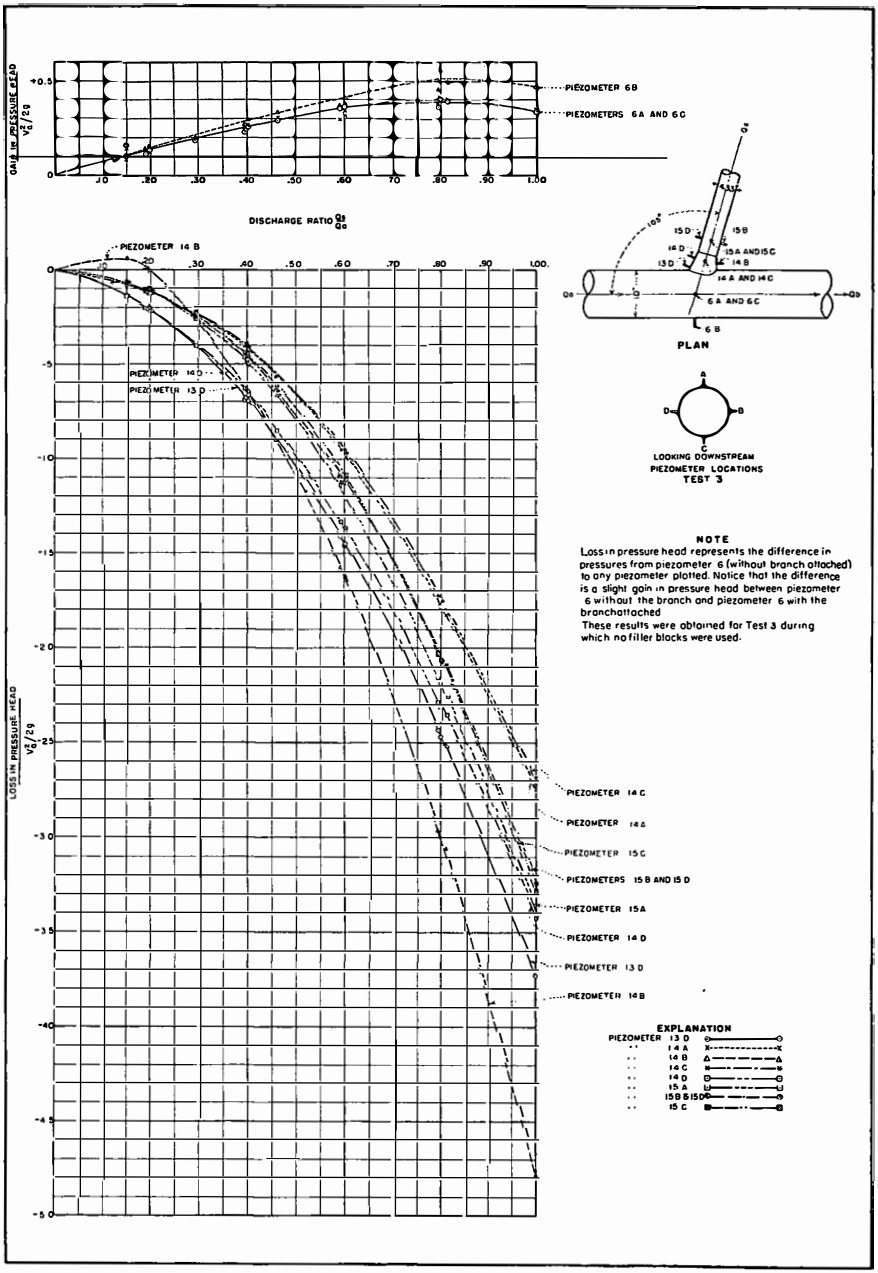

FIGURE 23—PRESSURES AT 105-DEGREE JUNCTION

signed. It was expected that the junction losses would increase for values greater than the designed ratio. The improvement, contrary to expectations, was so small that the benefit derived from filler blocks of this type would hardly be worth the expense of installation. It is possible, however, that for penstock installations where discharge ratios for the branches remain nearly constant and power head at the turbines is at a premium, filler blocks may prove to be of some value. These, however, would not be a practical installation at Boulder Dam.

17. Static Pressures at 105-Degree Junction.—In the design of thin-walled pipes, maximum and minimum pressures developed at junctions are important. To determine more in detail these pressure conditions, additional piezometers were installed in the model of the junction. Piezometer 13-D and piezometer rings 14 and 15 were placed as shown in figures 10 and 23, in the section of the branch immediately downstream from its intersection with the main pipe. During test 3, these pressures were read simultaneously with the other piezometers. Pressures at three of the piezometers of ring 6 were also read; the fourth was eliminated by the installation of the branch pipe.

The pressure at each of these points was compared with the average pressure condition at piezometer ring 6, measured during previous runs without the branch installed. The drop in pressure between each piezometer and piezometer ring 6, measured before the branch was installed, expressed in terms of the velocity head in the main pipe upstream from the junction, is shown on figure 23. As it is possible to calculate the pressure at any point in a straight pipe, a condition which is not true after a junction is installed, the pressure obtained at ring 6, without the branch, was used as the reference pressure in these experiments.

A slight increase in pressure was found at piezometers 6-A, 6-B, and 6-C, due to the introduction of the junction. For discharge ratios up to 0.20, a decided increase was indicated by piezometer 14-B; but for ratios above this value, the pressure diminished rapidly. For lower ratios, the gain in pressure indicated by this piezometer was probably caused by impact; while for the larger ratios, the loss in pressure may be attributed to turbulence and complicated eddy formations.

As an aid in visualizing the pressure distribution in a junction of this type, diagrams of the actual observed pressure intensities

at piezometer rings 14 and 15 are shown on figure 24 for several runs of test 3. Pressures were measured in feet of water above the center of the pipe and are plotted both vertically and horizontally, using the intersection of the two axes as the origin. The circumferential pressure at piezometer ring 15 was quite uniform in each case. Pressures recorded at ring 14, however, varied greatly with discharge conditions. Considerable variation can be noted in the pressure distribution for the extreme cases where $Q_s/Q_a = 0.151$, and 1.00.

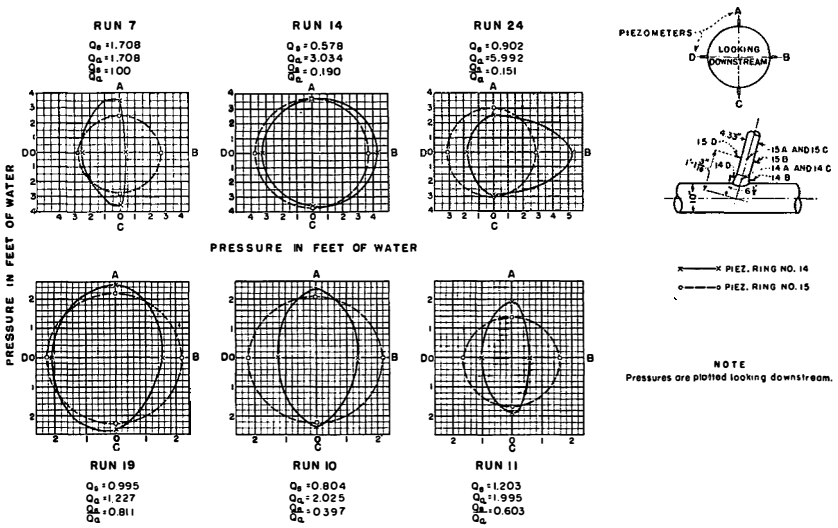

FIGURE 24—PRESSURE DISTRIBUTION AT 105-DEGREE JUNCTION

18. **Tests on a Right-Angle Junction.** — As previously mentioned, experiments of a similar nature have been performed by Professor Thoma and his associates at Munich, Germany. Translations of their work have been used quite extensively for reference in the design of pipe junctions. This was the case in the early designs for the Boulder Dam penstocks. There was some question at that time as to the validity of applying Professor Thoma's data to such extremely large penstocks, particularly in view of the fact that his experiments were performed on relatively small brass pipes.

To make a definite check on Professor Thoma's experiments, two tests were made for the determination of junction losses, using

a 3.49-inch branch pipe connected to the 10-inch main pipe at an angle of 90 degrees as shown on figure 25. In test 10, the branch was connected directly to the main pipe; while in test 11, the branch was joined to the main pipe by a cone having a total central angle of 13 degrees and a length of 2.1 D_s. The ratio of the diameters, D_s/D_n, of 0.35 and the proportions of the cone were directly comparable with two of Professor Thoma's experiments.[4]

The 3.49-inch branch, with an extra section of pipe upstream, was first connected to the forebay bulkhead and calibrated by the procedure previously used to calibrate the 4.33-inch branch. The friction factor curve obtained from this calibration was plotted with respect to Reynolds' number as test 9 on figure 14. This curve falls below the curve for the 10-inch pipe which tends to substantiate the previous explanation that the smaller pipes were subject to lower friction factors because they contained fewer joints per diameter than the larger pipes. Calibration curves representing the pipe friction from piezometer ring 6X to any piezometer in the branch, for various discharges at a temperature of 60 degrees Fahrenheit, are shown on figure 26. Temperature correction curves used in converting pipe friction losses in the 3.49-inch branch to a constant temperature are shown on figure 27.

Calibrations of the 10-inch pipe, before and after tests on the 90-degree branch, are indicated as tests 2Y and 2Z on figure 14. Little change in friction was evidenced in the 10-inch pipe throughout the entire set of experiments. Calibration curves representing pipe friction from piezometer 6X to any piezometer in the main pipe, for different discharges at a temperature of 60 degrees Fahrenheit, are shown on figure 28.

The procedure for determining junction losses in tests 10 and 11 was the same as in test 3, except that an additional piezometer ring, 6X, was used as the reference point. P_x in tests 10 and 11 represented the average readings of piezometers 2, 3, 5, and 6 rather than piezometers 2, 3, 4, and 5. Piezometers on ring 4 had been damaged and readings from it were no longer included in the average.

The results of test 10, without the cone, and test 11, with the cone, are plotted in three forms on figures 29 and 30. Figure 29 shows junction losses measured in the branch, expressed in terms

[4]Vogel, Gustav, Losses in Right Angle Pipe Tees, Mitterlungen des Hydraulischen Instituts der Technischen Hochschule, Part 1—1926.

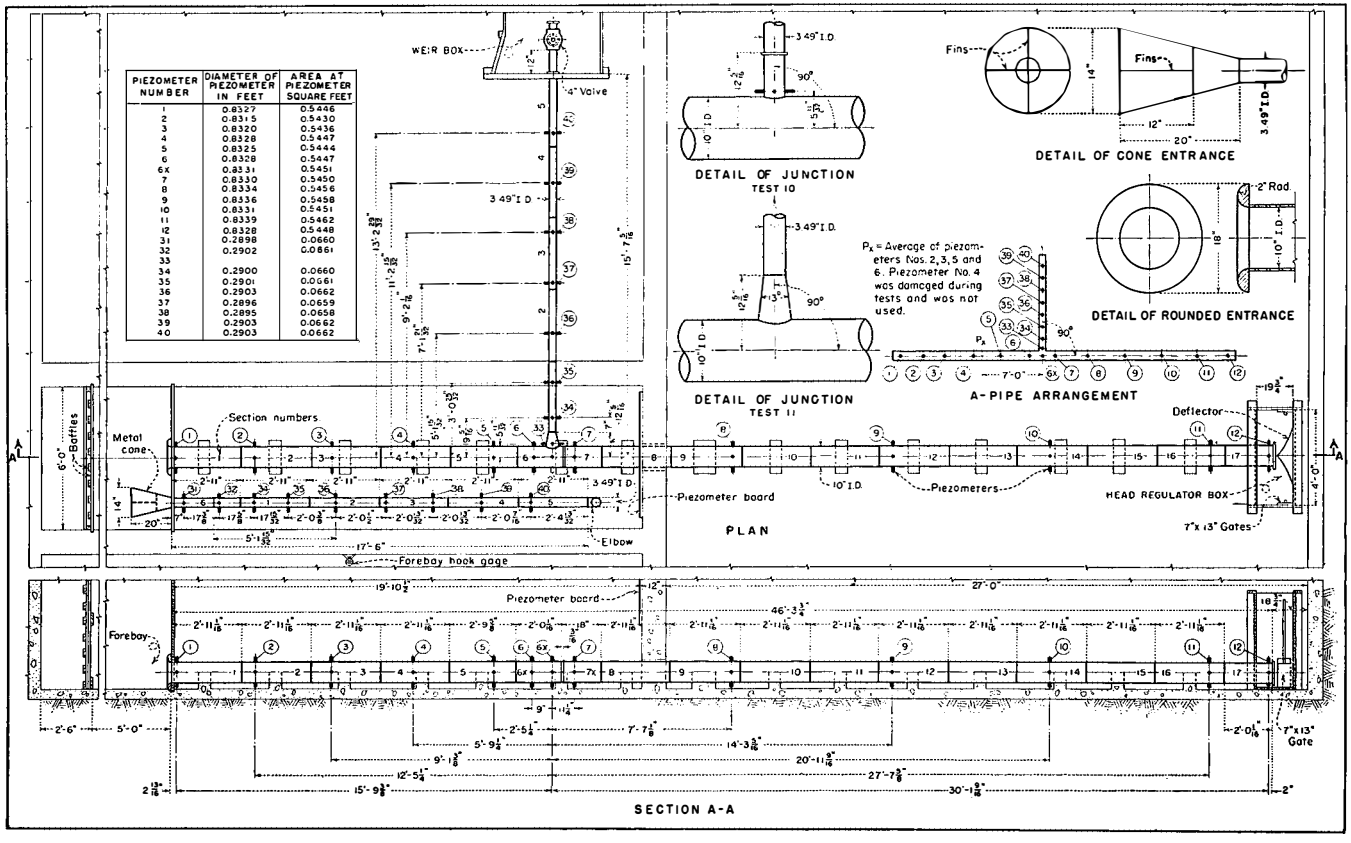

FIGURE 25—LABORATORY ASSEMBLY OF MODEL, 3.49-INCH 90-DEGREE BRANCH

of velocity head in the main pipe upstream from the junction. Figure 30-A shows the same losses in terms of velocity head in the branch. Junction losses measured in the main pipe, expressed in terms of velocity head in the main pipe upstream from the junction, are shown on figure 30-B.

Professor Thoma's junction loss coefficients for an exactly similar layout in which he used a 43-millimeter smooth brass pipe

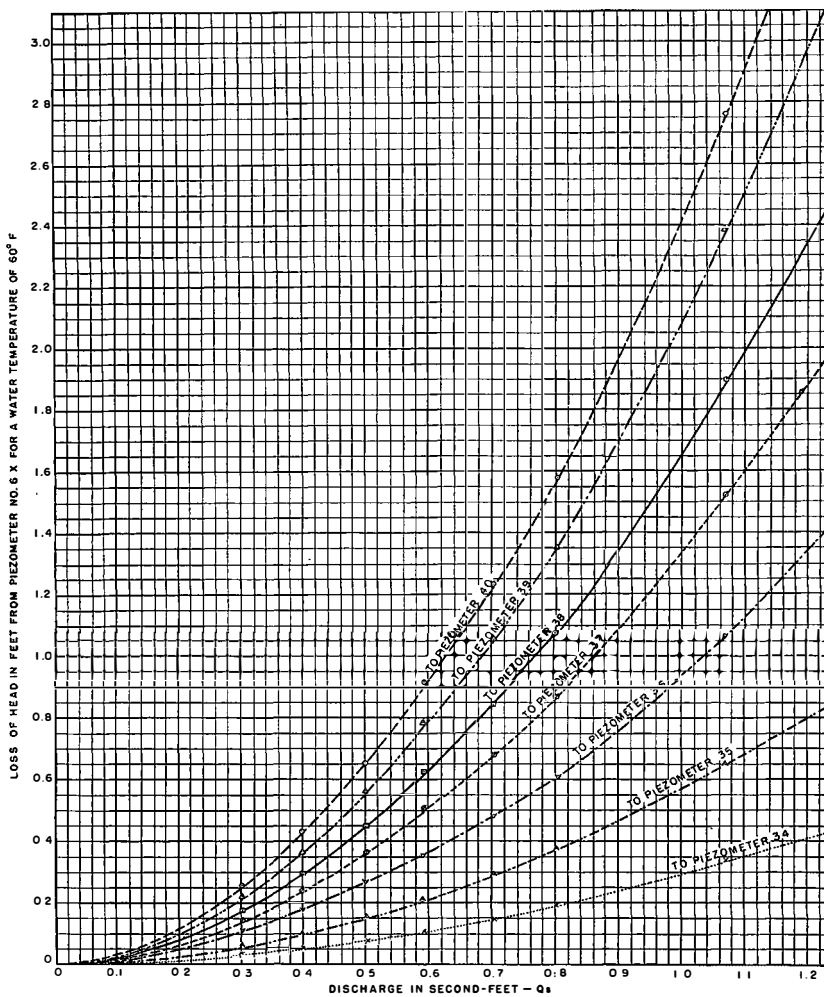

FIGURE 26—FRICTION CALIBRATION CURVES FOR 3.49-INCH BRANCH

with a 90-degree 15-millimeter branch, with and without cone, are plotted on figure 29. These coefficients on small pipes are considerably higher than those obtained by the Bureau of Reclamation on larger pipes, which would indicate that viscous effects, in small junctions as well as in small pipes, are appreciable. It is believed that the surface roughness in the two pipes was very nearly to scale. If this is true, the results indicate that experimental data on small junctions for small values of Reynolds' number are not particularly applicable for computing losses in large penstocks where large values of Reynolds' number are involved. Professor Thoma's work dealt with Reynolds' numbers up to 100,000, while the Boulder Dam penstocks involve Reynolds' numbers as large as 90,000,000. Considerable recent data are available which indicate that losses tend to decrease with the use of larger models, in spite of the fact that little change in the loss coefficient is observed for varying velocities in a model of given size. If junction losses in large smooth penstocks, such as those at Boulder Dam, were computed on the basis of Professor Thoma's experiments, the existing losses would undoubtedly be less than those computed.

Professor Thoma's junction loss coefficient curve for the cone installed is unquestionably in error as a few rough computations will show. The addition of the cone should produce a very notice-

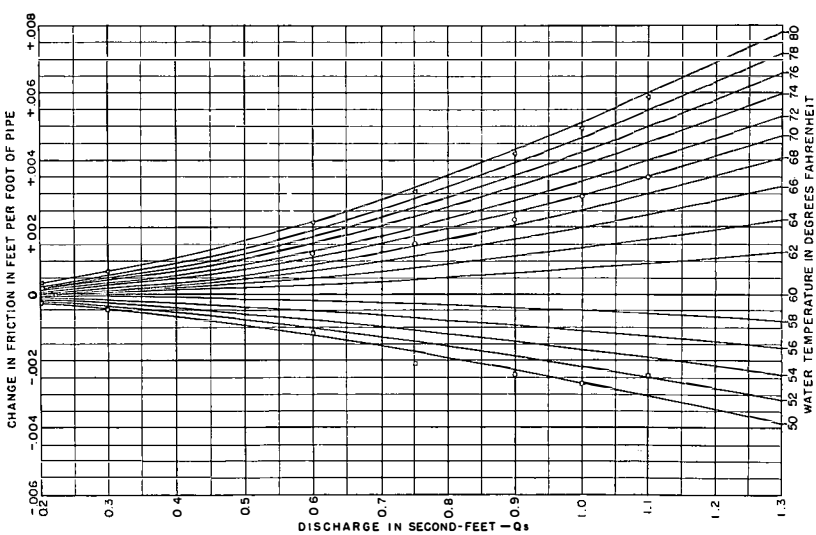

FIGURE 27—TEMPERATURE CORRECTION CURVES FOR 3.49-INCH BRANCH

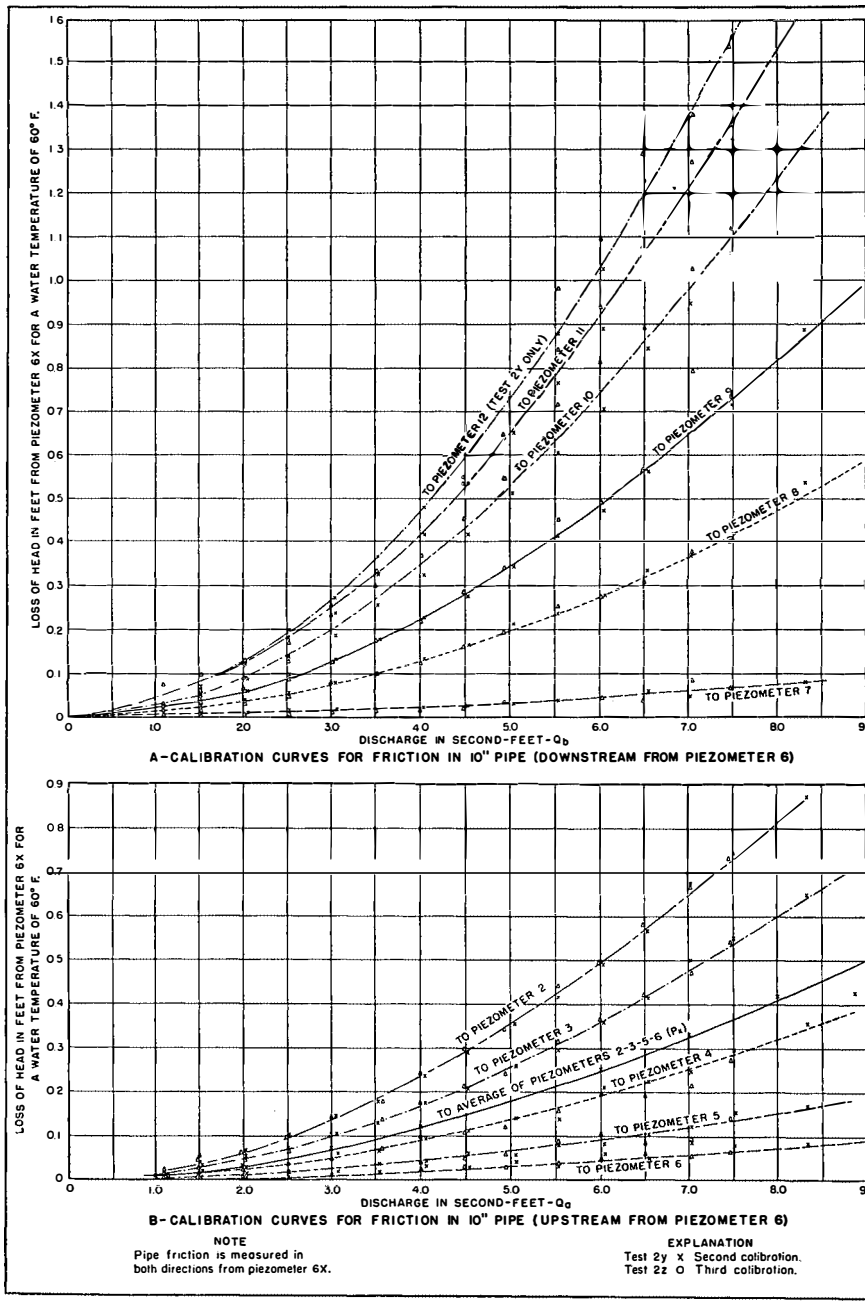

FIGURE 28—FRICTION CALIBRATION CURVES FOR 10-INCH PIPE

able improvement in entrance conditions at the branch. The Bureau's experiments show that the addition of a cone reduced the junction loss coefficient to approximately one-third of its original value. As a matter of interest, it is possible to compute junction losses for the layouts in tests 10 and 11, with a limited degree of accuracy, by a method similar to that used previously for test 3.

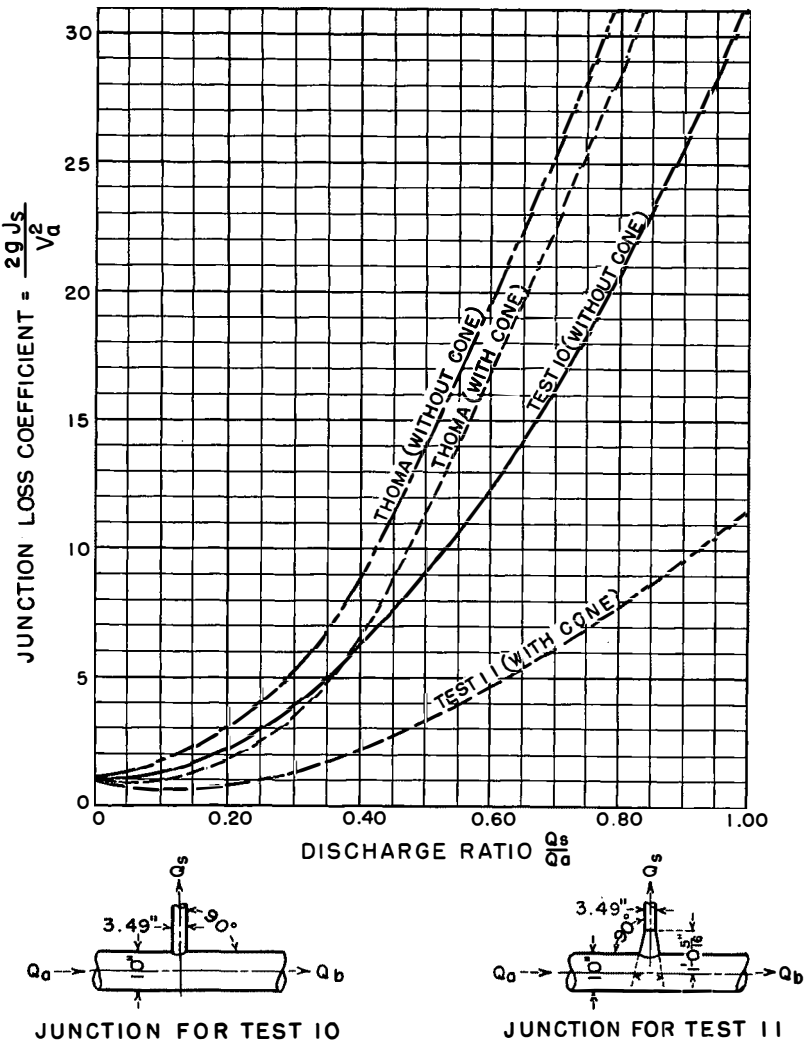

FIGURE 29—JUNCTION LOSSES IN BRANCH IN TERMS OF VELOCITY HEAD IN MAIN PIPE ABOVE JUNCTION

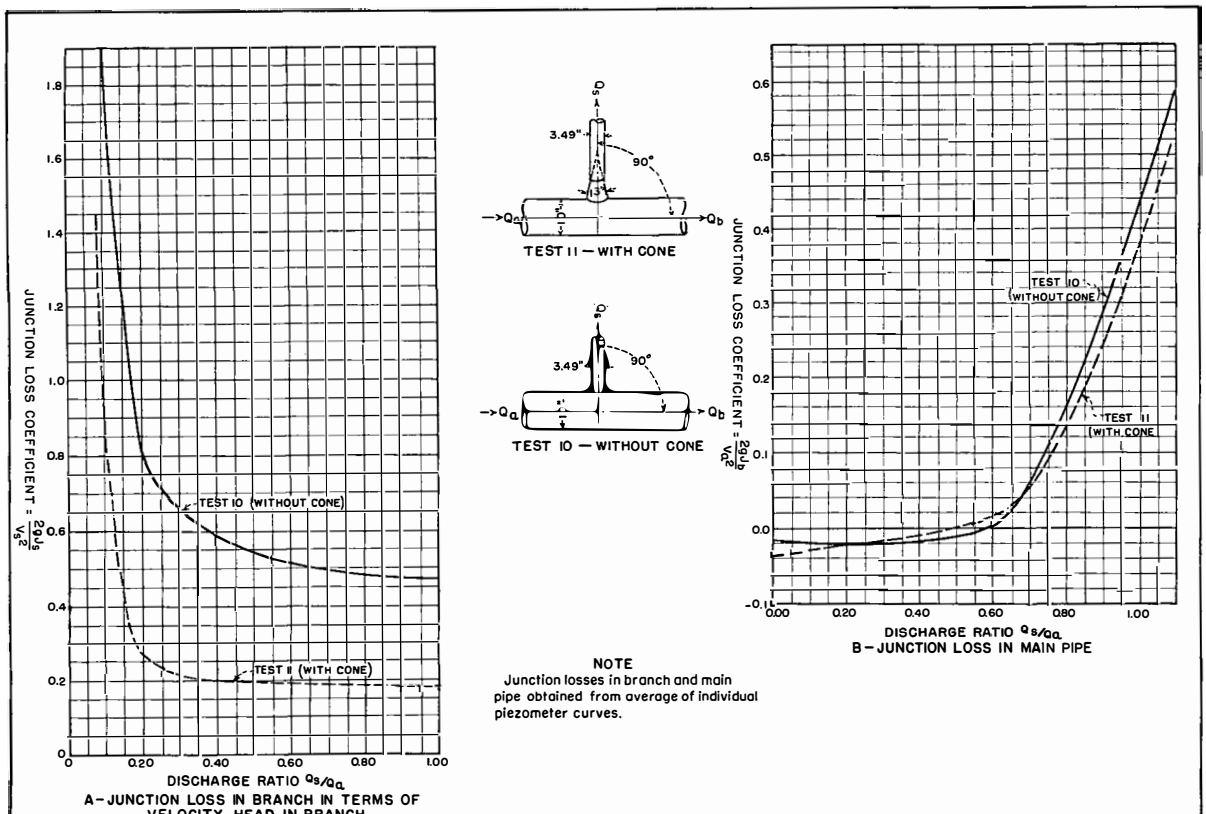

FIGURE 30—JUNCTION LOSSES IN BRANCH AND MAIN PIPE

The layout in test 10, without the cone, will be considered first. For an ordinary sharp-edged pipe entrance leading from a quiet reservoir, handbooks show the entrance loss to be approximately $0.5\ V_s^2/2g$. In the case of a junction, various conditions of flow exist at the entrance to the branch and an additional loss, of approximately $0.8\ V_a^2/2g$, should be combined with the entrance loss. The total junction loss for the branch is:

$$J_s = 0.5\ V_s^2/2g + 0.8\ V_a^2/2g.$$

The second term is a variable but is approximately correct for the lower values of Q_s/Q_a where it is effective. For the larger values of Q_s/Q_a this term is neglible compared to the first. Expressing the equation in a more practical form, the junction loss coefficient for the branch is:

$$\frac{J_s}{V_s^2/2g} = 0.50 + 0.8\left(\frac{Q_a A_s}{Q_s A_a}\right)^2 \quad \text{where} \quad \frac{A_s}{A_a} = 0.1216.$$

Upon substituting values of Q_a/Q_s in the above equation a curve is obtained which approximates the one for test 10 on figure 30-A.

The junction loss for test 11, with the cone, may be estimated in the same manner by substituting the proper coefficients in the equation. Comparing the entrances to the branch in the two tests with cones, one would expect the entrance for test 3 to be slightly superior to that of test 11. It therefore seems logical to substitute the following coefficients in the formula:

$$J_s = 0.2\ V_s^2/2g + 0.5\ V_a^2/2g.$$

Expressing this in the alternate form, the junction loss coefficient becomes:

$$\frac{J_s}{V_s^2/2g} = 0.20 + 0.5\left(\frac{Q_a A_s}{Q_s A_a}\right)^2$$

The curve obtained by substituting values of Q_a/Q_s in this equation closely approximates the curve for test 11 on figure 30-A.

19. Static Pressures at a Right-Angle Junction.—Piezometer rings 33 and 34 were installed in the branch near the junction, as shown on figure 25, for the purpose of studying pressures in the junction zone. These were read with the other piezometers during tests 10 and 11. The drop in pressure between each of the piezometers and the piezometers at the theoretical junction, without the branch, is plotted on figures 31 and 32, respectively. These differences in pressure, expressed in terms of velocity head in the

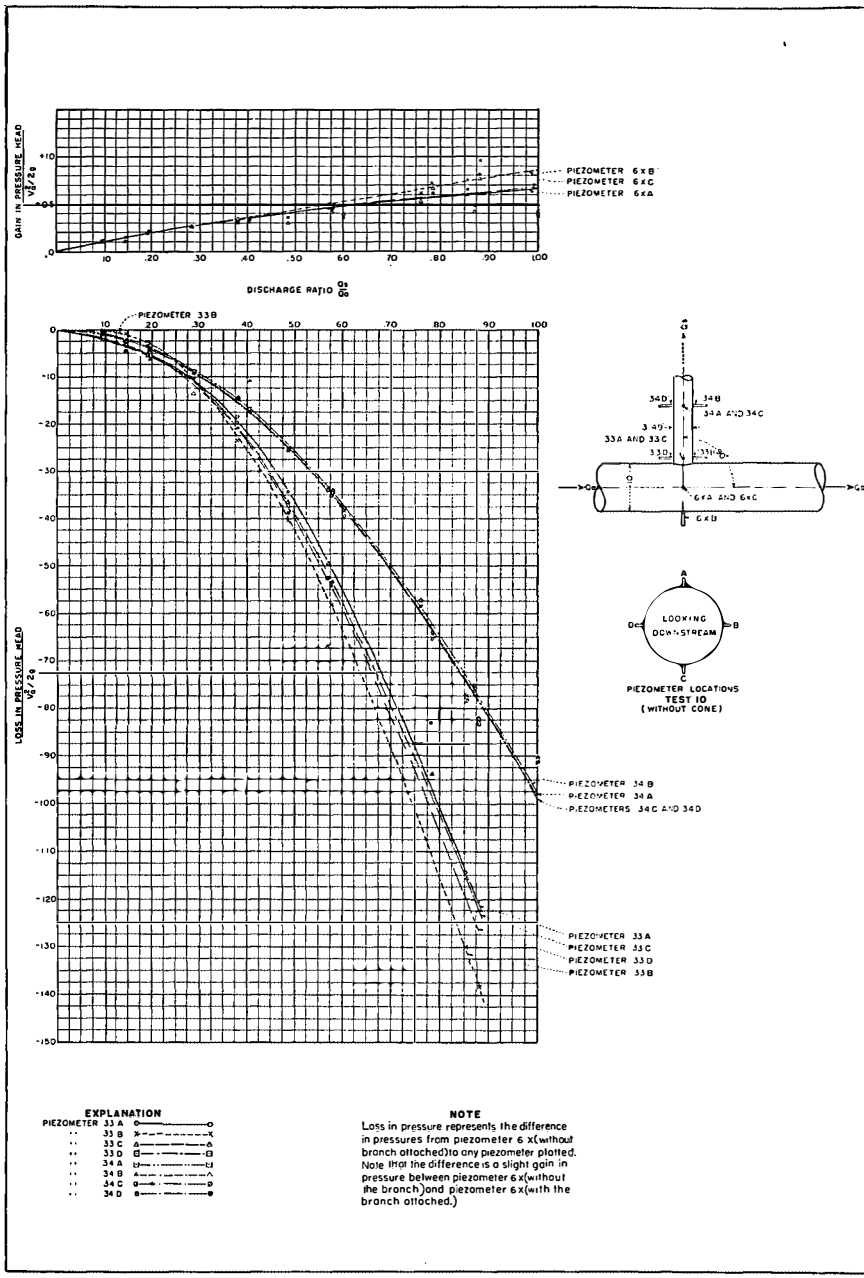

FIGURE 31—PRESSURES AT 90-DEGREE JUNCTION, TEST 10

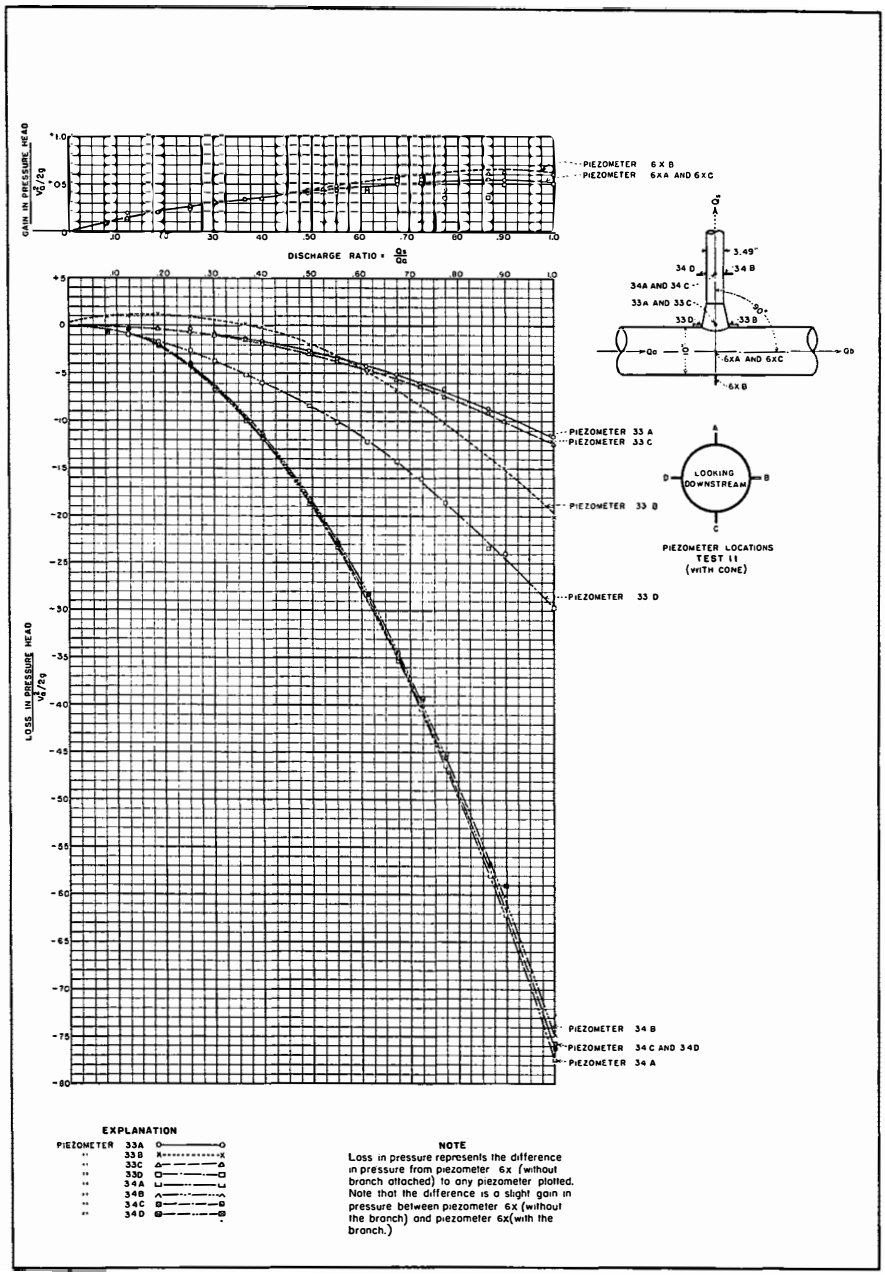

FIGURE 32—PRESSURES AT 90-DEGREE JUNCTION, TEST 11

main pipe above the junction, are plotted with respect to the discharge ratio. In both tests 10 and 11, piezometers 6XA, 6XB, and 6XC, show pressures above the average obtained at ring 6X without the branch attached. Higher pressures were developed in the main pipe for test 10 than for test 11. The curve for piezometer 33-B in figure 31 is similar to the curve for piezometer 14-B in figure 23; but no increase in pressure was developed in the right-angle junction without the cone. The curve for piezometer 33B in figure 32 shows the effect on the pressure at this point produced by the addition of the cone. An increase in pressure was recorded at piezometer 33-B for discharge ratios below 0.40. Small drops in pressure were observed for ratios above this value.

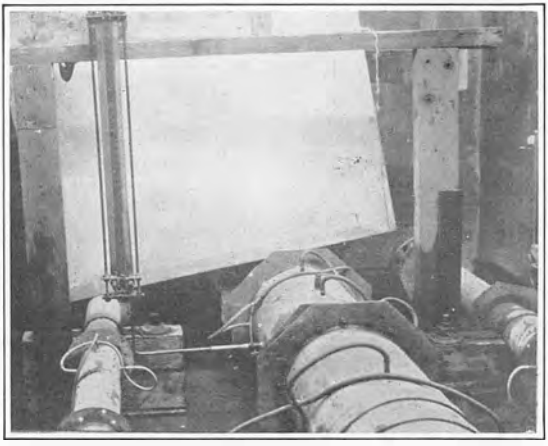

FIGURE 33—PITOT TUBE APPARATUS FOR MEASURING VELOCITIES

20. Velocity Distribution in Main Pipe.—At the conclusion of the experiments on the quantitative model of the pipe junction, measurements of velocity distribution in the 10-inch pipe were made with the branch removed. A pitot tube, shown in figure 33, was mounted near piezometer 6, or approximately 18 diameters downstream from the pipe entrance. Traverses were made in both horizontal and vertical planes passing through the center line of the pipe. Five pitot-tube readings were taken at each point shown in figure 34-A. Actual velocities measured at the several points are plotted in figure 34 for six discharges. Isotachs, representing

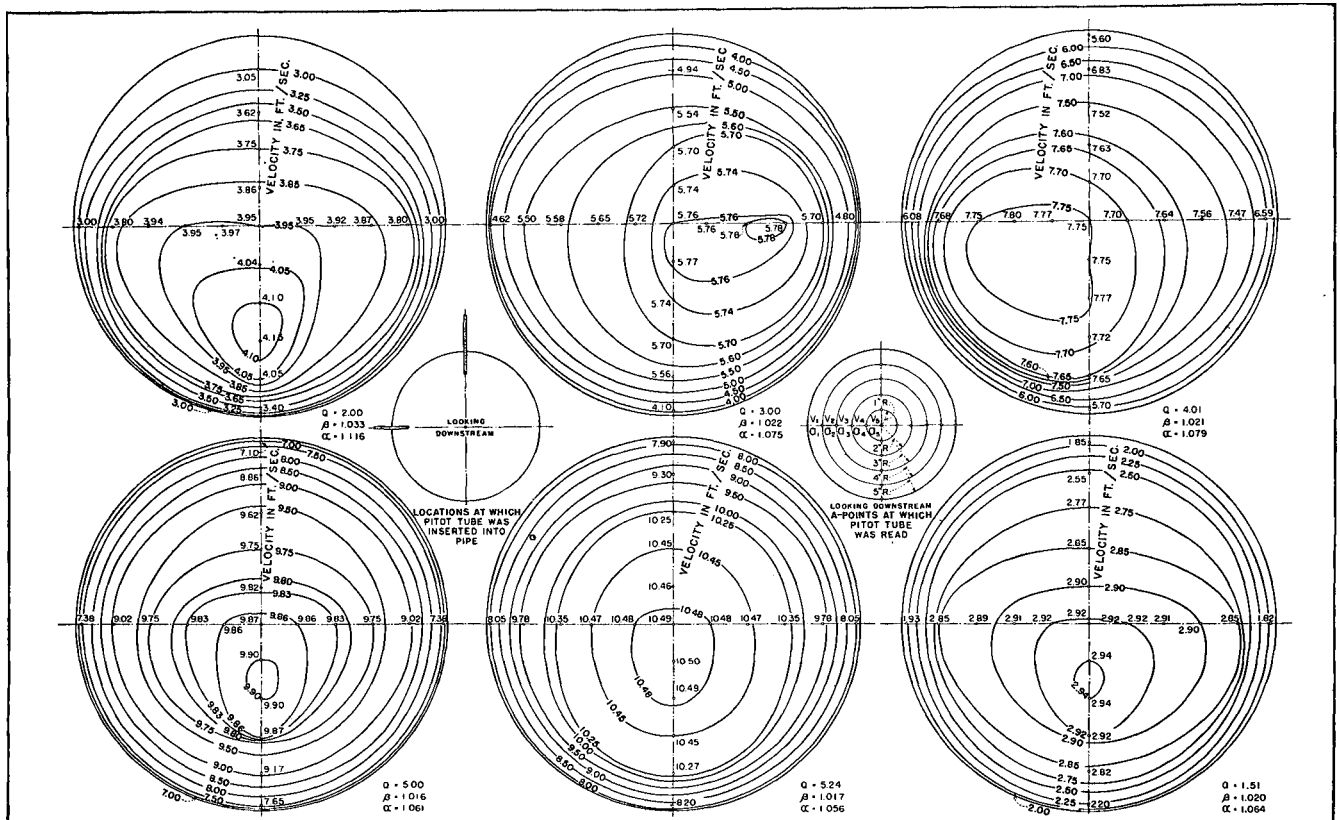

FIGURE 34—VELOCITY DISTRIBUTION IN 10-INCH PIPE FROM PITOT TUBE MEASUREMENTS

points of equal velocity, were drawn, and the areas between these lines were obtained by the use of a planimeter. The non-uniformity in velocity distribution is probably due to the unsymmetrical entrance conditions.

The coeffficient of velocity in a circular pipe is expressed[5] as $\beta = \int \frac{v^2 dA}{V^2 A}$, where v is the velocity in each individual area bounded by the isotachs, V is the mean velocity in feet per second, and A is the total area of the pipe in square feet. If the areas of the annular rings between the velocity contour lines in the figure 34-A be denoted as a_1, a_2, a_3, etc., and the mean velocity in each respective area be indicated as v_1, v_2, v_3, etc., the numerator of the above equation can be expressed as $\Sigma\ (v_1^2\, a_1 + v_2^2\, a_2 + v_3^2\, a_3 + \text{---})$ or $2g\ \Sigma\ (h_{v1}\, a_1 + h_{v2}\, a_2 + h_{v3}\, a_3 + \text{---}) = 2g\ \Sigma\ (h_v a)$, where h_v is the velocity head of each individual area between isotachs.

The mean velocity V in the pipe is equal to

$$\frac{\Sigma\ (v_1\, a_1 + v_2\, a_2 + v_3\, a_3 + \text{---})}{A}$$

or

$$\frac{\Sigma\ (q_1 + q_2 + q_3 + \text{---})}{A} = \frac{Q}{A}$$

The denominator of the equation is then simply Q^2/A which can also be expressed as $2g\ H_v A$, where H_v is the total mean velocity head in the pipe.

Substituting the numerator and denominator into the original equation, the result is

$$\beta = \frac{\Sigma h_v a}{H_v A}$$

Experimental values were substituted in the above equation for six discharges investigated. It was found that the value of β varied from 1.016 to 1.033, as indicated on figure 34. The energy head correction factor[6], expressed as $\alpha = \int \frac{v^3 dA}{V^3 A}$ where $v =$ velocity in each individual area bounded by isotachs, $V =$ mean velocity in pipe in feet per second, and $A =$ total area of pipe in

[5]Powell, Ralph W., Branch Losses in Pipes by the Momentum Method.

[6]O'Brien, M. P. and Johnson, J. W., Velocity-Head Correction for Hydraulic Flow, Engineering News-Record, August 16, 1934.

square feet, was computed for the six runs shown on figure 34. The integration of the expression $\int v^3 dA$ was accomplished by plotting a mass diagram, the coordinates of which were the area of the pipe and the cube of the individual velocities at isotachs. The numerator of the above equation was obtained by measuring the area under the curve with a planimeter. The denominator was obtained by multiplying the total area of the pipe by the sum of the cubes of the individual velocities in the areas between isotachs. The velocity head coefficient, α, varied from 1.020 to 1.116. These values are listed under their respective discharges on figure 34. The true velocity head is then αH_v, where H_v = total mean velocity head in the pipe.

The junction loss results would have appeared slightly different had the true velocity head been used in the computations rather than the mean velocity head; since the coefficient varied with the length of the pipe used in the experiments. It is evident, therefore, that numerous measurements would have been required to obtain a true interpretation of velocity conditions throughout the pipes. The results of these experiments together with other similar studies indicate that the velocity head coefficient for a given pipe decreases with an increase in Reynolds' number; and, for a given Reynolds' number, the coefficient decreases as the size of pipe increases.

It was realized that additional measurements of velocity distribution would have been interesting, and perhaps valuable; but the requirements of this particular problem did not justify them, and time limitations prohibited additional studies. Furthermore, such work would have required a material refinement of the available apparatus.

21. Summary and Conclusions.—Results of the foregoing tests may be summarized as follows:

1. The installation of filler blocks at the 105-degree junction, to displace the eddy formation existing at this location, produced no material improvement in the efficiency of the junction.

2. Comparison of results obtained by Professor Thoma and the Bureau of Reclamation on geometrically similar junctions of different size indicated that the junction loss decreased as the size of the model increased. The increased

loss indicated by the smaller junction is primarily due to viscous effects and to the fact that the straight pipe friction is seldom to scale, although the junctions may be geometrically similar. It is therefore logical to assume that the greater deviations in junction losses occur for the smaller pipe sizes.

3. The addition of a cone connecting the right-angle branch with the main pipe reduced the junction loss coefficient to approximately one-third of its original value.

In conclusion, it may be well to emphasize the fact that the foregoing experiments were performed for a specific purpose and were not intended to constitute a general study of pipe junctions. The results of these tests may prove of value for a similar case in the future which complies with similar limitations. The majority of the graphs have been expressed so that the values are dimensionless; thus it would appear that the same values indicated by the graphs apply for both model and prototype. Strictly speaking this is not entirely true, especially on very small models, due to the above mentioned factors. It is expected that actual junction losses in the Boulder Dam penstocks will be slightly less than those indicated on the model, in the same way that the losses in the model were less than those obtained by Professor Thoma on a smaller but similar junction. The variation between prototype and model is expected to be less than the variation between the model and the small brass pipe, because the model was large enough to reduce viscous effects considerably.

ACCURACY OF RESULTS

22. General.—The model tests on junction losses in the Boulder Dam penstocks, comprising approximately 25,000 separate observations, made with accurate equipment and with multiple readings of piezometers located every four to six diameters over the entire length of pipe tested, afford an exceptional opportunity to evaluate experimental errors, to analyze the distribution of hydraulic losses, and to develop a procedure of maximum efficiency for future tests.

In this report, the energy loss due to a junction has been defined as the sum of the piezometric drop and the difference in mean velocity heads, less the normal friction loss between the two piezometer stations. This equals the true energy loss when

the two piezometer stations are located sufficiently far upstream and downstream from the junction that normal velocity distribution exists in the stream cross sections. Theoretically, a complete loss determination requires the simultaneous measurement of two mean velocity heads, two piezometric elevations, and the loss which would exist in the same total length of pipe if it were uniform. Since simultaneous readings were impractical, certain errors were introduced.

23. Errors in Mean Velocity Head.—The rate of discharge was measured by weirs which had previously been calibrated

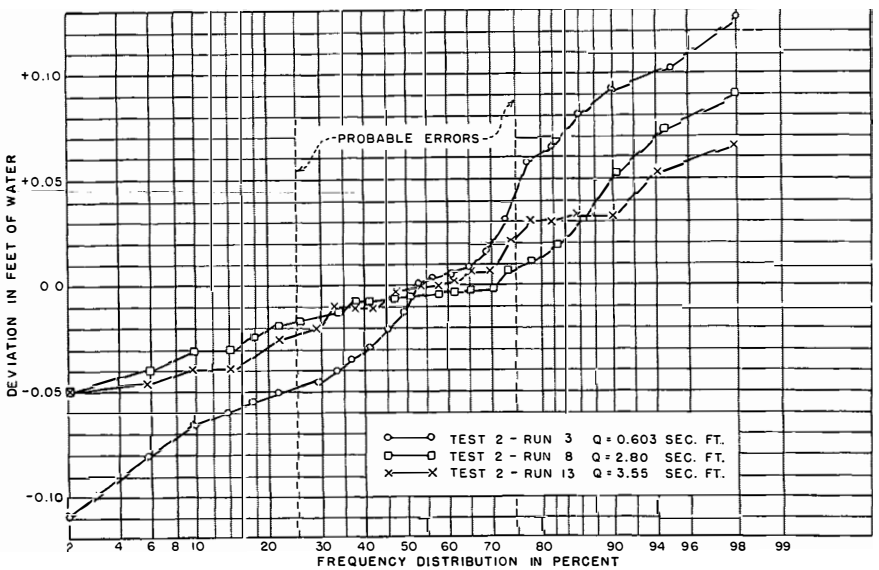

FIGURE 35—FREQUENCY DISTRIBUTION OF FLUCTUATIONS IN STILLING BASIN

volumetrically. It is believed that absolute errors in mean discharge as determined from the measurements did not exceed one-half of one percent. From the weir, the water passed to a stilling basin, thence to the equipment under test. Although nearly an hour was allowed before each test for the flow to stabilize, fluctuations persisted in the stilling basin. The water rose and fell slowly with a probable deviation of 0.025 foot from the mean elevation as shown in figure 35 at any instant. At the end of

each run, the average discharge was obtained by correcting the mean of the weir readings, to allow for any storage which had occurred in the forebay. The correction for even the lowest discharge was less than 0.2 percent. Nevertheless, an observational error was introduced by the momentary changes in the total head on the apparatus. Since the head on the apparatus approximated $3h_v$, for velocity heads of one foot and over, this error for a single observation is $\frac{1}{3} \times \frac{0.025}{1.0} = 0.8$ percent of h_v. Sixteen readings were made on each piezometer, therefore the probable error[7] of the mean would be only $\frac{0.8}{\sqrt{16}} h_v = 0.2$.

Repeated microcaliper measurements showed that the diameters of the pipes did not vary more than 0.003 inch, or 0.1 percent for the 3.49-inch branch. This variation would cause an error of approximately 0.4 percent in the mean velocity head. The previously mentioned error of 0.5 percent in the weir discharge is equivalent to an error of $(1.005)^2$—1.00, or one percent in the mean velocity head. Combining, the total probable error in the mean velocity head is:

$\sqrt{(0.01)^2 + (0.002)^2 + (0.002)^2}$, equivalent to about one percent.

In accordance with usual practice, the mean velocity head was used in this report for the computation of kinetic energy head. It is known, however, that because of the non-uniform distribution of velocity, the kinetic energy is from nine to two percent in excess of the mean velocity head for Reynolds' numbers between 50,000 and 1,000,000. Furthermore, the corrections may be much larger for sections less than thirty diameters downstream from fittings due to non-symmetry of velocity distribution. Information concerning the magnitude of this correction, measured at a location immediately upstream from the junction in the 10-inch pipe, approximately 18 diameters below the entrance, is given in section 20. Numerical values of junction losses have been computed on the basis of mean velocity heads. The error involved in this procedure will be further discussed.

---

[7]For a detailed discussion of the application of the theory of least squares to the interpretation of errors, see Root: "Mathematics of Engineering." Williams and Wilkins Co., Baltimore.

24. Errors in Determination of Hydraulic Grade.—The determination of the hydraulic grade at any point was subject to the following errors:

1. Fluctuations in headwater elevations.
2. Fluctuations due to turbulence.
3. Errors due to mechanical construction of piezometers.
4. Errors due to lack of parallelism of flow.
5. Various errors due to capillarity, temperature, entrained air, etc.

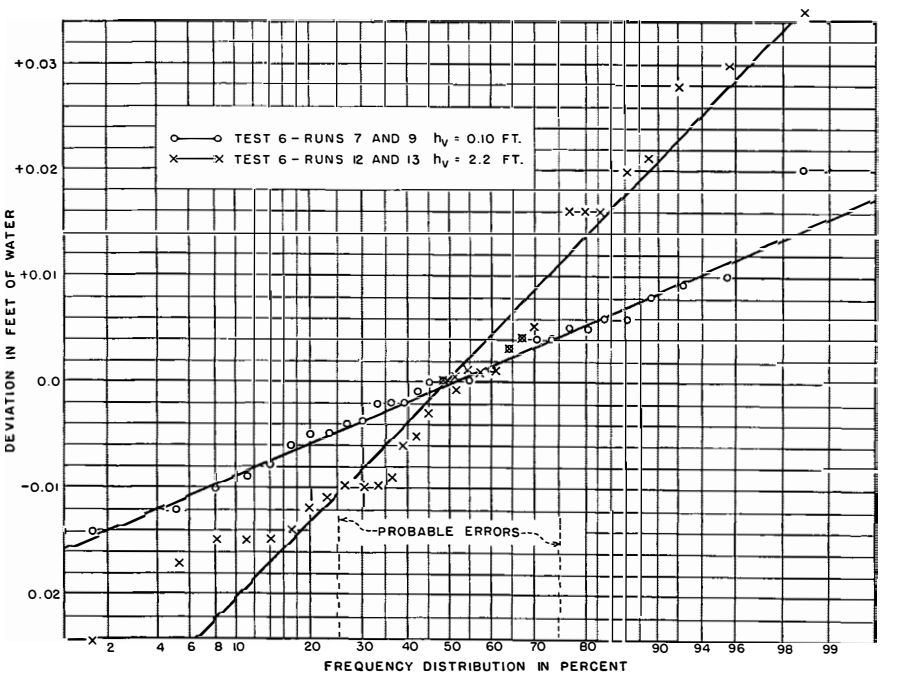

FIGURE 36—FREQUENCY DISTRIBUTION OF FLUCTUATIONS IN PIEZOMETER READINGS

Since approximately half the total pressure head on the apparatus was transformed into velocity head at the entrance, the effect of reservoir fluctuations, error 1, on oscillations in the pipe piezometers is expected to be reduced one-half. Figure 35 indicates that the probable fluctuation in the reservoir was about 0.025 foot; so the expected fluctuation in a piezometer was of the

order of 0.012 foot. Results showing fluctuations at 16 different piezometers for two discharges are plotted on figure 36. These indicate a probable error for a single observation of 0.008 foot. These data take into account changes in piezometric levels caused both by headwater and turbulence fluctuation; and as the error is less than that expected by headwater fluctuations alone, a reasonable conclusion appears to be that turbulence surges, error 2, were of relatively little importance.

Four readings of each piezometer were taken at about ten-minute intervals during each run. The fluctuation error for a set of readings from a single piezometer would therefore be $\frac{0.008}{\sqrt{4}}$ $= 0.004$ foot. Since four piezometers comprised a ring, the error of the piezometric grade as determined by the ring, caused by fluctuations only, would be 0.002 foot.

Due to slight roughness at the edges of openings, error 3, or non-parallelism of flow, error 4, most piezometers exhibited constant positive or negative errors varying with velocity head. Assuming the correct piezometric elevation at a given ring to be that of the mean of the four piezometers, each read four times, a study was made of the variation of the individual piezometers from the mean. For this purpose the experiments made to determine friction losses in the 10-inch straight pipe were used, the analysis being based on the piezometer errors of rings 6, 10, and 11, located 18, 44, and 52 diameters downstream from the rounded intake.

Eight runs with velocity heads varying from 1.5 to 3.5 feet were used, and the differences from the mean piezometric level of each run for each ring were expressed in terms of velocity head. The distribution of the mean error for the twelve piezometers is shown on figure 37. The indicated probable error for a single piezometer due to mechanical defects is $(0.01 \pm 0.0015)\, h_v$ percent. With a mean velocity head equal to 2.5 feet, the corresponding error is 0.025 foot. For a ring containing four piezometers, the probable error is 0.012 foot which is comparable to the 0.002 foot caused by headwater fluctuations. Although the constant error due to mechanical defects of the piezometers may appear large, previous work on the subject[8], indicates that it is within the limit of practical accuracy.

[8]Allen and Hooper, "Piezometer Investigations," Trans. A.S.M.E. HYD. 54-1-1932.

In connection with lack of parallelism of flow, error 4, there is reason to believe that water, entering a pipe system through an imperfectly shaped mouthpiece, passes through the same phenomena of contraction and expansion that is experienced by a free jet issuing from an orifice. In the straight pipe experiments

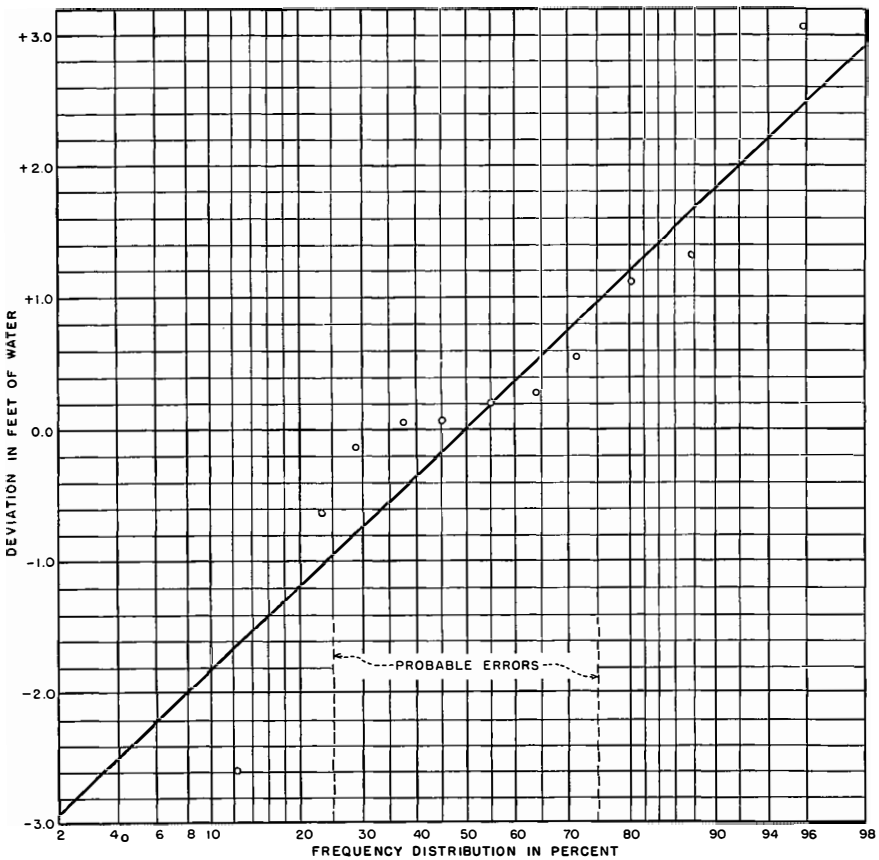

FIGURE 37—FREQUENCY DISTRIBUTION OF CONSTANT ERRORS IN PIEZOMETERS DUE TO MECHANICAL IMPERFECTIONS

on the 3.49-, 4.33-, and 10-inch pipes, with piezometers located 3.5 to 7 diameters along the pipes, the experimental data indicated that points of low and high pressure, analogous to waves, occurred downstream from the entrance at intervals of 6 to 8 diameters. The amplitude of the pressure deviation was about one percent

of the velocity head, and was not entirely damped in a length of 50 diameters. Although the experimental data are not conclusive, it is estimated that there was a probable error from this cause in the order of 0.7 percent of the velocity head at the upper end and 0.2 percent of the velocity head at the lower end.

No attempt has been made to evaluate errors due to temperature, entrained air, and capillary effects, error 5. In comparison with the other errors it is believed that these may be neglected.

25. Errors in Obtaining Energy Grade.—For a given run, the energy grade at any piezometer ring was determined by averaging the 16 separate readings from the four piezometers and adding to it the mean velocity head. The probable error in the result was as follows:

$$\gamma^2 = (\text{velocity head error})^2 + (\text{error due to standing pressure waves})^2 + (\text{mechanical error of piezometer})^2 + (\text{fluctuation error})^2.$$

Assuming the fluctuation error to be equal to or less than 0.002 h_v for velocity heads of one foot and over, the experimental error in the energy grade at any piezometer ring for a given run becomes

$$\gamma = h_v\sqrt{(0.002)^2 + (0.002)^2 + (0.005)^2 + (0.002)^2} = 0.006\ h_v.$$

For velocity heads of three feet or more this error amounts to 0.02 foot. Variations of this magnitude revealed by the plotted energy grades on figure 17 are common. These errors are exclusive of those previously mentioned, resulting from inaccuracies in weir measurements.

26. Errors in Straight Pipe Losses.—At the beginning of the experimental program, it was contemplated that the straight pipe losses required by the experimental procedure would be obtained, once for all, by tests made for this purpose. The following apparatus was available:

1. 3.49-inch pipe: Entrance, 29-degree cone with 16:1 entrance-to-throat area ratio; calming length, 38 diameters containing 6 piezometer rings; end length, 14 diameters with 3 piezometer rings.

2. 4.33-inch pipe: Entrance, 27-degree cone with 10:1 entrance-to-throat area ratio; calming length, 26 diameters containing 4 piezometer rings; end length, 16 diameters with 3 piezometer rings.

3. 10-inch pipe: Entrance, semicircular beading on face of wall with radius equal to 0.4 that of pipe; entrance-to-throat area ratio 2:1, calming length, 36 diameters containing 8 piezometer rings; end length, 16 diameters with 3 piezometer rings.

Since the pipe used was of the same quality throughout and all piezometer rings were of equal accuracy, the distinction between calming length and measuring section is a nominal one, but is useful for analyzing errors.

The velocity distribution is nearly uniform at the throat of a well-rounded pipe entrance whose shape is such that no contraction occurs. For smooth pipes, the distribution changes into the typical velocity profile within a distance of 25 to 40 diameters downstream. The energy loss during this transition must be very small, and may be even less than in the portions of pipe subjected to normal flow. The change in velocity distribution results in a conversion of potential to kinetic energy. The hydraulic grade line for this case, tends to take the form of a falling curve, concave upward, steeper at the upstream end, and flattening into a straight slope descending toward the outlet. If entrance conditions are not ideal and a tendency toward contraction exists, the kinetic energy at the contracted section will be much higher than would be indicated by the calculation from the mean velocity corrected for normal distribution. The static pressures would show a drop from the actual entrance to the vena contracta followed by a sharp rise and subsequent gradual drop, the latter being subject to damped oscillations. The experimental measurements of static pressures began approximately at the probable location of this contraction, and show the sharp rise and succeeding drop with oscillations. When a constant kinetic energy term, based on downstream conditions, is added to this pressure distribution, the resulting nominal energy grade line shows the same variations as the measured pressures. It is thus too low at the first point, probably too high at its peak, and may oscillate about the true grade line with diminishing amplitude thereafter.

It is evident, therefore, that to obtain the normal loss in a straight pipe, either the pressure drop must be obtained at locations sufficiently distant from the entrance that the velocity distribution is constant and the hydraulic grade a straight line, or the true value of the kinetic energy at the measured cross sections must be known. Unfortunately, in the Bureau's tests, the length

of pipe which could be accommodated was limited so that only 14 to 15 diameters at the downstream end could be considered as having approximately constant velocity distribution. The measured energy drop in this length was approximately 0.23 h_v. It has

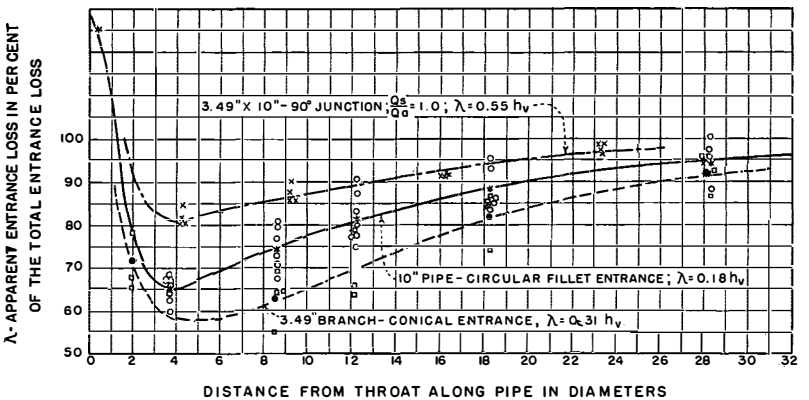

FIGURE 38—DISTRIBUTION OF THE ENTRANCE LOSS

been shown that the probable error in the mean results of a set of readings on a single piezometer ring is of the order of 0.006 h_v, for a single determination of the friction coefficient, calculated from the drop between two rings. Therefore the probable error in the friction coefficient is: $\frac{\sqrt{2} \times 0.006\ h_v}{0.23\ h_v} = 3.7$ percent. In addition, if calming lengths are inadequate, the true kinetic energies in the two sections may vary by an amount equal to 0.01 h_v, resulting in a persistent error of $0.01/0.23 \times 100 = +4.3$ percent in the friction coefficient, a value well within the possible range.

27. Entrance Losses.—During the tests for friction losses in straight pipes, advantage was taken of the opportunity to measure apparent entrance losses and their rate of development. Results obtained from this series of observations show that their probable deviations from the mean, based on 25 experiments, are as follows:

1. 3.49-inch pipe entrance, loss 0.14 $h_v \pm 2.5$ percent.
2. 4.33-inch pipe entrance, loss 0.11 $h_v \pm 3.33$ percent.
3. 10-inch pipe entrance, loss 0.18 $h_v \pm 2.5$ percent.

Details of pipe entrances are shown on figures 10 and 25.

The accumulative percentage of the total apparent entrance

losses at various diameters below the entrances are shown on figure 38. It is noted that, even at 30 diameters, only 95 percent of the total entrance loss has occurred.

Since this data was obtained from pipes of limited lengths, there is reason to believe that the determinations of both entrance losses and straight pipe losses include large persistent errors. Thus, in an experiment in which the calming length is only 30 diameters, followed by a test section 16 diameters long, if 5 percent of the entrance loss, assumed to be 0.20 h_v, takes place in the test section whose normal friction loss is 0.23 h_v, a persistent positive error of $\frac{0.05 \times 0.20}{0.23} \times 100 = 4.3$ percent would exist in the determination of the friction coefficient. This may explain the higher friction losses found for the 10-inch pipe which had the largest entrance loss. Such an overestimate of friction loss would, in turn, lead to a persistent underestimate of about 13 percent in the entrance loss, since the determination of the entrance loss involves the subtraction of the normal friction losses, in 40 diameters of pipe, from the measured energy drop.

28. **Branch Loss Errors.**—The true energy losses caused by the junctions were not required to satisfy the major purposes of these tests, and those shown in the graphs are the nominal losses as ordinarily used in hydraulic practice. Nevertheless, in some circumstances the true losses are important. The two examples following indicate the magnitude of the difference between the nominal and true losses.

The equation by means of which the coefficients were determined experimentally may be written:

$$\lambda = (1-K_2) + (P_x-P_o) - mK_1K_2.$$

The symbols have the meaning and values as follows; the experimental values are those obtained in one of the tests to determine the losses in the main pipe due to the diversion of six-tenths of the flow through the branch with Reynolds' number equal to 200,000, see figure 20-A, $Q_s/Q_a = 0.6$:

λ = Coefficient of junction loss in terms of $V_a^2/2g$

(P_x-P_o) = measured drop in hydraulic grade line across junction in terms of $V_a^2/2g$ $= -0.64$

K_1 = Friction coefficient in terms of $V_a^2/2g$ per diameter $= 0.019$

m = length of pipe in diameters between points of measurement of pressure drop; = 25

K_2 = ratio between mean velocity head below junction to that above; = 0.16

Substituting the experimental values in the equation gives

$$\lambda = 0.84 - 0.64 - 0.08 = 0.12.$$

This is the value plotted on figure 20-A.

In figure 34 are shown the coefficients by which the mean velocity heads must be multiplied to obtain the true kinetic energy head. It should be noted that these values are higher than nominal due to the nonsymmetrical velocity distribution. If, instead of using the difference between mean velocity heads for the term $(1 - K_2)$ the true energy head be used, from figure 34, Q = 2, the term $(1 - K_2)$ becomes $(1.12 - K_2)$; and, according to Nikuradse's[9] data for symmetrical velocity distribution, K_2 must be multiplied by 1.05. Using these values the equation becomes

$$\lambda = 0.95 - 0.64 - 0.08 = 0.23.$$

Thus the true energy loss caused by the junction in the main pipe for a discharge ratio of 0.60 is 95 percent larger than shown in figure 20-A.

Similar methods of computation show, on the contrary, that, for the same discharge ratio $Q_s/Q_a = 0.60$, and for the conditions plotted on figure 21-B, the true loss is only 77 percent of that plotted.

It is evident that where the desired quantity depends upon the differences of large terms of nearly equal magnitude, if accurate values are desired, great refinement is required in the experimental work.

29. **Conclusions on Errors.**—From a study of the errors in these tests, the following conclusions appear to be warranted:

1. The magnitude of the accidental error in the energy grade at a given ring for a single run was largely controlled by the mechanical errors in the piezometers. If in future tests the piezometers are placed in a spiral around the pipe over a length of about 3 diameters, errors due to pressure waves will be eliminated. Where fluctuations exist, similar to those

[9] Nikuradse. "Gesetzmäszigkeiten der turbulenten Strömung in glatten Rohren" (Laws of Turbulent Flow in Pipes) VDI Forschungsheft 356 (1932).

found in these tests, the piezometers can be read to the nearest 0.01 of a foot and the number of readings reduced by one-half without appreciable change in the accuracy.

2. Moving piezometers from locations near a fitting to points away from the fitting, where the straight pipe loss is known and the velocity distribution is nearer constant, will increase the accuracy of an experiment.

3. Where quantitative losses are sought, errors in energy correction factor and in straight pipe losses probably control the accuracy. The energy correction factor is of particular importance where anticipated losses are small. Neglect of this factor is probably responsible for many discrepancies in published data.

CHAPTER III—INTAKE TOWER AND PENSTOCK ASSEMBLY

INTAKE TOWER MODEL

30. Introduction.—Release of water for irrigation and power purposes is controlled by four intake towers adjacent to the upstream face of Boulder Dam.[10] Each intake tower is provided with two cylinder gates 32 feet in diameter. The lower gate is located in the base of the tower, at elevation 895; and the upper 150 feet higher, at elevation 1045. These gates control the flow through the 30-foot steel penstock headers which extend from the base of each tower to the turbines in the power plant and to either the canyon-wall outlet works or the tunnel-plug outlet works. The closure of the upper and lower gates in any intake tower permits the unwatering of the steel penstock and all its appurtenances for inspection and maintenance.

To determine the hydraulic action of the towers and control gates under the various conditions of discharge to which they may be subjected, a model of one of the towers, on a scale of 1 to 64, was constructed and tested in the hydraulic laboratory of the Colorado Agricultural Experiment Station, Fort Collins, Colorado. By means of this model, the distribution of flow through the two sets of gate openings was determined; methods of reducing the entrance losses studied; and the necessity for air vents below the lower cylinder gate investigated.

31. Apparatus.—The model consisted of a complete assembly of the upper Arizona 30-foot penstock header, intake tower, and branch penstocks leading to the turbines and needle valves as shown on figures 39 to 43, inclusive. Photographs of the model are shown on figure 42.

The intake tower and surrounding topography were located in the 10.5- by 10.25-foot tank, as shown in figure 2. The inner portion of the tower consisted of galvanized sheet-metal cylindrical

[10]Kinzie, P. A., Hydraulic Valves and Gates for Boulder Dam, Mechanical Engineering, vol. 56, July, 1934, p. 387.

shells, accurately built and carefully soldered together with butt joints, forming a true representation of the prototype in detail and dimension. Two independently operated cylinder gates were installed in the tower, similar to those in the prototype. The gates were made of 12-gage seamless steel tubing with the lower outside edges beveled sufficiently to insure a close fit with the base plates, forming a satisfactory water seal as shown in figures 43-A and 43-B. These were raised and lowered by three small rods attached to each gate at the third points on the circumference. The rods from the lower gate converged into one main rod which extended up the center of the tower to the hoisting apparatus. The upper end of the rod was threaded to permit raising and lowering the gate by a small crank in the upper part of the tower, see figure 43-C. The rods to the upper gate were similarly connected to a sleeve which enclosed the main rod leading to the lower gate. This sleeve was also threaded at the upper end, and was actuated by a second crank located in the upper part of the tower.

Bottom portions of the gate entrances were made from machined metal plates. The lower plate served both as a gate seal and as a base for the tower. Upper portions of the entrances were molded, using a mixture of beeswax and paraffin. With the exception of piers and pier spacers, which were of wood, and gate entrances, which were of wax and paraffin, the tower was constructed of metal. Piers and spacer blocks were protected with two coats of aluminum paint to prevent as far as possible any swelling of those parts of the model. The topography about the tower was constructed from contour maps of the canyon and consisted of a lean mixture of cinder concrete. Trash racks, shown on figure 42-B, were installed on the tower during a portion of the tests. These were constructed to scale, but due to their miniature size, there is some doubt as to the advisability of relying closely upon results obtained with them. Small edges and burrs which were practically impossible to remove, surface tension, and traces of grease and oil on the racks, all probably had some effect on test results. The racks, 182 feet long on the prototype, were constructed of thin strips of sheet metal, set with the thickness of the metal normal to the direction of flow and held in place by cross pieces to which the strips were soldered. Upon completion of the various parts, the tower was assembled on its base plate and bolted to a corresponding plate located in the floor of the model tank, to which the 30-foot diameter penstock header was connected. In

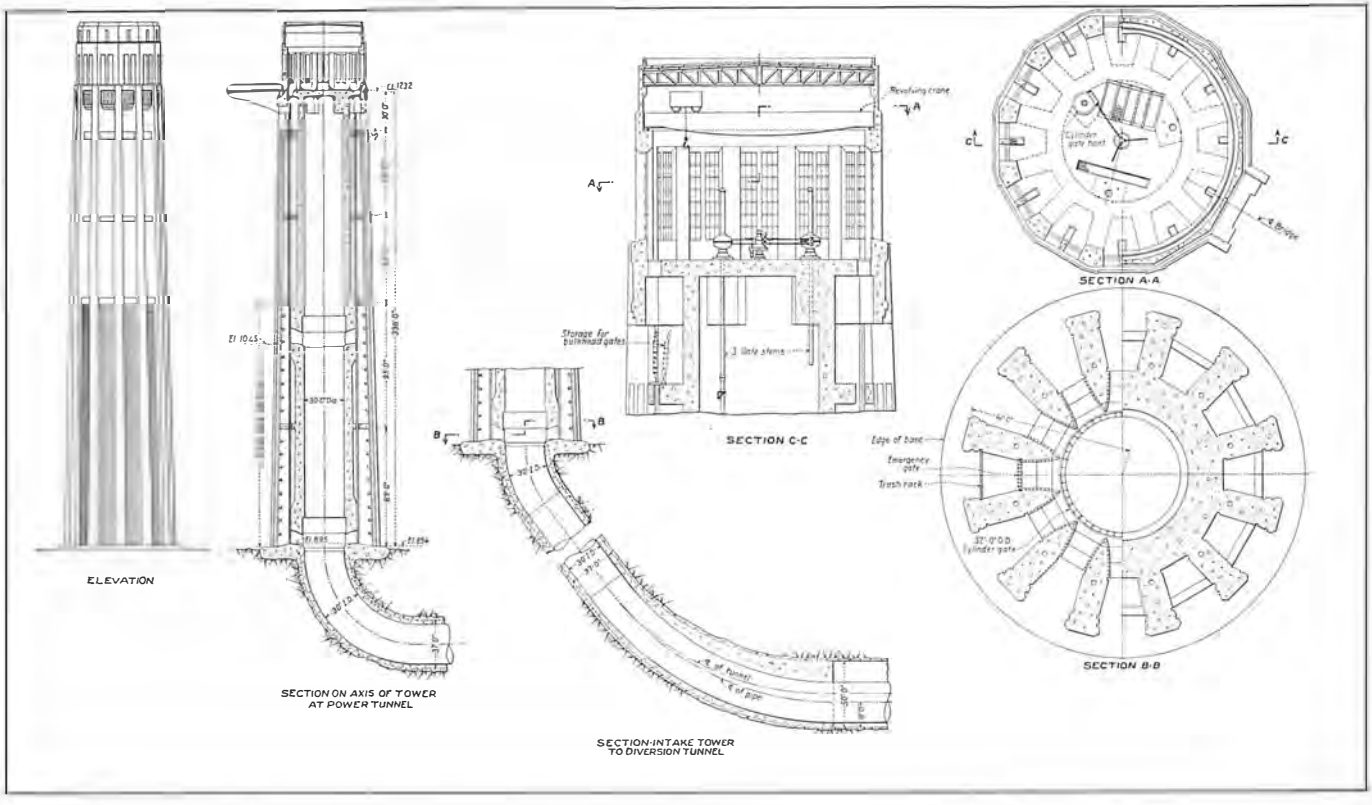

FIGURE 39—INTAKE TOWER AND INCLINED TUNNEL

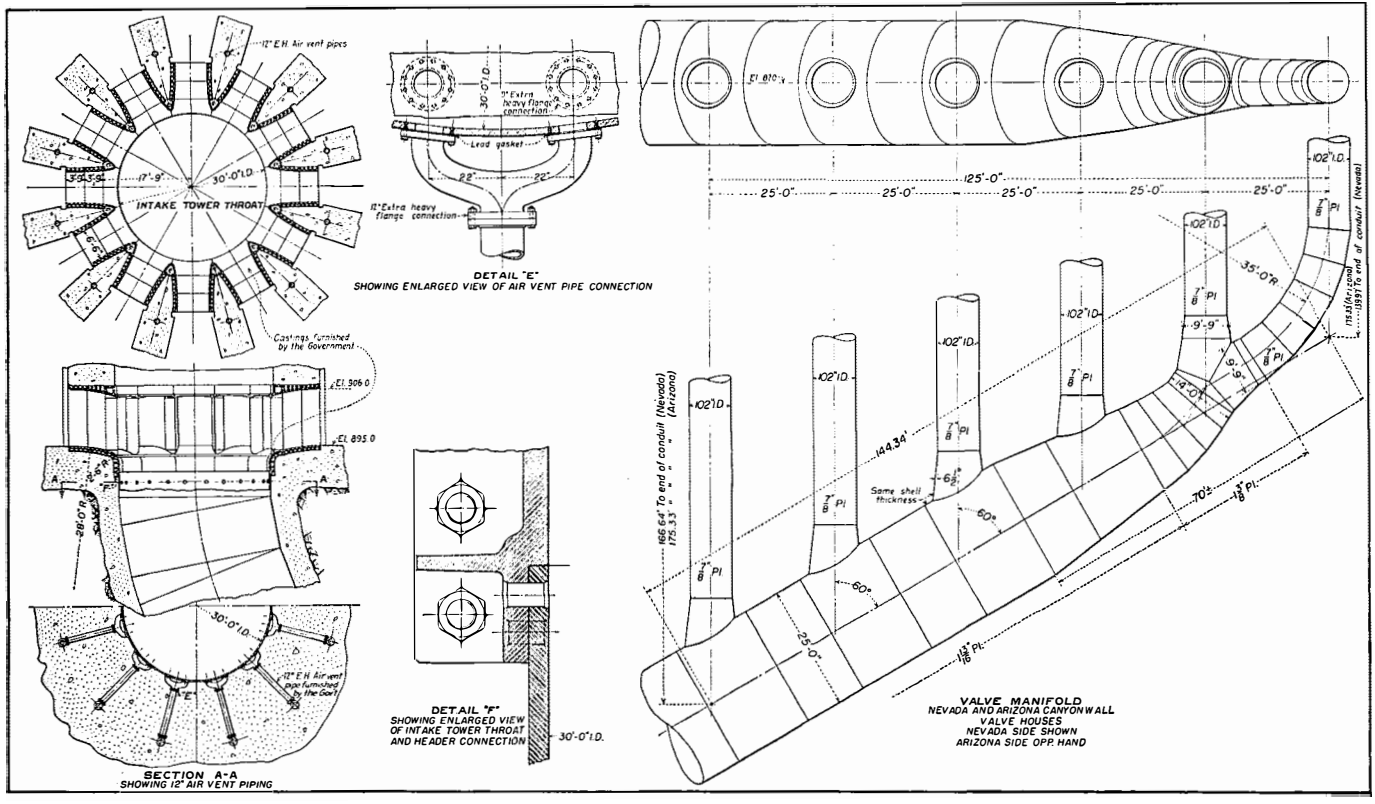

FIGURE 40—INTAKE TOWER CONNECTION AND MANIFOLD

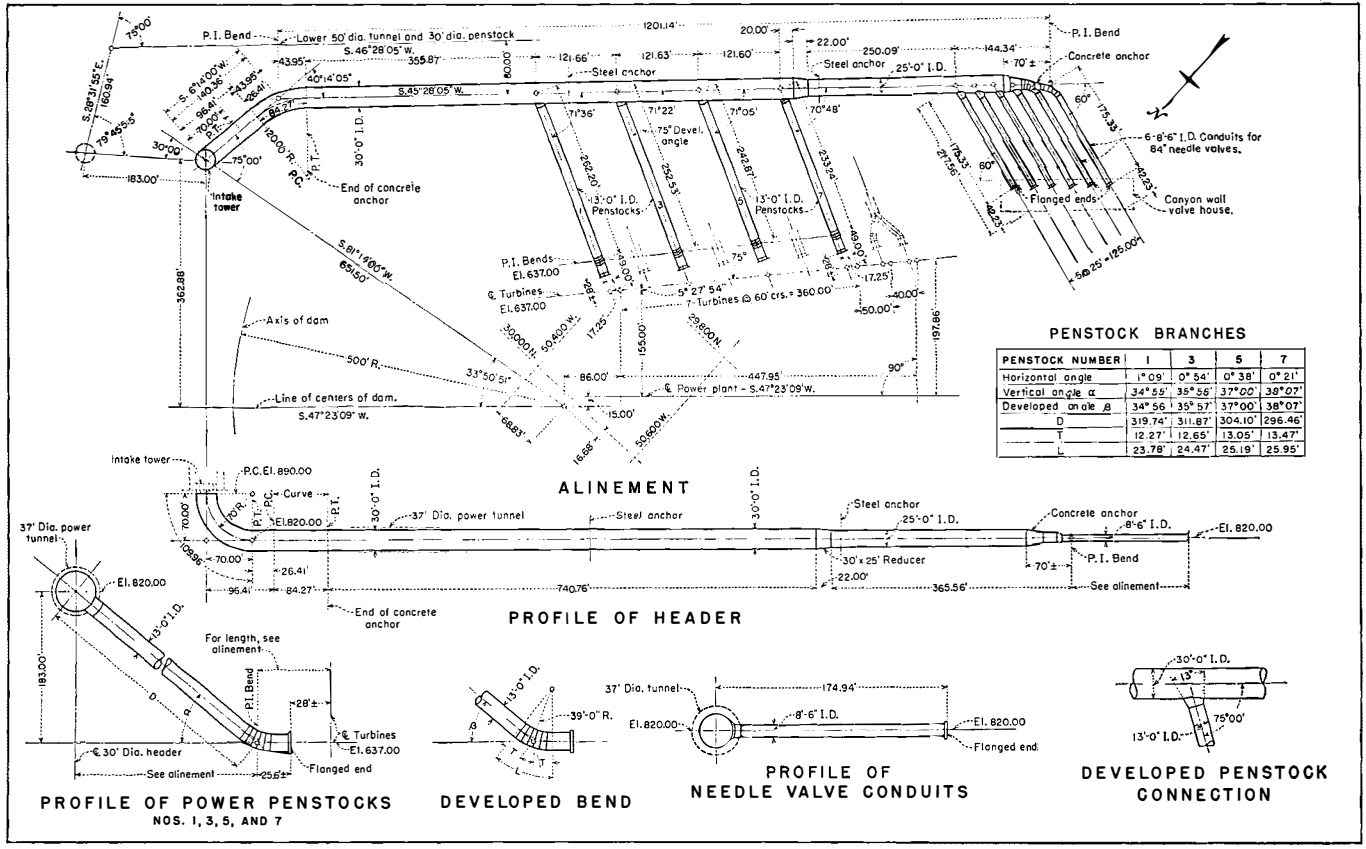

FIGURE 41—HEADERS, PENSTOCKS, AND CONDUITS FOR UPPER ARIZONA TUNNEL

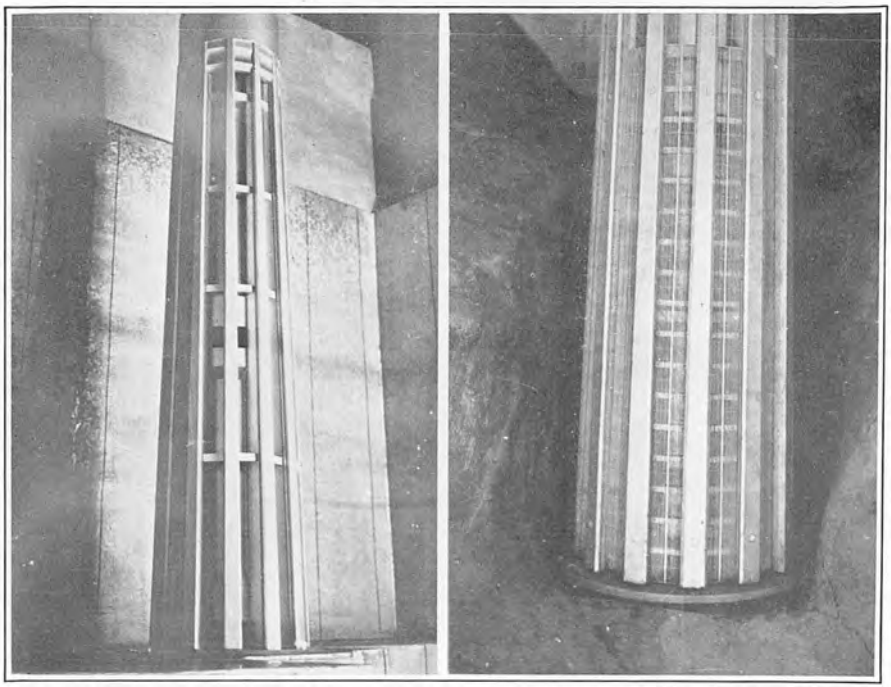

A. Intake Tower Without Trash Racks B. Intake Tower With Trash Racks

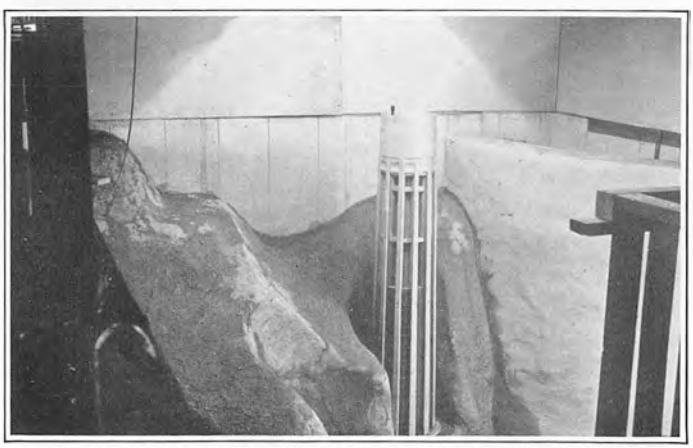

C. Intake Tower, Topography and Portion of Dam

FIGURE 42—MODEL OF ARIZONA TOWER LOCATED ADJACENT TO THE DAM

making alterations in the model, it was necessary to unbolt only the upper plate from the lower and remove the intake tower as a unit.

32. Analysis of Losses in Tower.—To aid in analyzing losses in the intake tower, a ring of piezometers was installed in the base, at elevation 890.0, see figure 43. It was anticipated, and later confirmed, that the vertical 90-degree bend in the penstock header, immediately below the tower, would produce an unbalanced effect on the flow in this portion of the model, causing a variation in pressure at the four piezometers. As losses to be measured in the model were small, averaging the readings of this ring of piezometers would have been inaccurate. Furthermore, the velocity distribution in the vicinity of the bend was unsymmetrical. To avoid complicating loss computations with errors from these sources, the penstock header was disconnected from the base of the tower model and a straight section of pipe, 3 feet in length was connected in its place, see figure 44-A. The lower end of this auxiliary section was fitted with a flange to which orifices of different size were fastened to regulate the discharge through the tower. Five rings of piezometers, designated as A to E, inclusive, were installed at 6-inch intervals along the auxiliary section of pipe, as shown on figure 44-A. Each ring consisted of four piezometers, spaced 90 degrees apart; and each piezometer was connected with a rubber hose to a single glass manometer reading tube. An average value for the pressure at the base of the tower, elevation 890.0, was obtained from these five rings of piezometers by adding the computed pipe friction, from each ring to elevation 890.0, to the corresponding observed gage reading of each ring. As this section of pipe was similar in construction to that used in the penstock experiments, the pipe friction was obtained from the curves plotted on figure 14.

Observed pressures at the five piezometer rings below the tower are shown on figure 45 for several runs with both gates open. Rings A and E were consistent with the other three; ring A appeared to be unaffected by the lower gate; and ring E was uninfluenced by the orifice. The data plotted for each run made essentially a straight line; thus readings from all five rings were used in the loss computations.

Two siphon piezometers were installed in the center of the tower; one midway between the upper and lower gates, and the

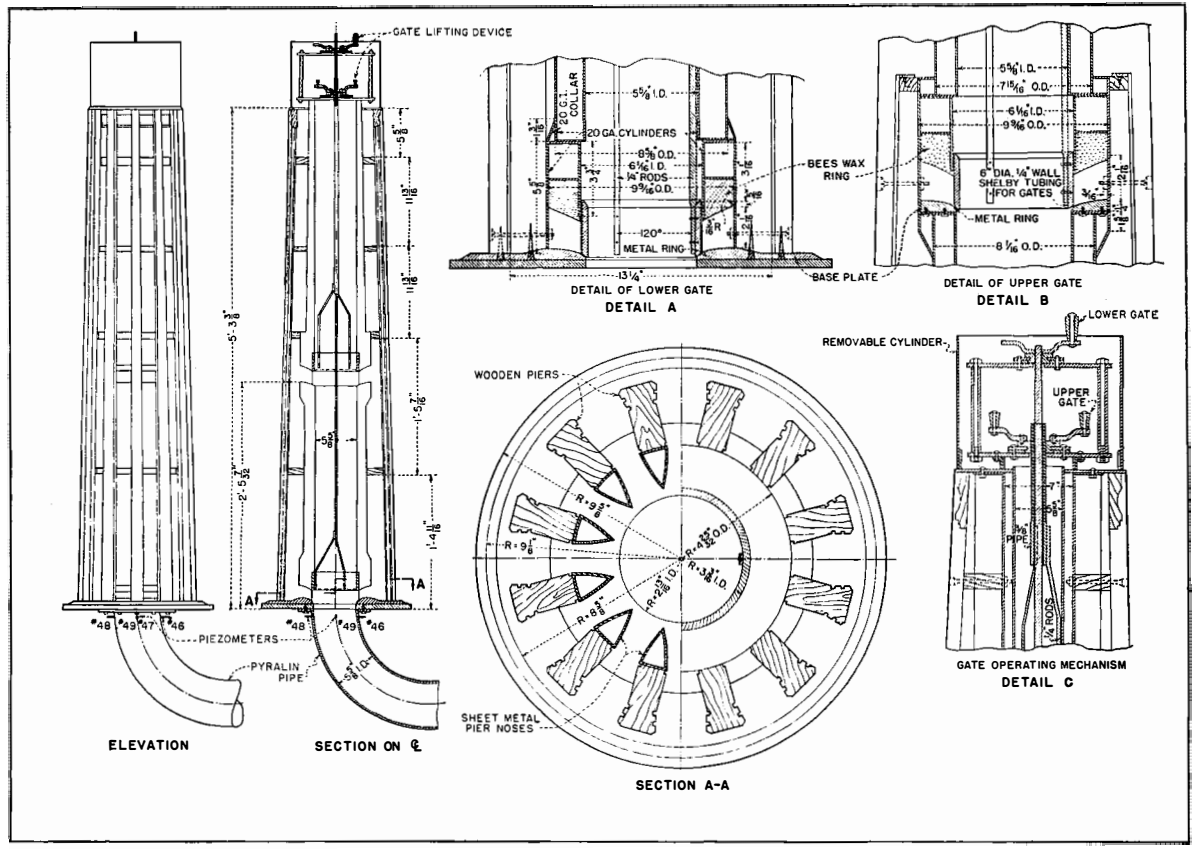

FIGURE 43—INTAKE TOWER MODEL, SCALE 1:64

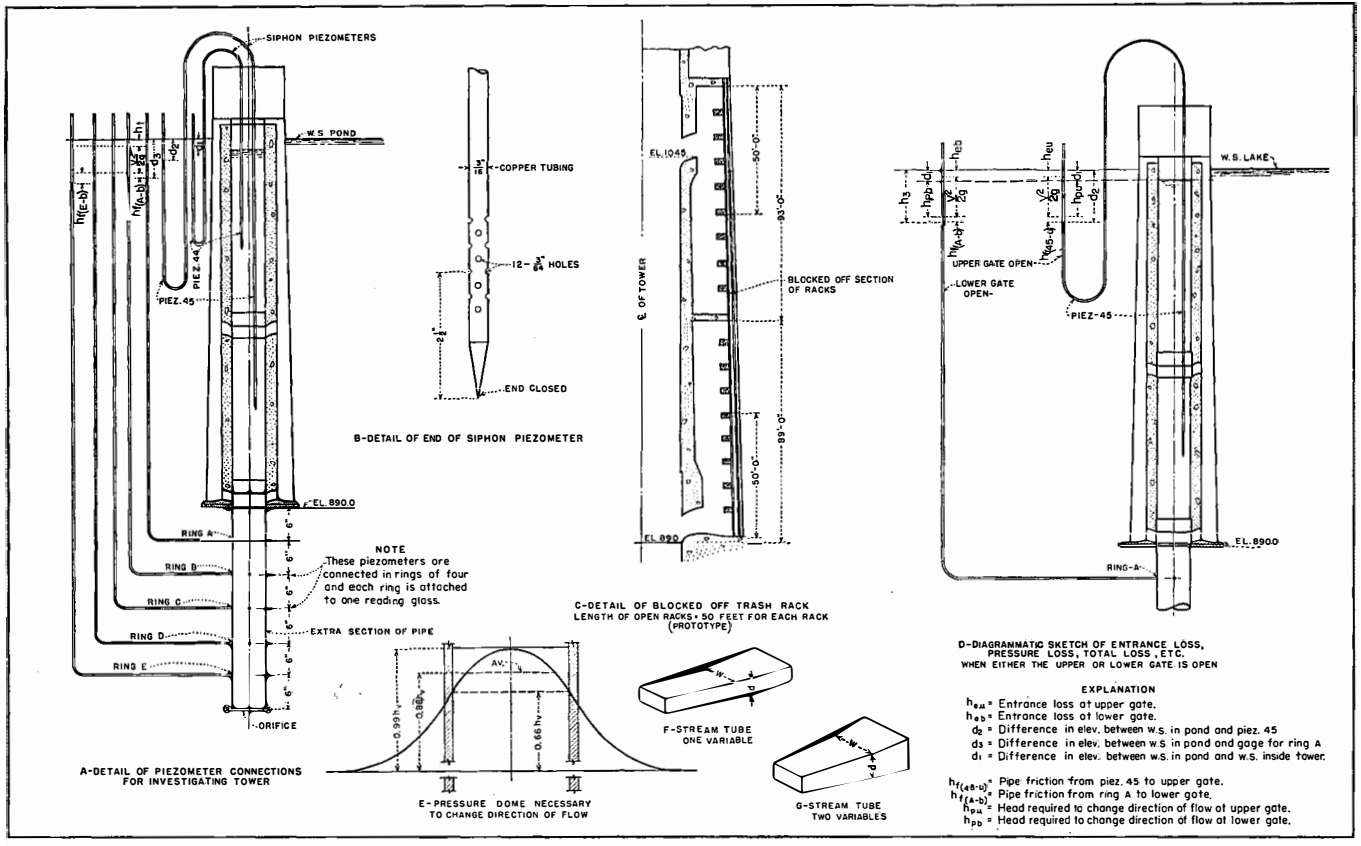

FIGURE 44—MISCELLANEOUS DETAILS OF INTAKE TOWER

other about a foot above the upper gate. Each consisted of a piece of 3/16-inch copper tubing, drawn to a point at the lower end as shown in figure 44-B. Twelve 3/64-inch holes were drilled in each tube, perpendicular to the walls, and the two piezometers were suspended vertically in the center of the tower.

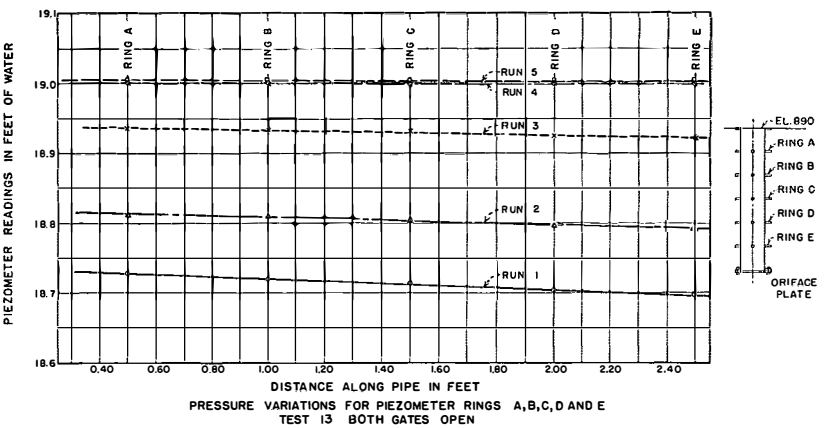

FIGURE 45—COMPARISON OF PIEZOMETER PRESSURES BELOW TOWER

One or both gates were always fully open in the tests as they are intended to be so operated on the prototype. The gates are provided for unwatering purposes and not for regulators. The total discharge was measured over the laboratory 90-degree V-notch weir. The magnitude of the discharge that could pass through the tower was regulated by the size of the orifice below the tower and the elevation of the water surface in the model reservoir. The model discharge ranged from 0.15 to 0.90 second-feet, which corresponds to a range of approximately 5,000 to 30,000 second-feet in the prototype.

33. Total Losses Through Tower.—Tests were made to determine losses through the tower, with and without trash racks, for either the upper, the lower, or both gates open and for a range of discharges. For all conditions, the total loss through the tower was computed by the formula,

$$h_t = d_3 - h_{f(A\text{-}b)} - V^2/2g$$

where h_t = Total loss through the tower to elevation 890.0.

d_3 = Difference in elevation between the water surface in the reservoir and the elevation of the water surface in the manometers connected to piezometer rings A to E, inclusive.

$h_{f(A\text{-}b)}$ = Pipe friction from elevation 890.0 to piezometers below.

$V^2/2g$ = Velocity head at elevation 890.0.

The pipe friction was computed using the combined observations at the piezometer rings below the tower. The results are plotted logarithmically on figure 46. The total loss through the tower, expressed in terms of velocity head in the tower at elevation 890.0, is plotted with respect to Reynolds' number rather than the model discharge; as it is possible to account for differences in temperature in the former but not in the latter. During the tests, the temperature of the water varied from 33 to 50 degrees Fahrenheit. The velocity and diameter of the pipe at elevation 890 was used to compute Reynolds' number.

The conversion of model losses to corresponding prototype values was one of the objectives in performing the experiments. The customary method in the past has been to convert from model to prototype by means of Froude's law, but this is not a valid conversion when small models are used and viscous effects are appreciable. To perform the transfer by this method, it is necessary to assume that the losses, expressed in terms of velocity head, are the same in model and prototype for the same value of Froude's number. With viscous effects present in the model, this assumption is not entirely correct.

Reynolds' law, on the other hand, takes into account viscosity in prototype and model; but is independent of the force of gravity, and consequently of centrifugal forces. If the model of the intake tower were exactly similar to the prototype, in dimension and roughness for all heads, and centrifugal forces were exactly similar, it would be possible to extend the model curves to prototype values of Reynolds' number as shown on figure 46. This would be a procedure similar to plotting the friction factor, f, for closed conduits, against Reynolds' number. All straight circular pipes are similar, except for roughness, and Reynolds' number offers the correct model-to-prototype conversion. In the intake tower, however, dissimilar centrifugal effects may be present in model and prototype; so that the Reynolds' number extrapolation is not directly applicable.

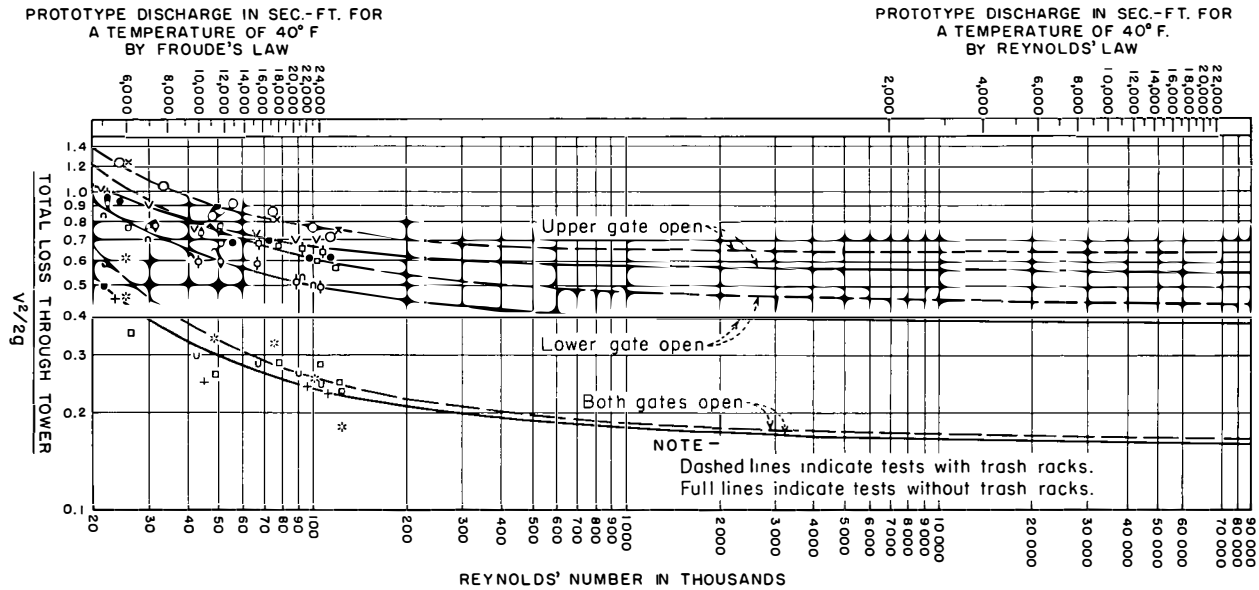

EXPLANATION

GATES OPEN	TEST NO.	WITH TRASH RACKS	TEST NUMBER (NO TRASH RACKS)
Upper	8 – × 11 – O	2 – 50' 1 – 182'	14 – ◊ 17 – v
Lower	9 – Δ 12 – o	2 – 50' 1 – 182'	15 – ◊ 18 – n
Both	7 – □ 10 – ✲	2 – 50' 1 – 182'	13 – + 16 – u

FIGURE 46—TOTAL LOSS THROUGH TOWER

Up to the present time, little success has been attained in expressing the relationship of all physical factors in a manner which will permit accurate extrapolation. It is necessary, therefore, to interpret prototype losses from models by one of two methods, first, by building a model large enough to reduce viscous effects to a negligible quantity; or, second, by constructing three or more smaller models to different scales. In the first method, the transformation can be made directly by Froude's law. In the second, the data from three or more models can be plotted with respect to Reynolds' number. By the latter method three or more sets of curves, one for each model, would be obtained on the graph instead

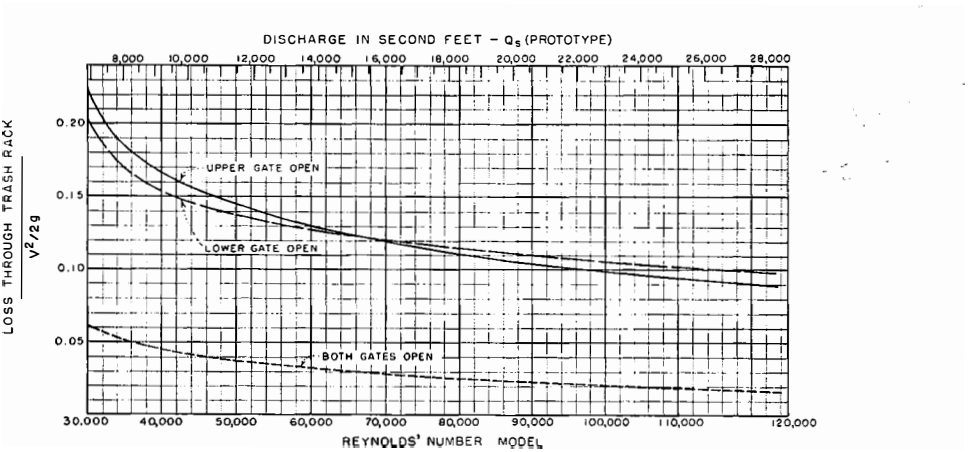

FIGURE 47—LOSSES THROUGH TRASH RACK

of continuous curves as shown on figure 46. Each set would resemble the set preceding it, but would be flatter and would be located lower on the graph. Lines representing similar heads could be drawn through the three or more sets of curves and extrapolated to include the desired prototype range.

Since only one small model was used for the intake tower experiments, the model-to-prototype conversion, for lack of better means, was made by the use of Froude's law. Due to viscous effects in the model, corresponding actual losses in the prototype will undoubtedly be smaller than those indicated by the following graphs. The actual amount of variation can be approximated by plotting the data by the two methods shown on figure 46 and interpolating between results. It can be stated with assurance that the

actual prototype losses will not exceed those obtained on the model when the conversion is made according to Froude's law.

34. Trash-Rack Losses.—The loss in head through the trash racks, for the three gate conditions, is represented by differences between the three pairs of curves on figure 46. These differences are plotted separately on figure 47, showing trash-rack losses directly for various conditions of flow.

Only reasonable reliance is assigned to the results of the trash-rack tests. As stated previously, the racks were constructed to scale and exhibited a commendable piece of workmanship; but their miniature size, small imperfections, surface tension, and traces of grease on the racks or oil in the water probably affected the results. In addition, it was physically impossible to construct the trash-rack bars in the model with a degree of roughness similar to that of the prototype.

Two lengths of trash rack were used in the tests, first, a rack 182 feet in length extending continuously over both gates; and, second, two racks 50 feet in length, each of which protected one gate. A detailed inspection of points from which lines were drawn on figure 46 shows that total losses through the tower for the two lengths of trash rack were analogous for the same conditions of flow. This indicates that above a certain length, factors other than length of racks determine their losses.

During the tests, the only place where trash collected on the racks was directly in front of the gates; the remainder of the racks were continuously clean. Trash racks are further discussed under the heading, "Intake Tower Electric-Analogy Studies", sections 44 to 48, inclusive.

35. Gate Entrance Losses. — The entrance loss through the upper gate is the difference between the energy head at the water surface of the reservoir and at the bottom of the upper gate. Trash racks were removed before individual losses in the gate tower were measured.

The entrance loss through the upper gate was computed using the equation:

$$h_{eu} = d_2 - h_{f(45\text{-}u)} - V^2/2g$$

where h_{eu} = Entrance loss through the upper gate.
d_2 = Difference in elevation between the water surface in the reservoir and the water surface in piezometer 45.

$h_{f(45\text{-}u)}$ = Pipe friction from piezometer 45 to the bottom of the upper gate.

$V^2/2g$ = Velocity head at piezometer 45.

The experimental values used in these calculations are shown on figure 44-D.

The entrance loss through the lower gate is the difference between the energy head at the water surface of the reservoir and at the bottom of the lower gate. This loss was computed using the equation:

$$h_{eb} = d_3 - h_{f(A\text{-}b)} - V^2/2g$$

where h_{eb} = Entrance loss through the lower gate.

d_3 = Difference in elevation between the water surface in the reservoir and the water surfaces in piezometer rings A to E, inclusive.

$h_{f(A\text{-}b)}$ = Pipe friction from elevation 890 to the piezometers below.

$V^2/2g$ = Velocity head computed at elevation 890.

Curves on figure 48 show entrance losses computed for two conditions of flow. Losses are expressed in terms of velocity head computed in the tower at elevation 890.0, and are plotted with respect to Reynolds' number for the model, computed at the same point. An additional scale is superimposed on the graph; so that

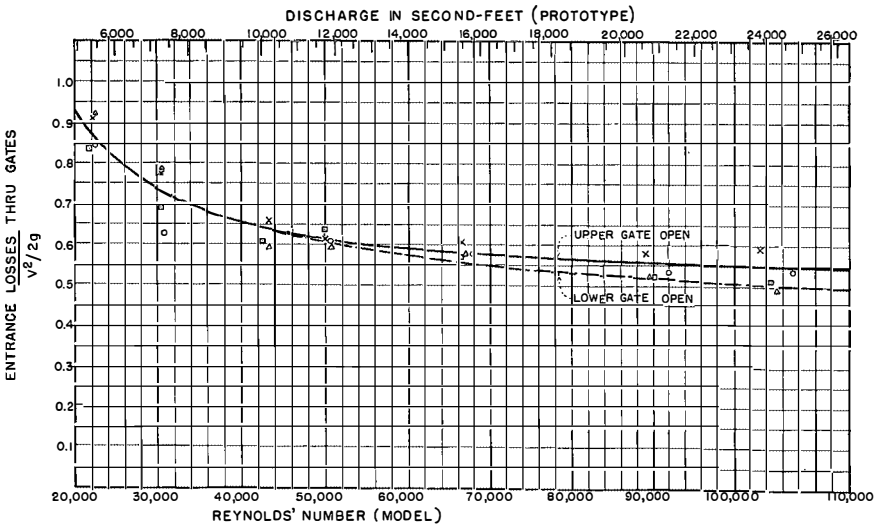

FIGURE 48—ENTRANCE LOSS AT GATES

entrance losses can also be expressed in terms of prototype discharge, computed according to Froude's law. Entrance conditions to the lower gate were slightly superior to those at the upper gate. It is evident from the preceding explanation that the entrance loss curve for the lower gate, shown on figure 48, is the same as that for the total loss curve, without trash racks, shown on figure 46; because the entrance loss was the total loss in this case. At the upper gate, the entrance loss was smaller than the total loss through the tower because it was necessary to deduct pipe friction.

Two sources of error exist in the analysis:

1. The mean velocity head was used in the computations because it was impractical to measure the velocity distribution in the tower to obtain the true energy head for each condition of flow. The velocity distribution in the tower was undoubtedly of a complex nature.

2. Where it was necessary to compute surface friction in the tower or in the auxiliary section of pipe below the tower, reference was made to the curves on figure 14. The pipes from which these curves were obtained were similar to the inner portion of the tower and any error that might arise from this source is small, since in no case did the length of pipe considered in the friction computations exceed 2.5 feet or 5.3 diameters. It should be noted again that prototype losses as shown on the graphs are approximate.

36. Head Required to Change Direction of Flow.—Water entered the gates in nearly a horizontal direction. Therefore a definite force was required to produce vertical acceleration. By measuring pressures directly above and below each gate, it was possible to compute the magnitude of the force acting within the tower. The original intention was to obtain hydraulic losses in the tower by observing the difference in elevation of the water surface outside and inside the tower. However, the force within the tower produced a rise in the surface level in the tower, and made the proposed method of computation impractical.

The head required to change the direction of flow at the upper gate with the lower gate closed, was found experimentally by the following equation:

$$h_{pu} = d_2 - d_1 - h_{f(45\text{-}u)}$$

where h_{pu} = Hydrostatic head in feet of water required to change the direction of flow at the upper gate.

d_2 = Difference in elevation between the reservoir water surface and the water surface in piezometer 45.

d_1 = Difference in elevation between the reservoir water surface and the water surface in the tower.

$h_{f(45\text{-}u)}$ = Pipe friction from piezometer 45 to the bottom of the upper gate.

The head required to change the direction of flow at the lower gate, with the upper gate closed, was computed in a similar manner, using the equation:

$$h_{pb} = d_3 - d_1 - h_{f(A\text{-}b)}$$

where h_{pb} = Hydrostatic head in feet of water required to change the direction of flow at the lower gate.

d_3 = Difference in elevation between the reservoir water surface and the water surface in piezometer rings A to E, inclusive.

d_1 = Difference in elevation between the reservoir water surface and the water surface in the tower.

$h_{f(A\text{-}b)}$ = Pipe friction from elevation 890 to the piezometers below.

The head required to change the direction of flow at the upper and lower gates, expressed in terms of velocity head, is plotted with respect to Reynolds' number for the model on figure 49.

A consideration of the principles of impulse and momentum provides a means of deriving, theoretically, the force required to change the direction of flow at the gates. It is not possible to obtain a rational theoretical solution from the forces acting entirely

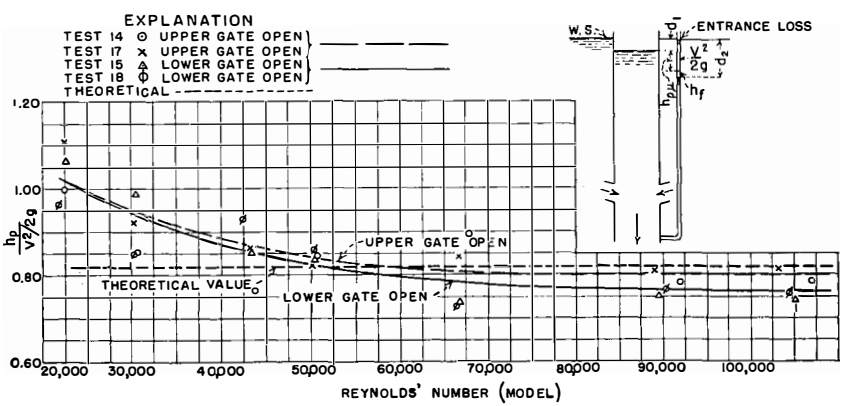

FIGURE 49—HEAD REQUIRED TO CHANGE DIRECTION OF FLOW AT GATES (MODEL)

within the tower, because conditions of flow at the gates are too indefinite. However, another logical method of attack is available, which is based on experimental data.

A free jet of water directed against a flat plate exerts a total force on the plate in the direction of the main jet equal to that given by the following expression:

$$F = wAV^2/g$$

where F = Total force exerted on plate.
w = Unit weight of water.
A = Area of main jet.
V = Velocity measured in jet.
g = Acceleration of gravity.

By analogy, if the direction of flow is reversed and water is assumed to flow radially inward toward the center of a circular plate and then turn downward away from the plate to form a solid column as in the case of the intake tower, the same law is assumed to apply. Professor A. H. Gibson[11] shows the bulb of pressure developed on a flat plate. The analogy with the intake tower is illustrated on figure 44-E. If it were possible to measure the pressure at a number of points within the tower, at one of the gates, the pressure distribution might resemble that shown on figure 44-E. From experiments by Gibson, it seems reasonable to assume that the maximum pressure head in the center of the tower is nearly equal to the velocity head, while the pressure at the inside face of the tower is approximately $0.66h_v$. By integrating pressures acting on individual small areas within the tower, an average pressure head of $0.82h_v$ is obtained. This is the average height at which water must stand within the tower to deflect the entering jets to a direction vertically downward.

The component of the total change in momentum per unit time, between any two points is the component of force in that direction required to produce this change. If the velocity of the water at the edges of the pressure bulb, outside the tower, is assumed to be in a horizontal direction, the vertical component of momentum at this point is zero. The change in momentum per unit time, or the total force in the vertical direction required to produce the change between the point outside the tower and a point in the vertical jet below the intake, is:

$$F = wAV^2/g$$

[11]Gibson, A. H., Hydraulics and its Applications, pp. 368 and 371.

This expression is identical with that for the total pressure on a flat plate.

If the pressure distribution required to produce the total force, F, is assumed to be similar to that of the flat plate, then the maximum pressure head is $V^2/2g$ and the distribution is as shown in figure 44-E. With this distribution, the average pressure head within the tower should be:

$$h_p = 0.82\ V^2/2g$$

Theoretical values are plotted on figure 49, together with

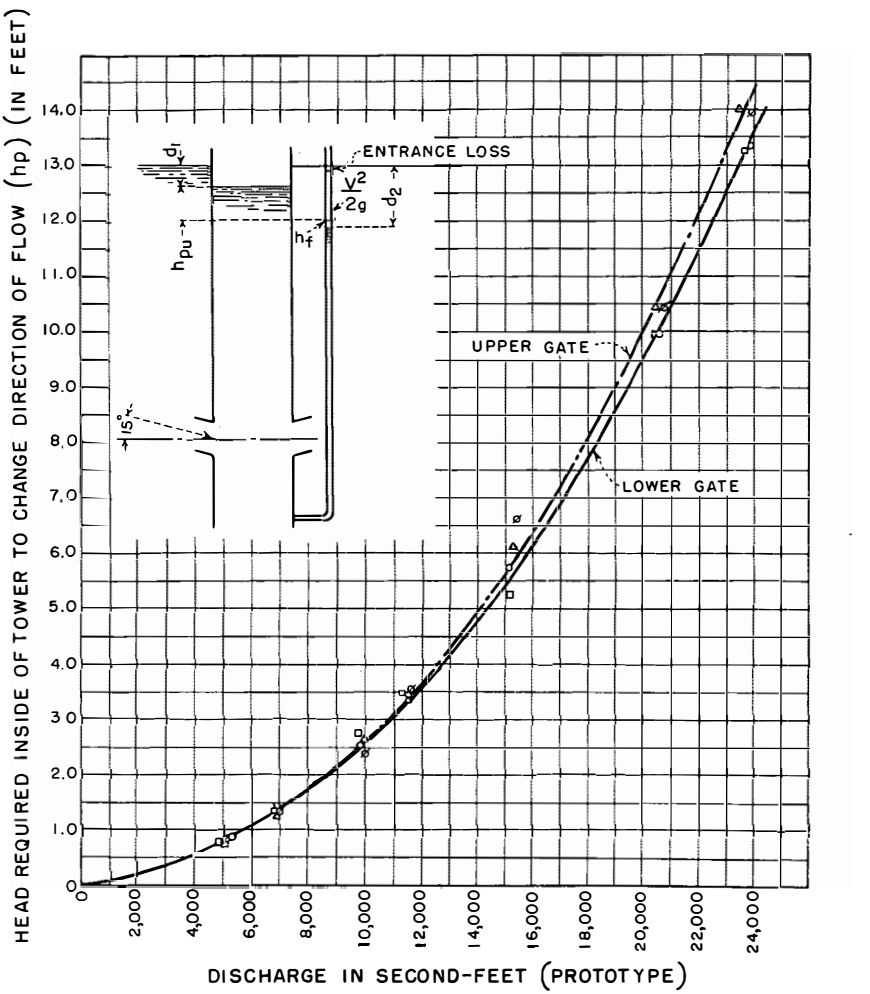

FIGURE 50—HEAD REQUIRED TO CHANGE DIRECTION OF FLOW AT GATES (PROTOTYPE)

actual values obtained on the model. The agreement is reasonably close and indicates that the analysis is a logical one. From the point of view of structural safety, it is of interest that substantial upward reactions exist in the converging intake passages; which, under some circumstances, might require special provisions in design.

To present the information obtained on the model in a more practical form, the results were transferred to prototype values according to Froude's law and plotted on figure 50. In this figure, the average head of water required inside the tower to change the direction of flow is plotted against the prototype discharge. These curves apply only for the upper and lower gate, operating separately.

37. Distribution of Discharge through Upper and Lower Gates. —It was desired to determine what portion of the total discharge passes through each gate when both gates are fully open. The piezometric drop, d_2, figure 44-D, bears a definite relationship to the discharge passing through the upper gate; the piezometric drop,

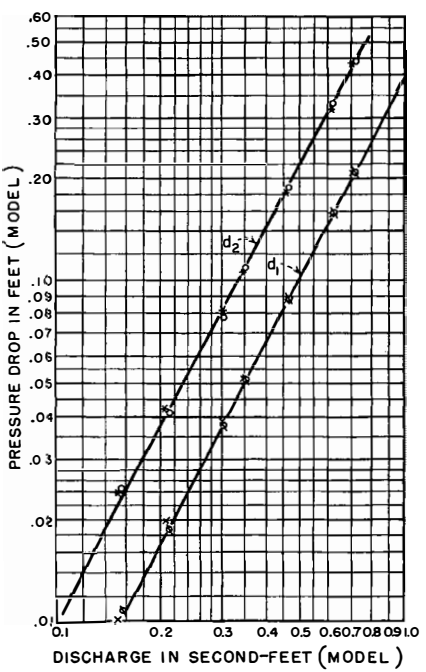

FIGURE 51—RELATION OF d_1 AND d_2 TO THE DISCHARGE

d_1, also shows a relationship to the discharge through the upper gate; and the two sets of data, when plotted logarithmically with respect to the model discharge, result in two straight lines as shown on figure 51.

Using these relationships, it is possible to compute the discharge through the upper gate when both gates are in operation. In other words, the pressure drops, d_1 and d_2, continue to be proportional to the discharge through the upper gate when both gates are in operation. These values are much smaller when both gates are open, since practically the same total discharge is divided between two gates.

For runs in which both gates were operating, the discharge through the upper gate was read from figure 51, for values of both d_1 and d_2, and the two discharges averaged for each run. The average was considered the discharge through the upper gate, while the remainder of the total discharge flowed through the lower gate. Figure 52 shows the percentage of total discharge flowing through each gate. The distribution of flow is expressed with respect to Reynolds' number, computed for the total flow passing elevation 890.0 in the model; and a second scale above the graph shows the approximate distribution with respect to the total prototype discharge. Figure 52 indicates that the flow through the upper gate is approximately 40 percent of the total, regardless of the reservoir elevation and magnitude of the discharge, providing the reservoir elevation remains above the upper gate.

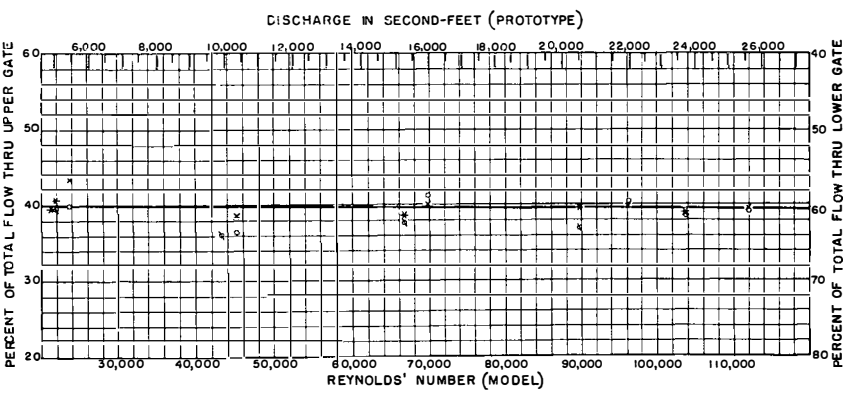

FIGURE 52—DISTRIBUTION OF FLOW BETWEEN UPPER AND LOWER GATE WITH BOTH GATES OPEN

38. Relation of d_1 and D_1 to Discharge.—Since the difference in elevation of the water surface outside and inside the tower, d_1, is proportional to the discharge, its relationship to D_1, the corresponding difference on the prototype, may have a practical value. Values of d_1 have been plotted on figure 53 with respect to Reynolds' number, computed at elevation 890.0 in the model, with the upper, lower, or both gates open. The drop, d_1, is the same for a given discharge with either the upper or the lower gate operating.

Although the drop, d_1, figure 44-D, consists of the gate entrance loss plus a small portion of the velocity head, it is a linear measurement; and by Froude's law was converted into an approximate prototype value by multiplying it by the model scale. This drop, d_1, is designated by the symbol, D_1, when converted to the prototype. Values of D_1 are plotted with respect to the prototype discharge on figure 54. This relation may prove useful for measuring the discharge through the prototype intake towers. The value of D_1 may be obtained by installing two float gages, one outside and one inside each tower. Entering the curves on figure 54 with these values the approximate discharge flowing through the towers may be obtained.

The relation of D_1 to discharge has been plotted on figure 54 for both conditions, with and without trash racks in place. It is believed that the curves shown for the prototype without trash racks are essentially correct. It has been previously stated that the friction loss through the model trash racks was undoubtedly excessive. Therefore, it can definitely be stated that the curves on figure 54, calculated from the model tests with trash racks, are

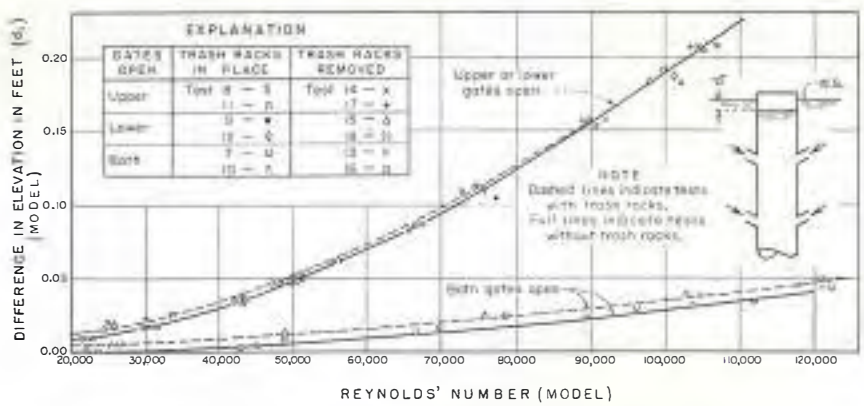

FIGURE 53—RELATION OF d_1 TO REYNOLDS' NUMBER (MODEL)

higher than would be similar curves made from actual tests on the prototype.

It is possible to actually calibrate the prototype intake towers by the Gibson Method[12] at the time acceptance tests are made on the turbines. With the information on figure 54 available, only a few points are necessary to establish a true calibration curve for the prototype.

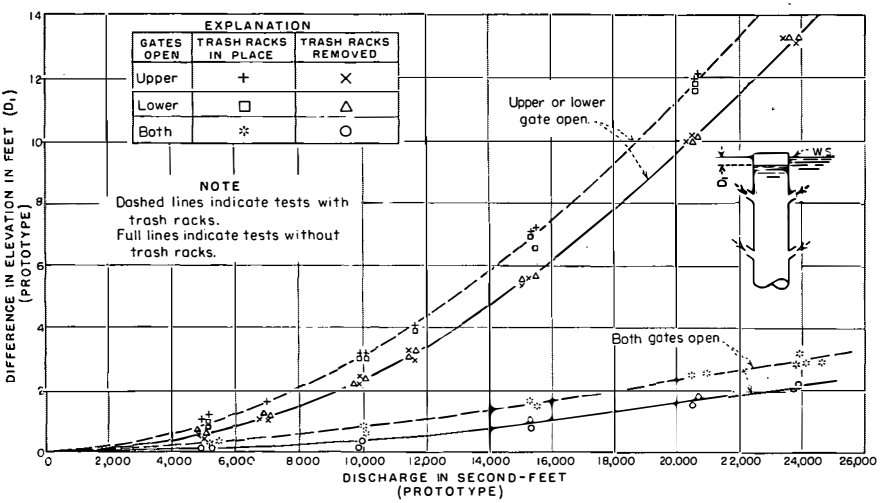

FIGURE 54—RELATION OF D_1 TO DISCHARGE (PROTOTYPE)

PENSTOCK ASSEMBLY

39. Apparatus. — At the conclusion of tests on the intake tower, the 3-foot vertical section of straight pipe below the tower was removed, and the penstock assembly model, constructed on a scale of 1:64, was connected in its place, see figure 55. The assembly consisted of accurate, butt-jointed, smooth, sheet-metal pipe, similar to that used in the penstock quantitative tests. The 90-degree, 5-5/8-inch diameter vertical bend directly below the tower, and a 40-degree horizonal bend of the same diameter located a short distance downstream, were molded of transparent pyralin. Four 2-7/16-inch diameter turbine penstocks, shown on figures 41, 55, and 56 were connected to the penstock header at a developed

[12]Gibson, Norman R., Pressures in Penstocks Caused by the Gradual Closing of Turbine Gates, Trans. Am. Soc. of Civil Engineers, vol. LXXXIII, p. 707.

angle of 105 degrees in a downstream direction as shown. Six 1-19/32-inch diameter branches leading to the canyon-wall outlets were connected to the downstream end of the penstock header by a reduction manifold.

Discharge through the four turbine branches was controlled and measured by sharp-edged circular orifices with diameters of either 0.75 or 0.875 inches. Flow through the six needle-valve branches was controlled and measured in a like manner by orifices with diameters of either 1.006 or 1.250 inches. The head on each orifice was observed from a piezometer located in the end of each branch. These orifices were previously calibrated in similar positions by weighing the discharge.

Piezometers for measuring pressure intensities were installed

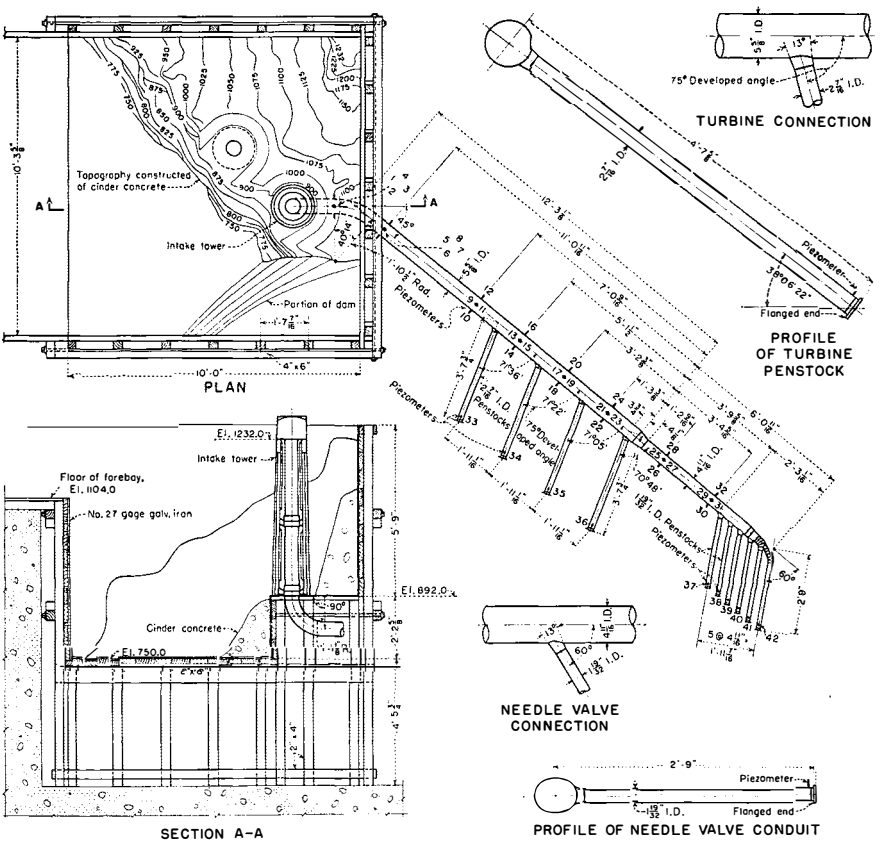

FIGURE 55—MODEL OF PENSTOCK ASSEMBLY—SCALE 1:64

in rings at intervals down the main header, as shown on figure 55. A ring consisted of four piezometers, spaced 90 degrees apart, and each piezometer was connected to an individual glass tube on the manometer board.

40. Pressures at Base of Tower.—In the original design of intake towers, air vents were provided in the region below the lower gate, to relieve any negative pressures which might be created by the flow conditions, see figure 40. A question arose as to the necessity for these vents and piezometers 46 to 49, inclusive, see figures 43 and 57-D and E, were installed to study pressure conditions in this region.

Tests were made with the upper, lower, and both gates open; and piezometric drops, d, between the water surface in the reservoir and the water surfaces in the four piezometers, were recorded. These drops, converted into prototype values, are plotted against discharge for the individual piezometers for the three conditions of gate opening, see figure 57. For the upper gate open and lower gate closed, the drop, d, recorded at piezometer 46, consists of the following:

$$d = h_{f(b\text{-}u)} + V^2/2g + h_{eu} + h_s$$

where d = Difference in elevation between the water surface in the reservoir and the water surface in piezometer 46.

$h_{f(b\text{-}u)}$ = Pipe friction from piezometer to bottom of upper gate.

$V^2/2g$ = Velocity head at piezometer 46.

h_{eu} = Entrance loss at upper gate.

h_s = Drop in pressure at the piezometer caused by irregularity of flow and suction effect.

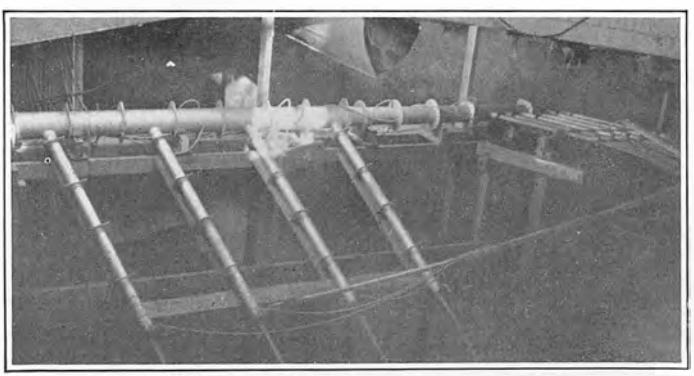

FIGURE 56—MODEL OF UPPER ARIZONA PENSTOCK

The largest piezometric drop occurred at piezometer 46 for the conditions of flow studied. The curves for piezometer 46, shown on figure 57, were replotted on figure 58 for the three conditions of gate opening. In addition, two other curves, which indicate the maximum approximate discharge obtainable with all needle valves operating and with all needle valves and turbines operating for various levels of the reservoir, have been superimposed on this graph. From these two sets of curves, the pressure at piezometer 46 may be obtained for any particular discharge. For example, with the water surface in the reservoir at elevation 1200, and a discharge of approximately 21,000 second-feet through the lower gate, the water surface in piezometer 46, expressed in prototype, would stand 42 feet below the reservoir water surface, or at elevation 1158, and a pressure of 268 feet of water would exist at the point where this piezometer is located. For the same discharge passing through the upper gate, the water surface in piezometer 46 would stand at elevation 1170. For a discharge of

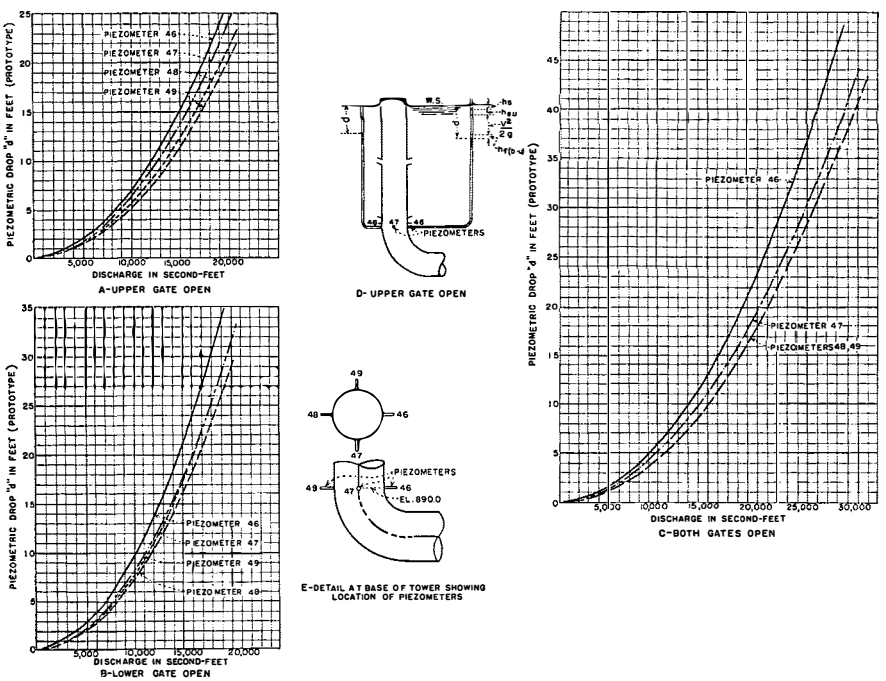

FIGURE 57—RELATION OF PRESSURE DROPS AT PIEZOMETERS 46, 47, 48, AND 49 TO THE DISCHARGE

21,000 second-feet flowing through both gates, the water surface in piezometer 46 would stand at elevation 1174. Water surfaces in the other three piezometers would stand above this elevation. From these results it is evident that a vacuum cannot exist at the base of the tower and that air vents are unnecessary.

41. Bend Losses.—The combined loss for the two bends di-

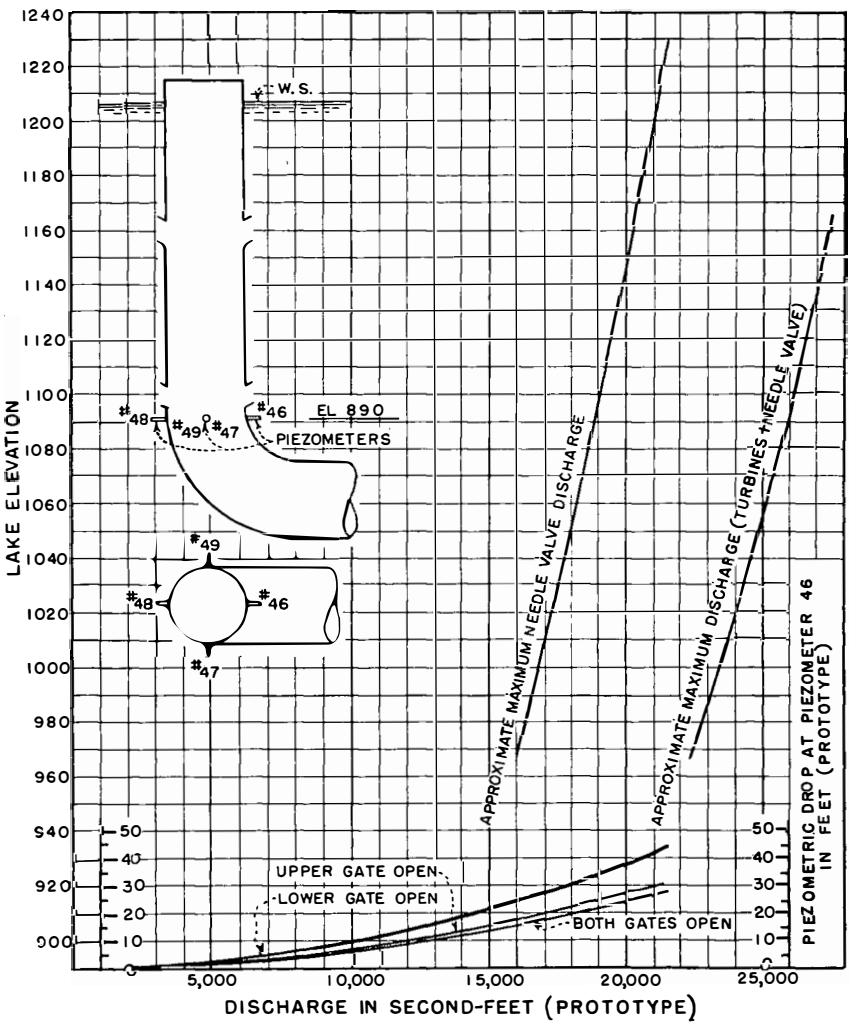

FIGURE 58—MINIMUM PRESSURES AT BASE OF INTAKE TOWER

rectly below the tower was obtained from runs in which only the upper gate was open. These bends, shown on figure 41, consisted of a 90-degree vertical bend and a 40-degree horizonal bend, interconnected by a straight section 0.88 diameters long. Flow through the lower gate would have materially affected the velocity distribution in the bends. The loss was obtained by the equation:

$$h_b = d_x - (V^2/2g + h_f + h_t)$$

where h_b = Combined bend loss.

d_x = Difference in elevation between the water surface in the reservoir and the average water surface in the manometer tubes connected to piezometers 9 to 12, inclusive, shown on figure 55.

$V^2/2g$ = Velocity head at base of tower, elevation 890.

h_f = Pipe friction from piezometers 9, 10, 11, and 12 to the downstream edge of the horizontal bend.

h_t = Total loss in intake tower.

A better velocity distribution existed at piezometers 9 to 12 than at 5 to 8 so the former were used in the computations.

The combined loss for the two bends, expressed in terms of velocity head at the base of the tower, is plotted with respect to Reynolds' number for the model on figure 59. An additional scale

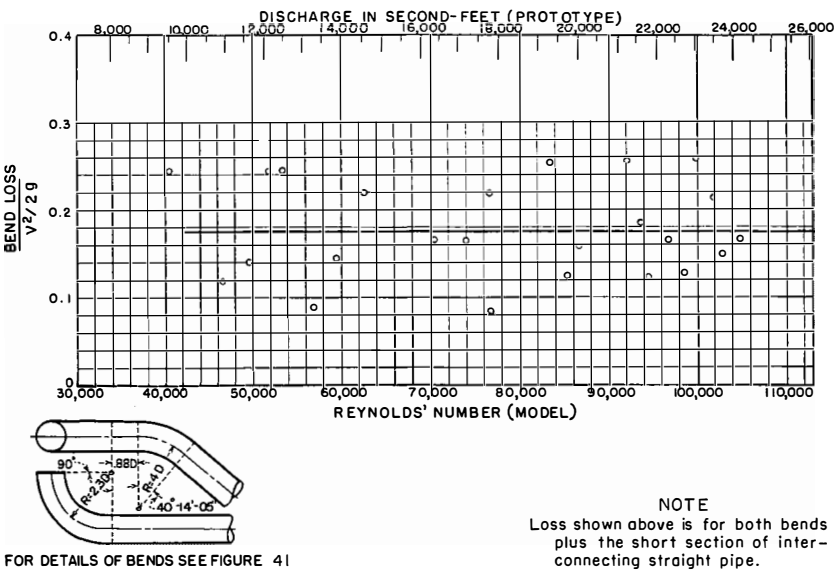

FIGURE 59—LOSS IN BENDS IN UPPER ARIZONA PENSTOCK

has been superimposed on the upper portion of the graph from which the approximate bend loss for the prototype can be obtained.

42. Tests on Penstock Assembly.—Tests were made on the complete penstock assembly, during which the discharge, head, and piezometer readings were recorded. From these tests the energy head at each piezometer ring was plotted as far down the penstock as possible. Energy head gradients for a few runs are shown on figure 60. The diagrams indicate a gain in energy head in the main penstock, immediately downstream from the first junction. A gain in energy head is evident at the next junction but is less than at the first. The third junction shows a slight gain in energy head and the fourth shows a loss. The gain was usually observed, even when there was no flow through the branch. It will be recalled that similar results were obtained in the penstock junction quantitative tests described in section 15. The apparent gain is undoubtedly due to an error in computing velocity head. Due to the irregular velocity distribution at these points, the mean veloc-

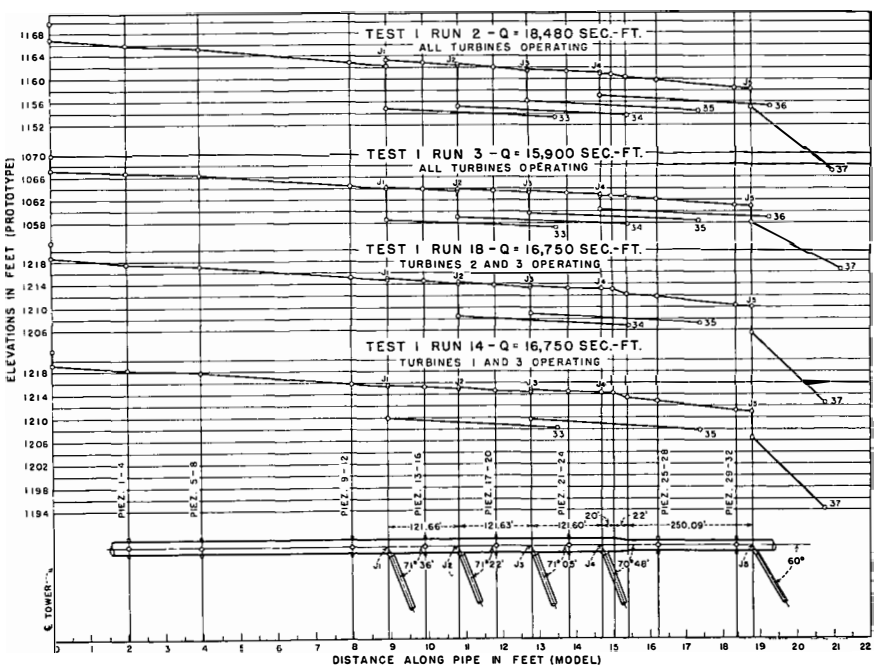

FIGURE 60—PRESSURE PLUS VELOCITY HEAD GRADIENT

ity head should be increased by multiplying it by a velocity head coefficient, a, which presumably lies within the limits of 1.03 to 1.15 and probably varied at each junction for each condition of discharge.

As an interesting comparison, pressure gradients for the runs shown on figure 60 are plotted on figure 61. There is a decided increase in pressure at each turbine junction, which is due to the reconversion of a portion of the velocity into pressure head. As the number of piezometers was limited, it was possible to plot only the pressures down to junction 5. An attempt was made to analyze junction losses in the assembly model, but the number of piezometers was insufficient to supply the necessary information.

43. Conclusions.—It is believed that the method employed in analyzing model results on the intake tower and penstock assembly was sufficiently accurate and that results are dependable insofar as the model data is concerned. It was desired, however, to extra-

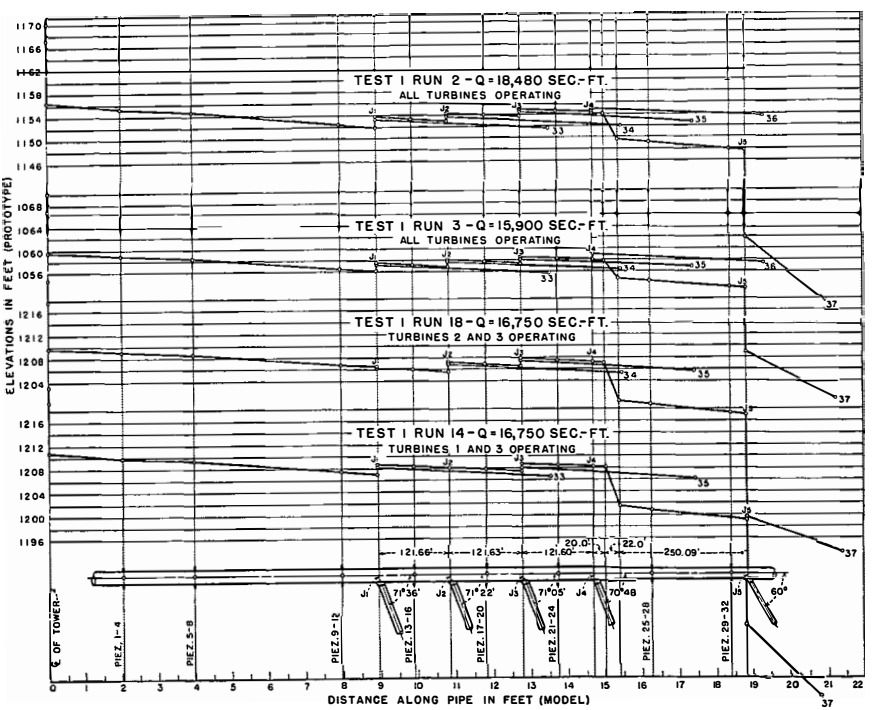

FIGURE 61—PENSTOCK PRESSURE GRADIENT

polate model results to obtain prototype values, since this was one of the objects in performing the experiments. With a single small model of this type it is not possible to accurately interpret conditions that prevail in the prototype.

The extrapolation from model to prototype has, in the foregoing graphs, been made according to Froude's law, for lack of a more accurate method. As a result, hydraulic losses, plotted with respect to prototype discharge, are unquestionably larger than those that may actually exist on the prototype. It is predicted that losses in the full-size structure will probably range from 5 to 20 percent less than those indicated by the graphs. For this reason, it is advisable to refer to the prototype values, as shown on the graphs, as approximate rather than exact values.

INTAKE TOWER ELECTRIC-ANALOGY STUDIES

44. Introduction. — The electric-analogy method, previously used in the analysis of problems of seepage through earth dams and under masonry dams on porous foundations[13], was applied as a means of determining the direction of flow of water entering the intake tower and incidentally to study the merits of the method itself. In this particular problem it was necessary to obtain a certain amount of information from the hydraulic model before the analogy model could be properly constructed.

45. Apparatus.—The apparatus consisted of a shallow glass tray, 39 inches long, 18 inches wide, and 3 inches deep, equipped with a leveling screw at each corner. A radial section of the tower, constructed of redwood, on a scale of 1:100, was cemented to the bottom of the tray. Copper plate electrodes were placed in position in the tray and a solution of sodium chloride used as a conductor. A drawing of the apparatus is shown on figure 62, and a photograph of the tray in a vertical position is shown on figure 63. The current used in the experiments was obtained from a 110-volt, 60-cycle source. By inserting a bank of lamps in series with the apparatus, as shown on figure 62, the potential across the electrodes was reduced to about 20 volts. A high-resistance wire, one meter in length, stretched on a meter stick on one side of the tray,

[13]Lane, E. W., Campbell, F. B., and Price, W. H., The Flow Net and the Electric Analogy, Civil Engineering, October 1934, p. 510.

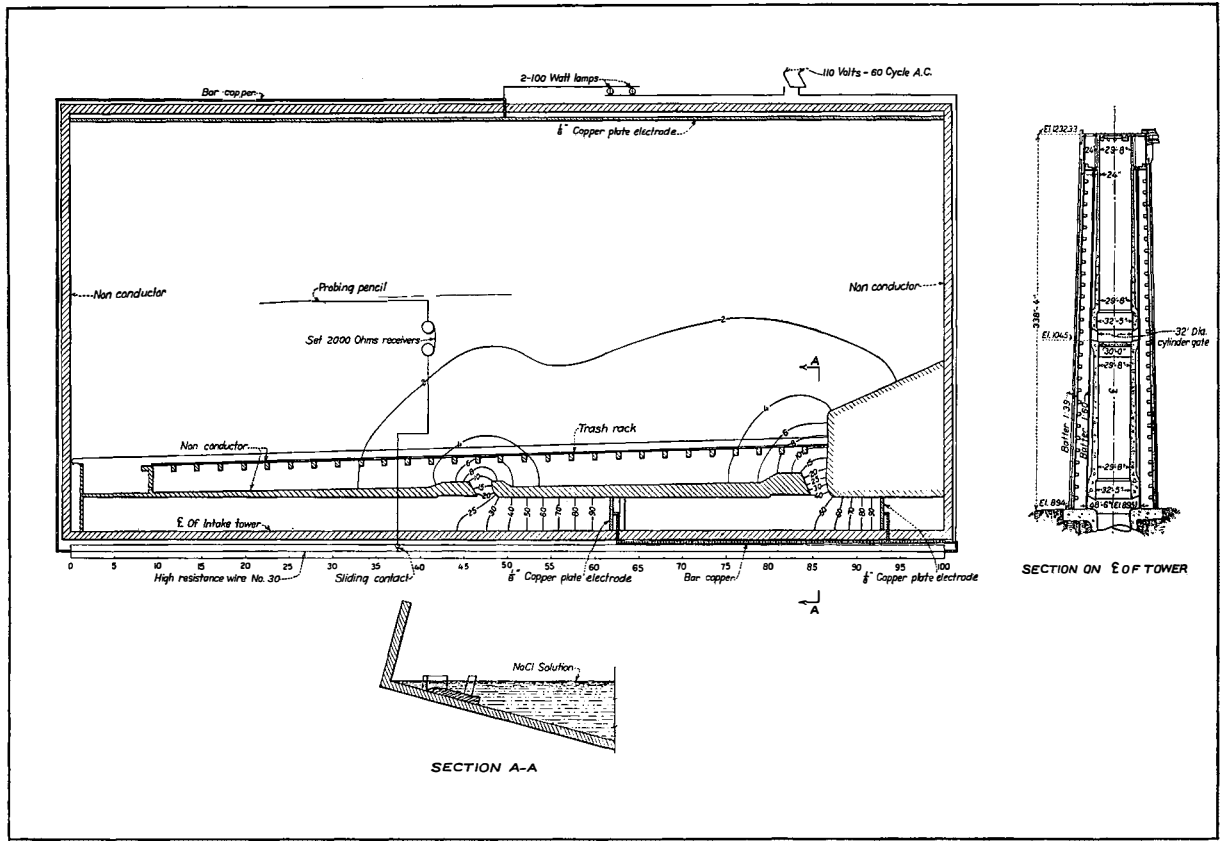

FIGURE 62—INTAKE TOWER ELECTRIC-ANALOGY MODEL

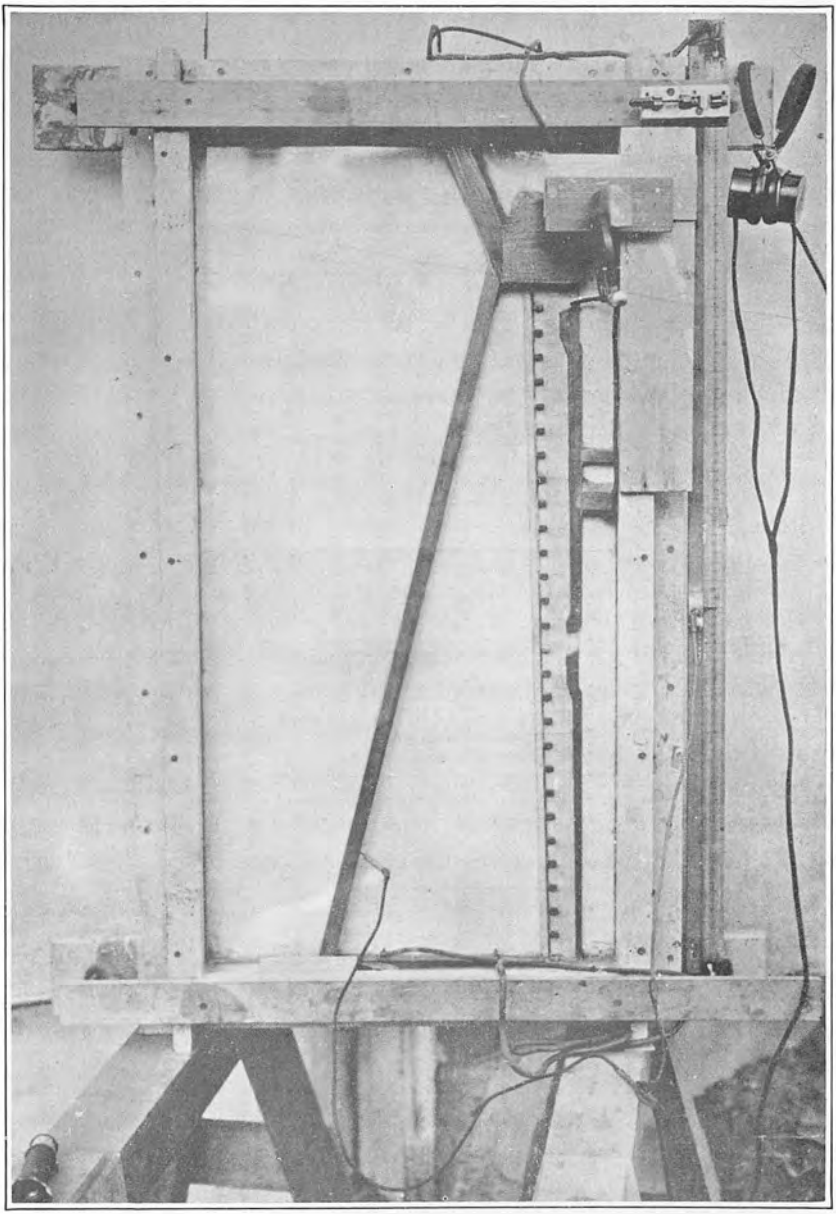

FIGURE 63—ELECTRIC-ANALOGY APPARATUS REPRESENTING A RADIAL SECTION OF THE INTAKE TOWER ADJACENT TO THE CANYON WALL

was connected in parallel with the circuit to constitute a Wheatstone bridge. A spring was attached to one end of the wire to keep it taut at all times, as the current raised the temperature of the wire and lengthened it. A metal terminal on one end of the meter stick made a continuous contact with the stretched wire, keeping the length connected in the circuit at exactly one meter, regardless of expansion or contraction. A circuit was established from a sliding contact on the high-resistance wire to the liquid conductor by a wire which had a set of head-phones and a probing pencil connected in series with it. All connections in the apparatus were made with heavy copper wire of very low resistance.

The radial section of the tower was represented by setting the tray on a slope with the electrolyte at zero depth on the center line of the tower, as shown in section A-A, figure 62. Variables in the experiment were length of trash racks, the three gate combinations, and positions of electrodes. The apparatus in figure 62 represents a section of the tower nearest the river with both gates open. The long electrode was connected to one side of the circuit and the two small electrodes in the tower were connected to the other side. The lines resembling contours represent points of equal potential. The purpose of the apparatus was to determine the position of these lines for different percentages of the total potential drop across the electrodes.

The position of any particular potential line was determined by setting the sliding contact on the resistance wire at the point giving the desired potential drop, and moving the probing pencil about in the salt solution until a point was reached at which the absence of a hum in the head-phones indicated that no current was flowing. To find the position of the potential line representing two percent of the drop between electrodes, the sliding contact was set at a point on the resistance wire representing two percent of its length, and the probing pencil moved about in the electrolyte until the alternating-current hum in the head-phones faded. This indicated that the probing pencil was at a point in the solution where the potential drop was two percent of the total drop across electrodes. Other points were located in a similar way, with the same setting of the sliding contact, until the number was sufficient to draw the two-percent line. Other potential lines were located in a similar manner.

46. Section of Tower Nearest the River.—The first tests were

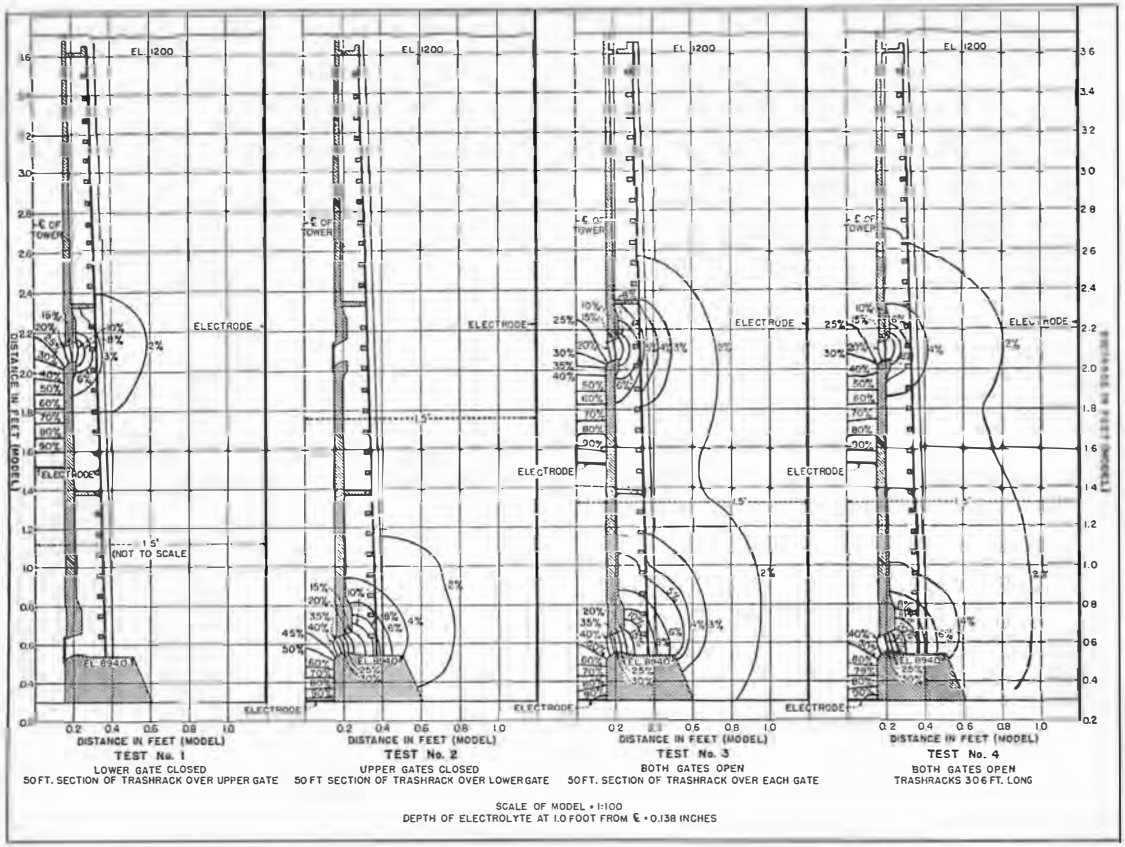

FIGURE 64—ELECTRIC-ANALOGY RESULTS ON RADIAL SECTION OF TOWER NEAREST TO THE RIVER

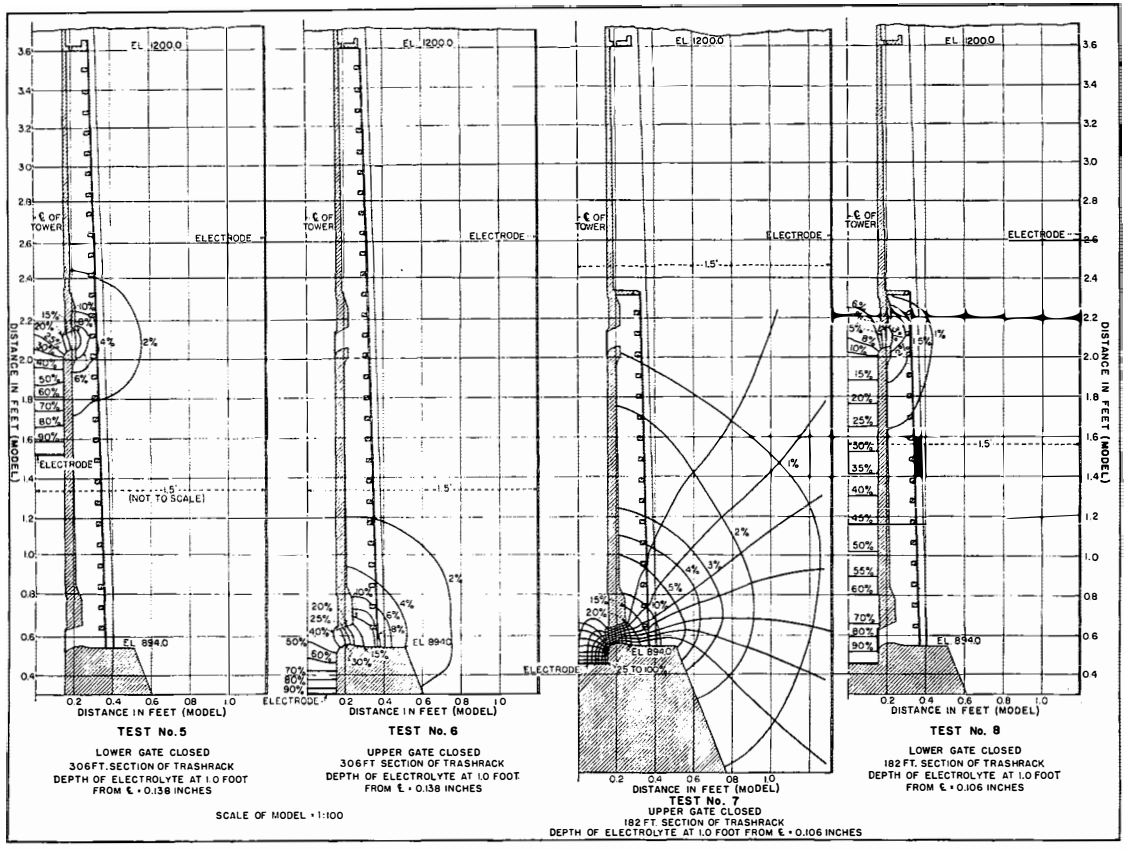

FIGURE 65—ELECTRIC-ANALOGY RESULTS ON RADIAL SECTION OF TOWER NEAREST TO THE RIVER

made on a radial section of the tower located nearest the river, with electrodes in the positions shown in figure 62. These tests were made with three different lengths of trash rack: 306 feet, 182 feet, and two 50-foot racks. The resulting equipotential lines are shown on figures 64 and 65.

Comparing tests 2 and 6, figures 64 and 65, in which the upper gate was closed and trash-rack lengths were 50 feet and 306 feet, respectively, the corresponding equipotential lines practically coincide, which indicates that the total potential drops between electrodes agree closely. This means that the resistance to flow through the 50-foot rack was no greater than that through the 306-foot rack.

Tests 1 and 5, shown on figures 64 and 65, were made under the same conditions, except that the lower gate was closed and the upper gate open. Again the potential lines show a close agreement, which indicates that the loss was no greater through the 50-foot rack than through the 306-foot rack.

Tests 3 and 4 on figure 64 were made on the same segment of the tower with both gates open. The potential lines for two 50-foot racks agree very well with those for the 306-foot rack. The agreement of potential lines is not so close for the range from one percent to five percent, because points for these lines were more difficult to locate than those for larger potential drops. The experiments, thus far, indicate that with racks free from trash, a length of 50 feet in front of each gate will provide sufficient rack area on the river side of the tower.

Tests 7 and 8, shown on figure 65, were made on the same radial section of the tower with a 182-foot trash rack, as used in the final design. These, however, cannot be directly compared with tests previously described, because the positions of the electrodes were shifted and the tilt of the tray changed. They are included as a matter of record.

47. Section of Tower Nearest the Canyon Wall.—A similar set of tests was made on a radial section of the tower located on the side nearest the canyon wall. Figure 63 shows the model for this condition. Tests 11 and 14, shown on figures 66 and 67, made with the upper gate closed, using two 50-foot and one 306-foot rack, respectively, show differences in positions of potential lines. This indicates that the total potential drop across the electrodes for the 50-foot racks was greater than for the 306-foot rack. The increase

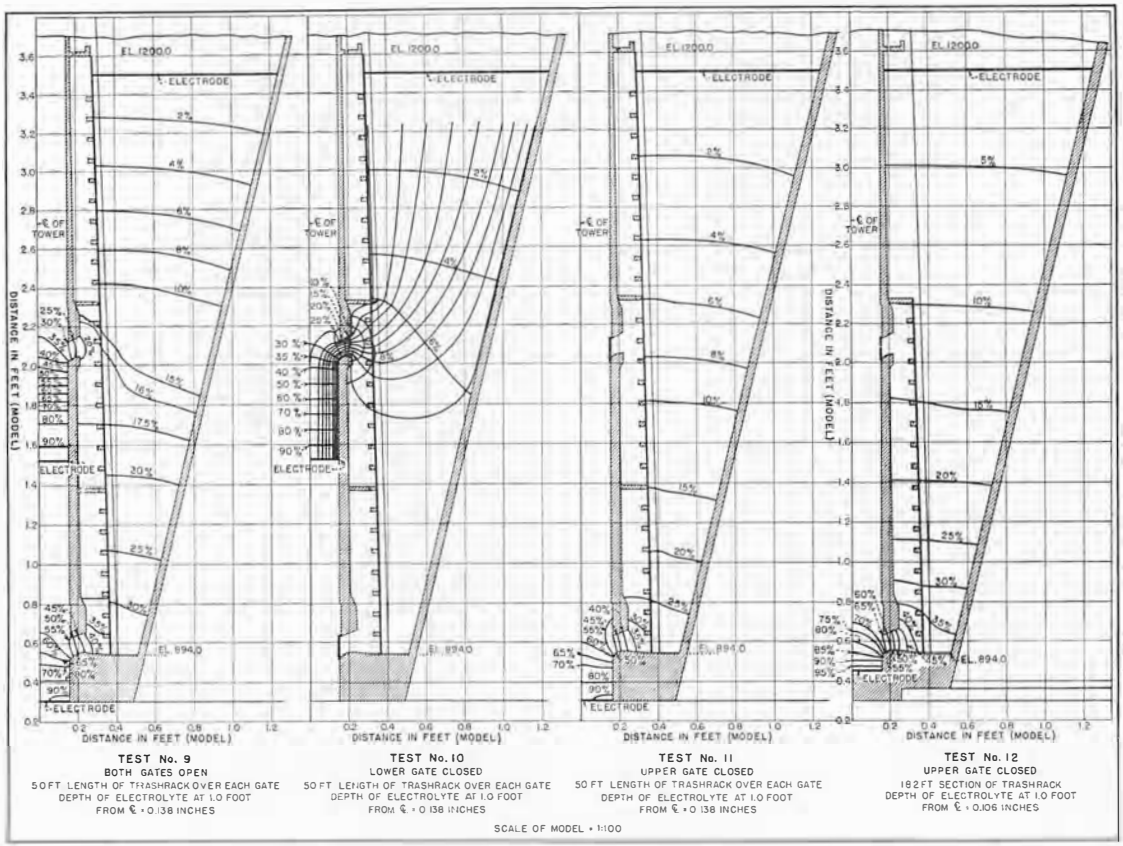

FIGURE 66—ELECTRIC-ANALOGY RESULTS ON RADIAL SECTION OF TOWER NEAREST THE CANYON WALL

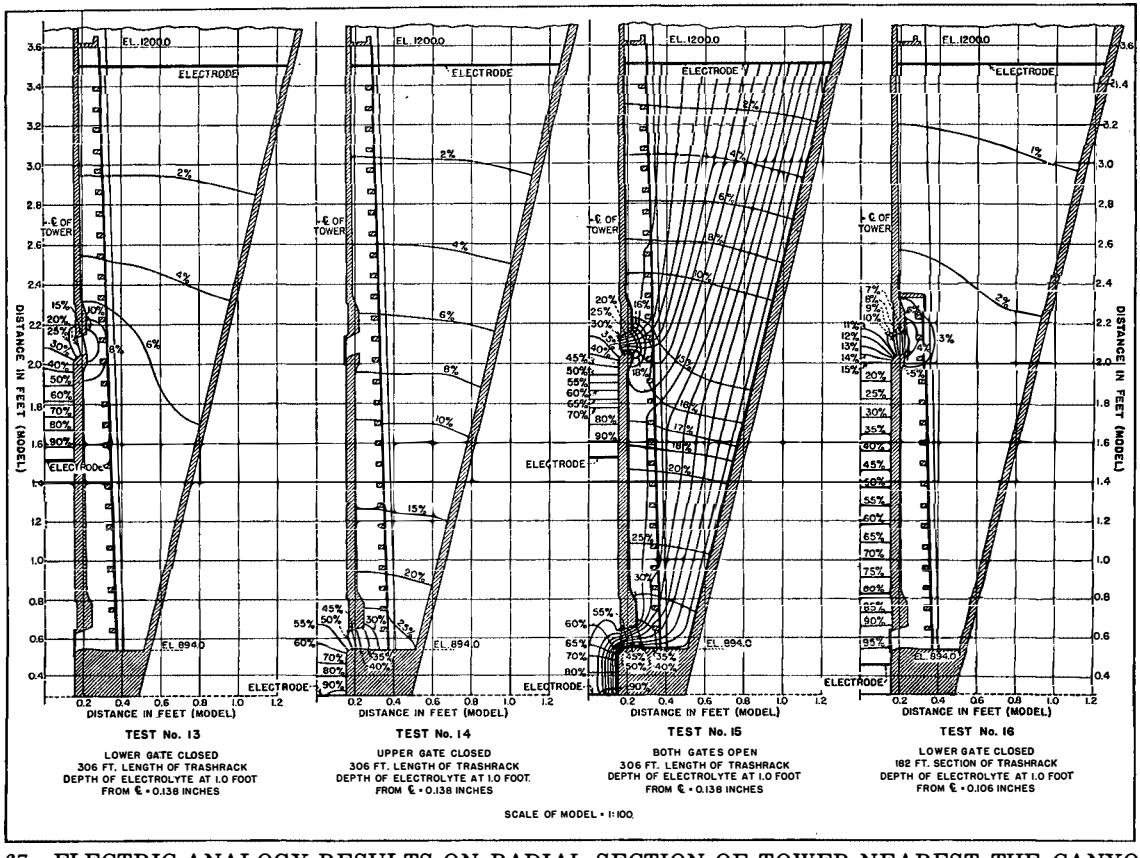

FIGURE 67—ELECTRIC-ANALOGY RESULTS ON RADIAL SECTION OF TOWER NEAREST THE CANYON WALL

is due to new boundary conditions which reduce the area of approach and change the direction of flow to the gates. With this decrease in approach area there must be an increase of velocity to maintain a continuity of flow. As velocity is proportional to potential gradient, the gradient must increase as the trash racks and gate openings are approached. The increase is indicated by a reduction in distance between equipotential lines. Closely spaced potential lines indicate flow concentrations and likewise high velocities.

Tests 10 and 13 on figures 66 and 67 were made with the upper gate open and the lower gate closed, using two 50-foot racks and one 306-foot rack, respectively. A noticeable increase in resistivity of the circuit was again witnessed when the 306-foot rack was replaced by the two 50-foot racks.

Tests 9 and 15, shown on figures 66 and 67, were made with both gates open, using two 50-foot racks and one 306-foot rack, respectively. Little difference in positions of potential lines was obtained. This could logically be expected, since the same discharge was divided between the two gates, and the effective rack area was doubled in the case of the two 50-foot racks. With one gate open, flow could occur only through one 50-foot rack.

Tests 12 and 16, shown on figures 66 and 67, represent flow through the upper and lower gate, respectively, with 182-foot trash racks as finally designed. These results, however, cannot be directly compared with others, as the tilt of the tray was changed and positions of electrodes shifted.

Losses shown by the experiments with the model section nearest the canyon wall are exceptionally high because actual flow conditions were not truly represented. In the experiment, all water was assumed to flow downward on the canyon-wall side of the tower, while actually a large portion will flow around the tower.

Flow nets have been drawn for tests 7, 10, and 15. According to hydrodynamics, flow lines should cross potential lines at right angles. The volumes bounded by flow lines may be considered as stream tubes, each carrying an equal quantity of water. To establish one end of each flow line, it was assumed that the velocity was constant across the electrode sections inside the tower. The electrodes were then divided into segments which, if revolved, would form annular rings. From these, flow lines were projected and drawn perpendicular to equipotential lines.

In the two-dimensional flow net, where the electrolyte is con-

stant in depth, a rectangle formed by the net bears a constant ratio to every other rectangle in the net, by which the average velocity in each stream tube can be determined. For the flow nets drawn for tests 7, 10, and 15 this ratio does not exist. With a sloping tray, the flow net is altered by a third dimension. Stream tubes in the three-dimensional net have no parallel sides and it is not possible to obtain velocities directly from the length or breadth of the rectangles, as in the two-dimensional system. The purpose in drawing flow lines in tests 7, 10, and 15 was merely to indicate the direction of flow. It is possible, however, to obtain velocities in these three-dimensional nets by a simple but laborious method.

There are eight stream tubes in test 7, figure 65, each carrying an equal quantity of water. The discharge through each tube is equal to one-eighth of the total discharge flowing into this radial segment of the tower. Figure 44-F shows a portion of a stream tube in a two-dimensional net, and figure 44-G, a portion of a stream tube in a three-dimensional net. In the first, d is a constant throughout, while in the second, it is a variable. The velocity at any point in either stream tube is $V = q/wd$, where q is the discharge through the stream tube. If the velocity is known at any point in the two-dimensional net, it is necessary only to measure w to obtain the velocity at any other point. In the three-dimensional net, d, a variable, but known at all points, must also be considered in computing the velocities.

The greatest source of error in obtaining velocities in a three-dimensional flow net of this type is not in the computations but in the construction of the net. It is usually necessary to make one or two assumptions before attempting to draw a net, and after these are made and the net commenced, it is still necessary to use a certain amount of judgment.

Seven stream tubes enter the upper gate and eight enter the lower, each carrying an equal discharge. This would indicate that 47 percent of the flow was passing through the upper gate and 53 percent through the lower. On the opposite side of the tower, where the area of approach is not restricted, the proportion of the total flow through the upper gate should be less, with the result that a greater percentage of the total flow should pass through the lower gate. To obtain the correct proportion of flow through the upper gate, electrodes in the tower were shifted by trial until the flow through each gate agreed with that measured on the hydraulic model. Results show that the electric-analogy method

is applicable to this type of problem, especially where only one intake is involved, since information can be obtained regarding trash-rack areas and obstructions to flow, readily and at little expense. The double intake on the Boulder Dam gate towers complicated the problem considerably.

48. Conclusions.—The outstanding advantages in using the electric-analogy method, where applicable, are its simplicity, its speed in obtaining results, and its low cost. It is important, however, in interpreting results of a study of this nature, to keep in mind limitations of the method. The symmetry and precision of results are a temptation to extend the method at the expense of factors which cannot be considered in the apparatus.

CHAPTER IV—TESTS ON TUNNEL-PLUG OUTLET

TUNNEL-PLUG OUTLET MODEL

49. Introduction.—It is intended to discharge surplus water at Boulder Dam through needle valves rather than over the spillways. Since 9,000,000 acre-feet of storage is to be held in reserve for flood control, water can be discharged over the spillways only when this space is filled to a large extent. The needle valves may, therefore, discharge large quantities of water over long periods. This will be particularly true after the reservoir is first filled and before the power demand requires the full stream flow.

Needle valves in the canyon-wall outlet works discharge into the open air. Those in the diversion tunnels are located a considerable distance from the tunnel portals to effect appreciable economy in the cost of the steel-plate outlet pipe, and to avoid disadvantages of large quantities of spray in the vicinity of the powerhouse and the high-voltage switching facilities.

Since the tunnel-plug needle valves are located a considerable distance from the portals, they discharge into a closed space. The combined discharge of the six valves in each tunnel may be as much as 21,400 second-feet with a maximum head of 454 feet, releasing energy equivalent to 1,100,000 horsepower. Great care is necessary to prevent damage resulting from this release of energy. Six 72-inch needle valves are required in each outlet, each valve being capable of discharging a maximum of 3,670 second-feet at a velocity of about 175 feet per second. Figure 68 shows the preliminary design for the lower Arizona penstock and figure 69 shows the tunnel-plug outlets. It is important that the six valves in each outlet be arranged so that the jets will not concentrate at one point and produce unnecessary disturbances in the tunnel.

It was at first expected that tunnels would be necessary to supply air downstream from the valves to replace that ejected by streams of water from the valves. Experience with other installations has demonstrated that in certain cases this is necessary.

An extensive series of tests was conducted on models using three different scales to observe the action of the needle-valve jets in the tunnels and to determine the feasibility of installing air-

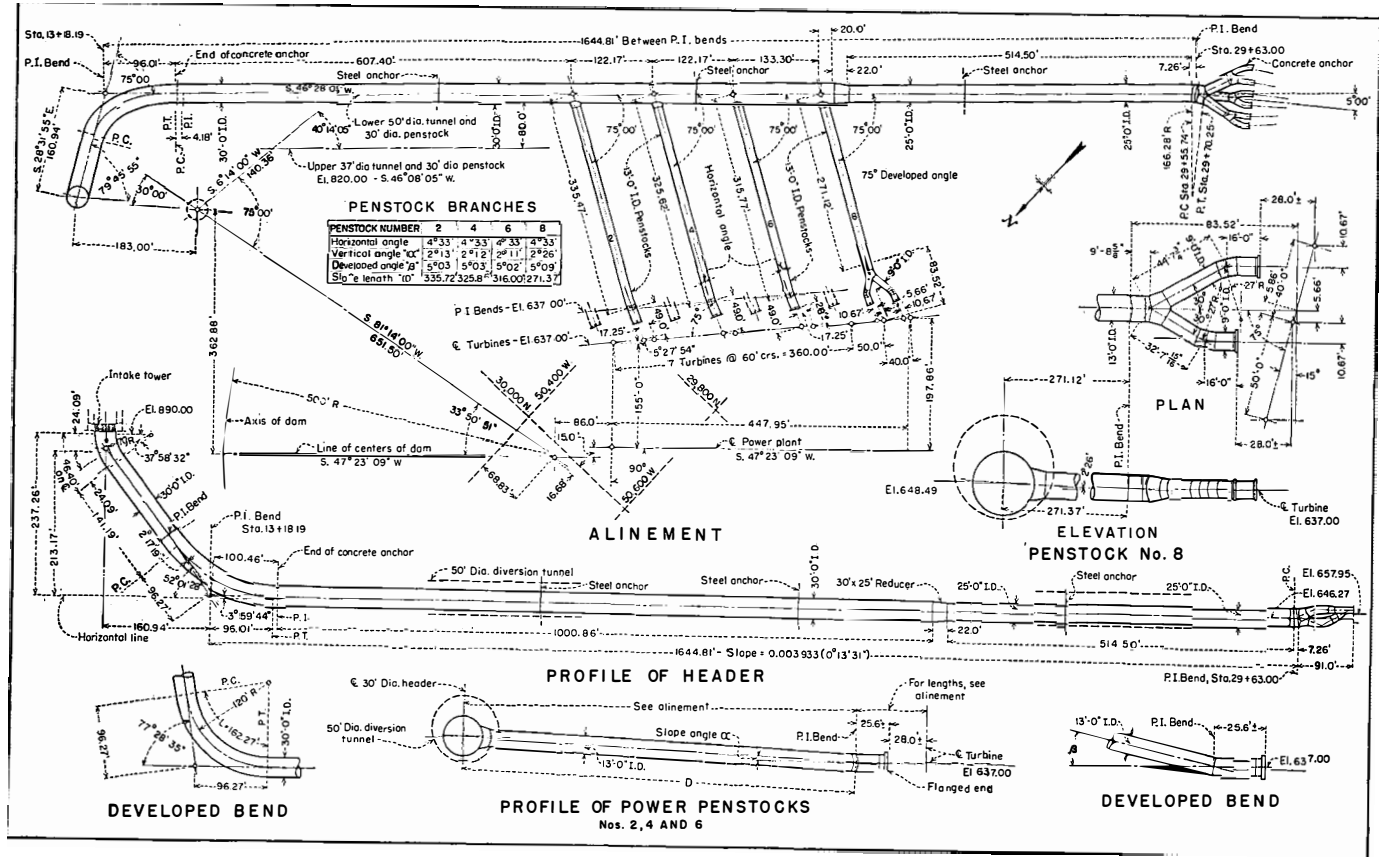

FIGURE 68—HEADERS, PENSTOCKS AND CONDUITS FOR LOWER ARIZONA TUNNEL

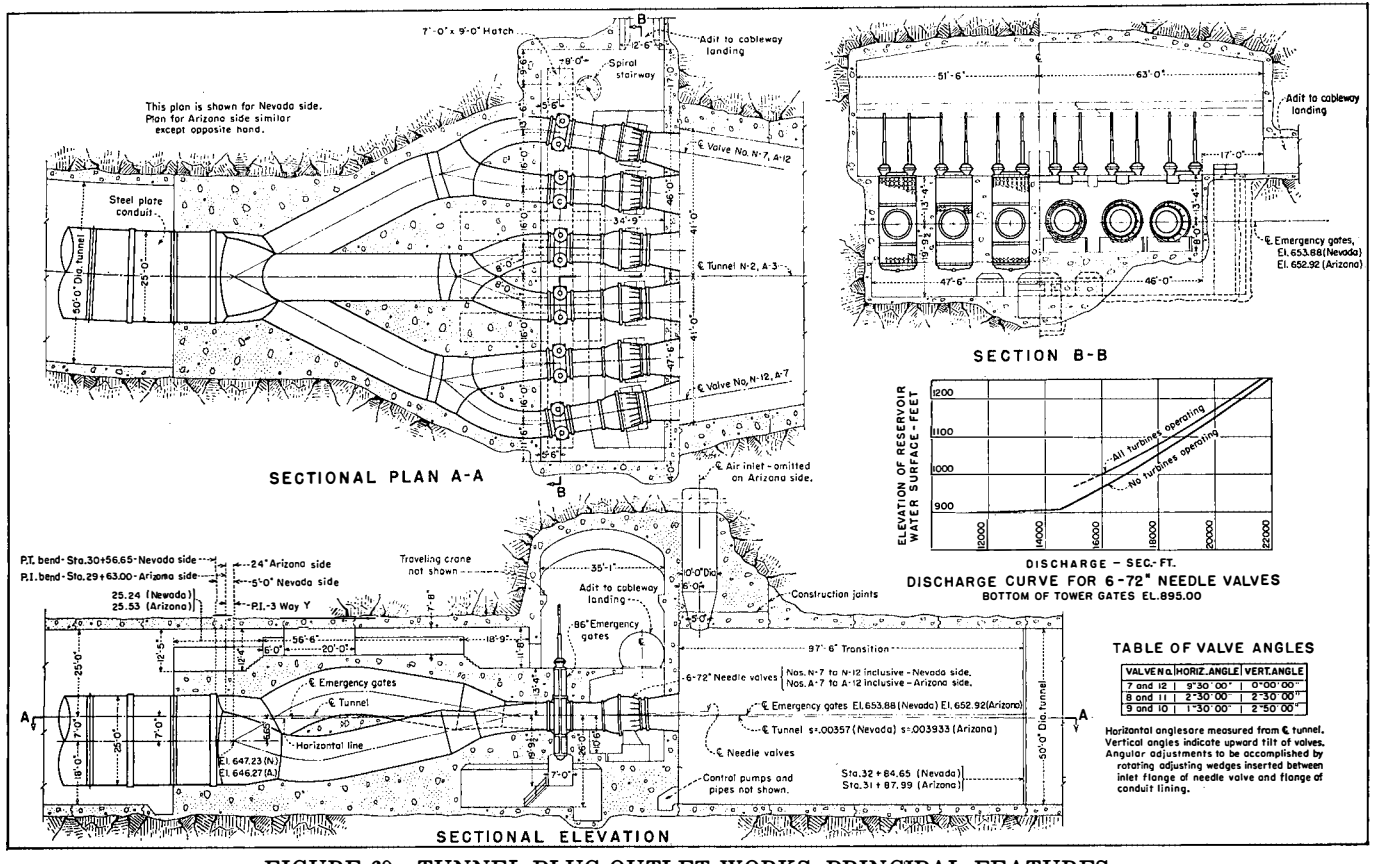

TABLE OF VALVE ANGLES

VALVE No.	HORIZ. ANGLE	VERT. ANGLE
7 and 12	9°30'00"	0°00'00"
8 and 11	2°30'00"	2°30'00"
9 and 10	1°30'00"	2°50'00"

Horizontal anglesare measured from ℄ tunnel. Vertical angles indicate upward tilt of valves. Angular adjustments to be accomplished by rotating adjusting wedges inserted between inlet flange of needle valve and flange of conduit lining.

FIGURE 69—TUNNEL-PLUG OUTLET WORKS, PRINCIPAL FEATURES

vent tunnels. The action of the three models was very similar and the results of the tests permitted the selection of an arrangement that minimized flow disturbances and erosive tendencies. The results also showed that the comparatively large air-vent tunnels that had been planned may not be necessary.

50. Results on 1:106.2 Model.—The first model, built on a scale of 1:106.2, was constructed and tested in the Fort Collins laboratory, using the arrangement of needle valves proposed by the design department. The model, see figures 70-A and C, was built so that needle valves could be adjusted both horizontally and vertically. The tunnel was made of pyralin to allow visual study

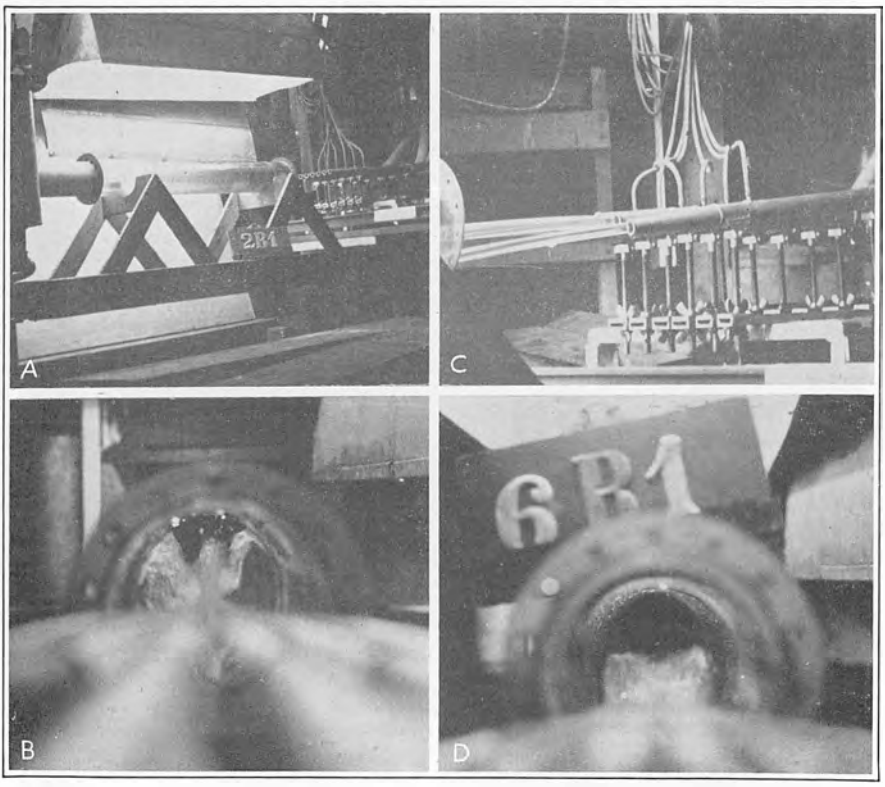

A. View of Model
B. Action in Tunnel with Original Design
C. Model in Operation
D. Action in Tunnel with Revised Design

FIGURE 70—TUNNEL-PLUG OUTLET MODEL, SCALE 1:106.2

of flow conditions. The spacing and angularity of the needle valves as originally proposed was as follows:

Valve Number	Distance of Center Line of Emergency Gates Above Tunnel Invert	Spacing of Emergency Gates	Valve Angle in Relation to Tunnel Centers	
			Horizontal	Vertical
1 and 6	30 feet	16 feet	11°57′	0°00′
2 and 5	30 feet	16 feet	7°14′	0°00′
3 and 4	30 feet	16 feet	2°25′	0°00′

Needle valves were represented in the model by conical nozzles that produced smooth jets. They gave little indication as to the aspirator action of the jets. The model, however, showed that the impact of the jets in the 50-foot diversion tunnel and the resulting turbulence was unsatisfactory. Flow conditions with the original design, see figure 70-B, were such that a large fin formed in the center of the tunnel and a wave carried up each side practically to the top.

Slight changes in the angles of the needle valves with relation to the center line of the 50-foot tunnel produced much better flow conditions, see figure 70-D. The most satisfactory arrangement of the valves in the initial tests on the 1:106.2 model was as follows:

Valve Number	Distance of Center Line of Emergency Gates Above Tunnel Invert	Spacing of Emergency Gates	Valve Angle in Relation to Tunnel Centers	
			Horizontal	Vertical
1 and 6	20.45 feet	16.04 feet	10°25′	0°00′
2 and 5	20.18 feet	16.04 feet	4°44′	0°08′
3 and 4	21.28 feet	16.04 feet	2°26′	1°48′

Positive vertical angles indicate that the valves were tilted upward with relation to the center line of the tunnel. The improvement obtained was so encouraging that it was decided to continue the studies on a larger scale model, where the details of the prototype could be duplicated to better advantage.

51. Results on 1:20 Model.—The large model shown on figures 71-A and C was built on a scale of 1:20 at the outdoor laboratory of the Bureau of Reclamation at Montrose, Colorado. The 50-foot concrete-lined tunnel was represented by a 30-inch wood-stave pipe; and the needle valves, mounted on frames which permitted horizontal and vertical adjustments as in the 1:106.2 model, were duplicated to scale in their full-open position. The tunnel-plug out-

let transition was constructed as an airtight compartment fitted with a hinged cover.

Jets from the 1:20 model needle valves were undoubtedly rougher, with respect to the scale ratio, than they will be in the prototype, because the model valves were iron castings with a higher degree of surface roughness than required by the scale of the model. At the present state of development of model testing, it is difficult to determine the exact similarity relations of model to prototype; but the streams from the model valves appeared from visual observations to be quite similar to those from large needle valves now installed and in operation. With the original valve positions used in the 1:106.2 model, flow conditions in the tunnel were extremely turbulent, see figure 71-B. Adjusting the positions

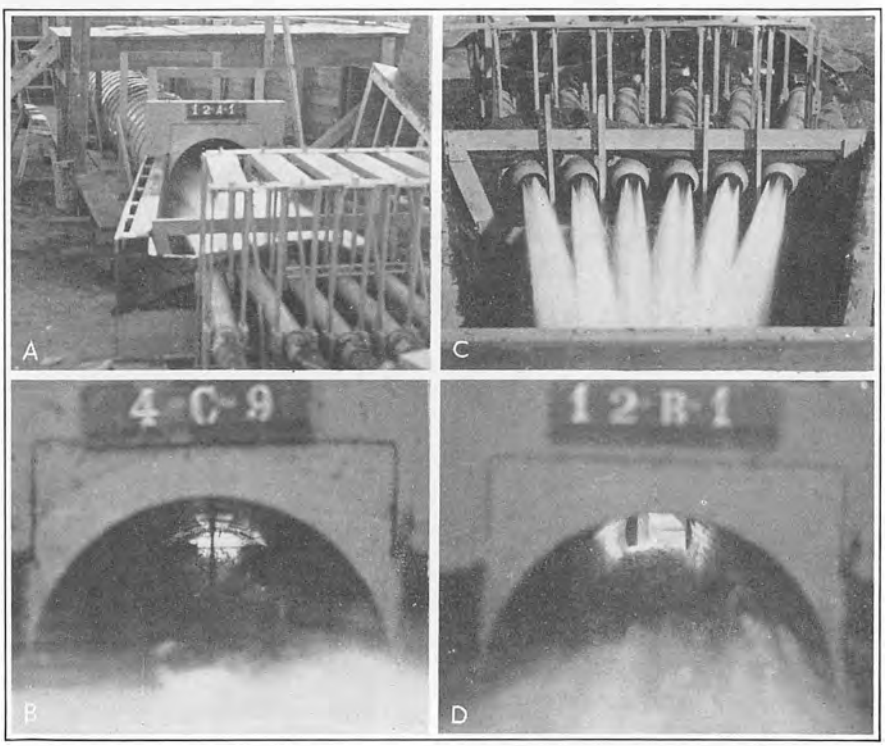

A. View of Model
B. Action in Tunnel with Original Design
C. Model in Operation
D. Action in Tunnel with Revised Design

FIGURE 71—TUNNEL PLUG OUTLET MODEL, SCALE 1:20

of the needle valves improved conditions of flow in the tunnel, and the results agreed closely with those obtained on the 1:106.2 model, see figure 71-D. Positions of the valves for the most satisfactory set-up on the 1:20 model were as follows:

Valve Number	Distance of Center Line of Emergency Gates Above Tunnel Invert	Spacing of Emergency Gates	Valve Angle in Relation to Tunnel Centers	
			Horizontal	Vertical
1 and 6	25 feet	16 feet	9°35′ 39″	0°00′ 00″
2 and 5	25 feet	16 feet	2°30′ 27″	2°28′ 56″
3 and 4	25 feet	16 feet	1° 2′ 41″	4°19′ 24″

Positive vertical angles indicate that the valves were tilted upward with relation to the center line of the tunnel. With the valves set as indicated above, the jets of water fell to the bottom of the tunnel at different locations, so that the impact was not concentrated at any point. The jets then combined and flowed along the invert in a smooth stream with surprisingly little turbulence, leaving a free air space, during normal tailwater in the river, of about 85 percent of the cross-sectional area of the tunnel. This action was not changed by completely closing the cover of the tunnel transition. During the course of experiments on both the 1:106.2 and 1:20 models, considerable data were obtained. Eight different arrangements were studied in the initial tests of the 1:106.2 model in the Fort Collins laboratory and fourteen were tried on the 1:20 model at the Montrose laboratory. Complete data were taken on each set-up, as it was not known at the time which would be the most satisfactory. Only initial, semifinal, and final plans are discussed in this report.

After a satisfactory plan was found for all six needle valves operating at full capacity, studies were made of flow conditions in the tunnel for different combinations as illustrated on figure 72. Poor conditions prevailed when one, two, three, or four valves on one side were discharging; while conditions were satisfactory when either the two center or four center valves were discharging. Upon completion of tests on the 1:20 model, results were checked by duplicating the schemes on the 1:106.2 model.

52. Results on 1:60 Model.—Neither the 1:106.2 nor the 1:20 model had approach conditions similar to the prototype, shown on figure 69. Both had been built with a canvas hose connecting each needle valve to a common water supply. The manifold and emer-

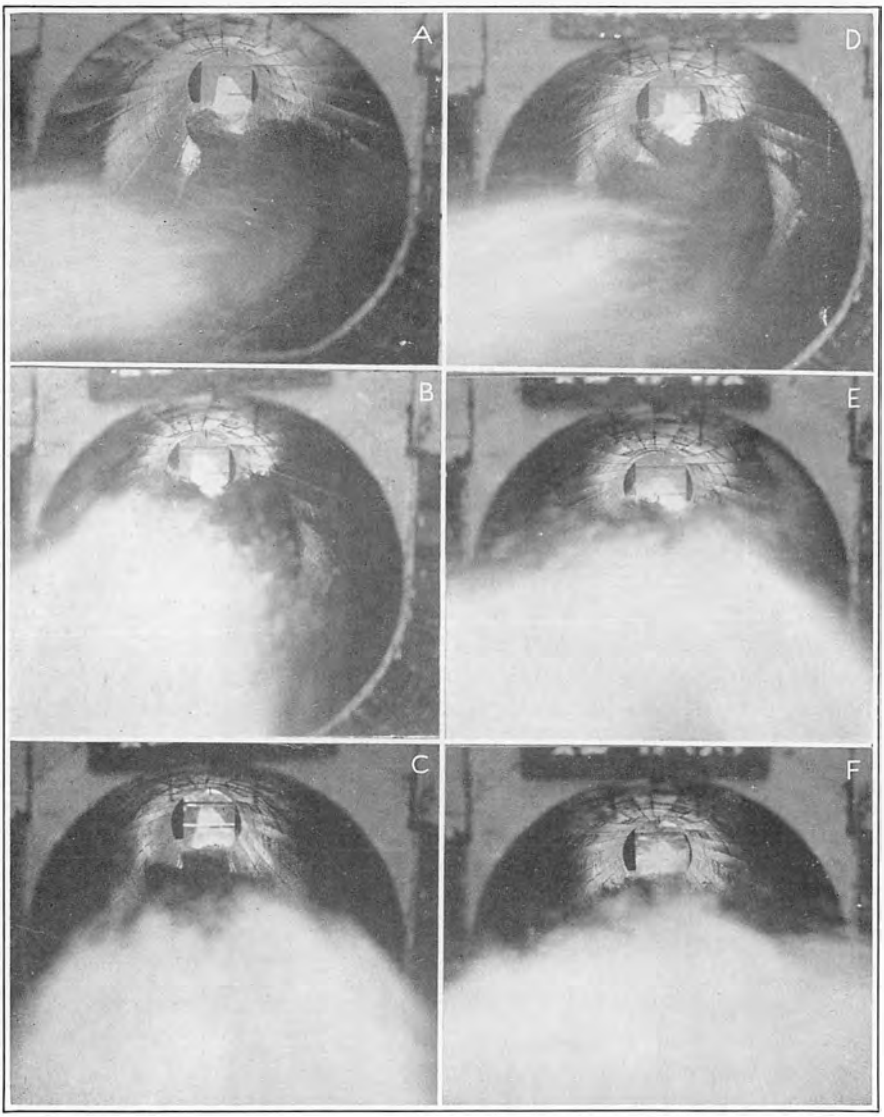

A. Valve 1
B. Valves 1, 2 and 3
C. Two Center Valves
D. Valves 1 and 2
E. Valves 1, 2, 3, and 4
F. Four Center Valves

FIGURE 72—CONDITIONS IN TUNNEL FOR VALVE COMBINATIONS, SCALE 1:20

gency gates were not incorporated in the 1:106.2 model because of its small size and because of the preliminary nature of the tests; nor were they incorporated in the 1:20 model on account of the high cost of construction. In order to study the effect of the manifold and emergency gates on flow conditions, a model, on a scale of 1:60, figure 73, was constructed and tested in the Fort Collins laboratory. This model was first tested using the most satisfactory arrangement derived from the 1:20 model tests, figure 73-C. Indications were that improvement could be accomplished by further adjustment of horizontal and vertical angles. With further testing, the following combination of valve positions was developed and recommended for final design, see figure 73-D.

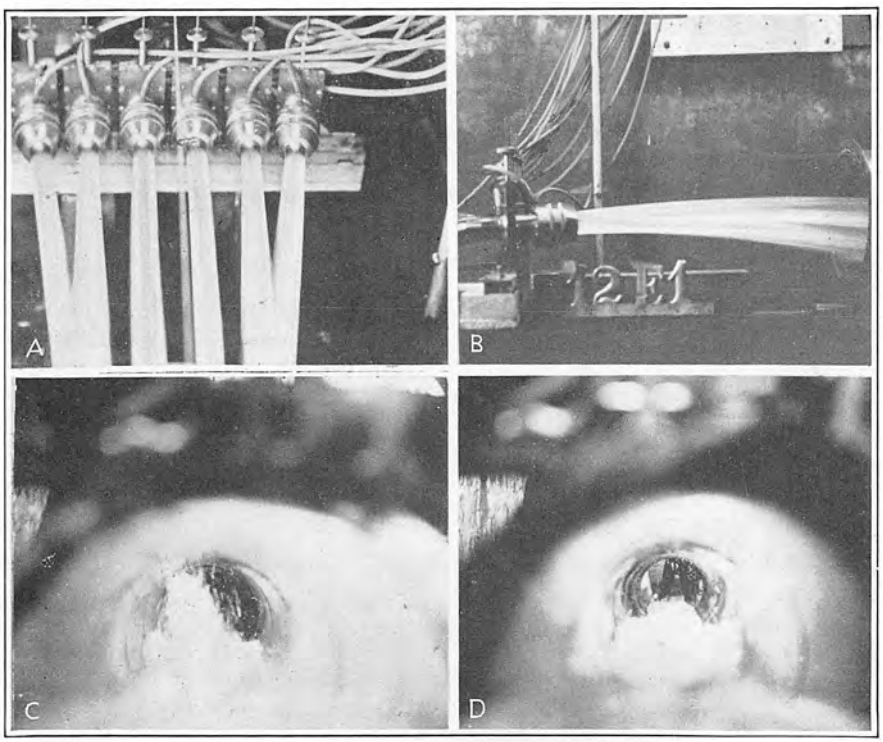

A. View of Model Looking Upstream
B. Side View of Model
C. Action in Tunnel—Setting from 1:20 Tests
D. Action in Tunnel—Setting from 1:60 Tests

FIGURE 73—TUNNEL-PLUG OUTLET MODEL, SCALE 1:60

Valve Number	Distance of Center Line of Emergency Gates Above Tunnel Invert	Spacing of Emergency Gates	Valve Angle in Relation to Tunnel Centers	
			Horizontal	Vertical
1 and 6	25 feet	16 feet	9°30′	0°00′
2 and 5	25 feet	16 feet	2°30′	2°30′
3 and 4	25 feet	16 feet	1°30′	2°50′

Positive vertical angles indicate an upward tilt of the valves.

In evolving correct positions of the tunnel-plug outlet needle valves from a hydraulic standpoint, it was necessary to consider mechanical limitations of proposed arrangements. In the original design, all needle valves were level in the same plane, with their center lines 30 feet above the invert, 5 feet above the center line of the 50-foot tunnel, and spaced 16 feet between center lines of emergency gates. The distance of 16 feet was the minimum because of mechanical requirements of assembly. In certain tests, good hydraulic conditions were obtained in the tunnel with the outer valves inclined downward; but this was objectionable on account of lifting reactions. Practically the same hydraulic action was obtained in the recommended design by inclining the center valves upward, thereby eliminating objectionable reactions.

TUNNEL-PLUG NEEDLE VALVES

53. Operating Program.—Since the designs provided a total of twelve needle valves in the tunnel-plug outlets, six in each of the lower Arizona and Nevada tunnels, it was believed desirable to determine the best procedure in opening the valves to obtain the most satisfactory flow conditions. The best discharge combinations of valves on the 1:20 model, two and four center valves discharging, see figures 72-E and F, were checked on the 1:60 model. The first combination was satisfactory, but the second was too turbulent. It was later determined that the combination of valves 1, 3, 4, and 6 operating together was more satisfactory than the second combination.

Other combinations were studied and the following order of operating needle valves in the tunnel-plug outlets is suggested. The valves in each outlet are numbered as shown in figure 69.

1. One tunnel-plug outlet in operation:
    a. Open two center valves, (9 and 10)
    b. Open two outside valves, (7 and 12)
    c. Open remaining two valves, (8 and 11)

2. Both tunnel-plug outlets in operation:
   a. Open two center valves on Nevada side, (N-9 and N-10)
   b. Open two center valves on Arizona side, (A-9 and A-10)
   c. Open two outside valves on Nevada side, (N-7 and N-12)
   d. Open two outside valves on Arizona side, (A-7 and A-12)
   e. Open two remaining valves on Nevada side, (N-8 and N-11)
   f. Open two remaining valves on Arizona side, (A-8 and A-11).

The procedure of closing the valves should be the reverse of that of opening.

54. Coefficient of Discharge.—In the design of needle valves for the canyon-wall and tunnel-plug outlets, the discharge was computed using the equation:

$$Q = CA_2 (2gh_1 + V_1^2)^{1/2} \quad (1)$$

where Q = Discharge quantity, second-feet.
C = Coefficient of discharge.
A_2 = Nominal area of discharge outlet, square feet.
h_1 = Pressure head immediately above valve (measured above center line), feet.
$V_1^2/2g$ = Head on valve due to velocity of approach, feet.

Equation 1 was obtained[14] from the equation for discharge,

$$Q = A_2 V_2, \quad (3)$$

by applying Bernoulli's theorem between the approach and outlet sections, in which,

$$h_1 = \frac{V_2^2}{2g} - \frac{V_1^2}{2g}$$

and

$$V_2 = \left[2g \left(h_1 + \frac{V_1^2}{2g} \right) \right]^{1/2}$$

or

$$V_2 = (2gh_1 + V_1^2)^{1/2} \quad (4)$$

[14]Schoder and Dawson Hydraulics, pp. 136-139.

Since there is a loss between the two points, the actual velocity, V_2, is less than the theoretical velocity. To correct for that loss a coefficient of discharge, C, must be applied to equation 4.

Then

$$V_2 = C(2gh_1 + V_1^2)^{1/2} \tag{5}$$

and

$$Q = CA_2(2gh_1 + V_1^2)^{1/2} \tag{6}$$

The coefficient of discharge was assumed to be 0.725 in the design of the valves. A check was made of this value on the 1:20 tunnel-plug outlet model at the Montrose laboratory.

A mercury manometer was connected above each valve on the model to register pressure head. Manometers were read simultaneously with the head on the 12-foot sharp-crested suppressed weir used to measure flow through the model. Representative runs for low, medium, and high heads were selected from tests 12 and 14 to determine the coefficient of discharge. Since the experimental needle valves were constructed in full-open position, the data apply only to that condition. Computed values of the coefficient are tabulated in table 4 and are plotted on figure 74.

TABLE 4—COEFFICIENT OF DISCHARGE FOR NEEDLE VALVES BASED ON DATA FROM 1:20 MODEL

Test No.	Head Feet	A_1 Sq. Ft.	A_2 Sq. Ft.	Q_1 Sec.-Ft.	C
14-69	15.254	0.10083	0.07149	1.9052	0.7328
12-68	13.011	0.10083	0.07149	1.7269	0.7228
14-54	12.828	0.10083	0.07149	1.7269	0.7266
12-78	12.972	0.10083	0.07149	1.7270	0.7236
14-44	12.711	0.10083	0.07149	1.7163	0.7257
12- 1	17.243	0.10083	0.07149	2.0291	0.7337
14- 2	17.007	0.10083	0.07149	2.0138	0.7334
12-56	15.447	0.10083	0.07149	1.8950	0.7266
14-59	15.309	0.10083	0.07149	1.9160	0.7348

55. Air Demand Tests.—One of the primary problems studied on the working models of the tunnel-plug outlet was the necessity for an air vent immediately above the needle valves to relieve low pressure conditions in the tunnel which might develop due to the aspirator action of high-velocity jets. In addition to the high cost of such installations, these air vents would be objectionable, should they cause a considerable quantity of mist or spray to be

discharged in the canyon near the powerhouses and high-tension electrical facilities.

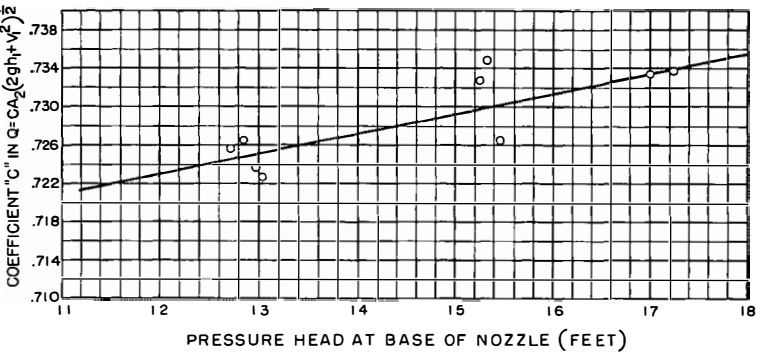

FIGURE 74—DISCHARGE COEFFICIENTS FOR NEEDLE VALVES IN TUNNEL-PLUG OUTLETS

The 1:20 scale model at Montrose was completely enclosed and a vent installed which could be controlled. With different operating heads on the valves, vacuum conditions were determined with the vent both open and closed. With improved conditions in the 50-foot tunnel, obtained by adjustment of positions of needle valves, a large space was available between the water surface and the roof of the tunnel to supply air deficiencies caused by the jets of high-velocity water. When air was not supplied by the vent and when normal tail-water conditions existed in the tunnel, the air in the upper part of the tunnel circulated, moving downstream near the water surface and upstream near the roof of the tunnel.

The maximum capacity of the Boulder Dam outlet works with the reservoir surface at elevation 1221.4, and spillway gates completely raised, has been estimated at 91,000 second-feet for the 24 needle valves, and 30,560 second-feet for the powerhouse operating at full capacity. A total discharge of 121,560 second-feet will produce a tail-water surface elevation of 669.0 at the diversion-tunnel portals under present conditions of river bed, see figure 75. The roof of the tunnel portal is at elevation 676; so that, with the possible maximum discharge of 121,560 second-feet from the outlet works, there will be a segment of the tunnel approximately 6.3 feet high, with a cross-sectional area of 143 square feet, available to relieve the low pressure created in the tunnel. The pro-

posed air vent was to be 10 feet in diameter with an area of 78 square feet.

It is expected that loose material in the river bed below the dam will be gradually eroded by clear water released from the reservoir; so that in the future, the tail water at the portals will be lower than at present. With this possibility an even larger segment of tunnel will be available for ventilation at maximum discharge. The only possibility of a larger flow in the river, and hence higher tail water, will be for the spillways to discharge. For this condition, the necessity for operating the tunnel-plug outlets will no longer exist and they can be closed.

Vacuum conditions on the 1:20 model, related to river elevations on the prototype, are shown on figure 76. The curves show that a slight vacuum will exist for flow conditions up to 70,000 second-feet, regardless of the head on the valves and the installation of an air vent. The vacuum increases quite rapidly up to 130,000 second-feet, but not sufficiently to be of serious consequence. A slight increase of vacuum was noted with an increase of

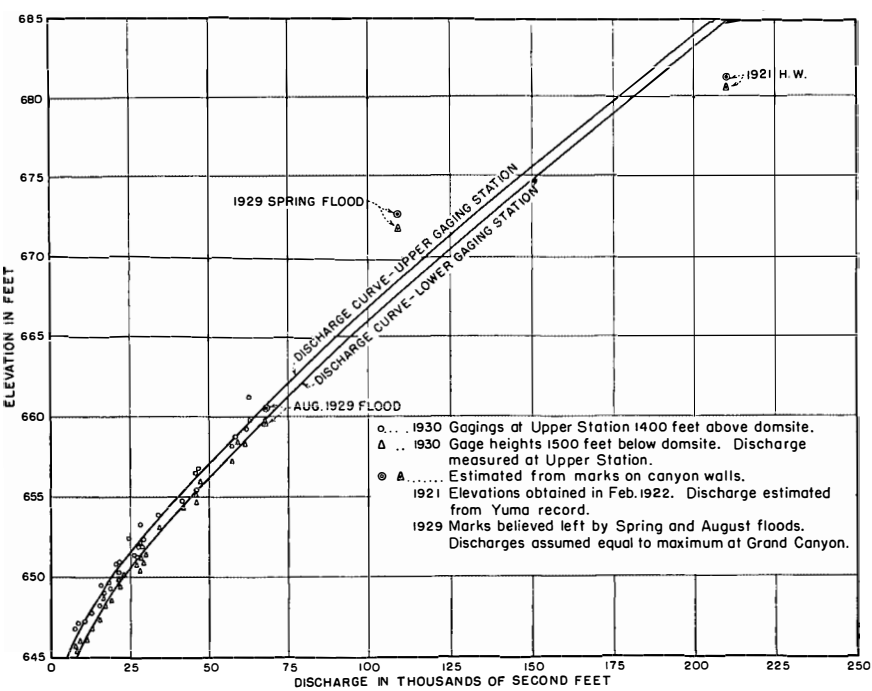

FIGURE 75—BLACK CANYON GAGING STATION DISCHARGE CURVES

head on the valves, but the amount was negligible. The data plotted on figure 76 are from tests on the model using heads corresponding to 340 to 475 feet on the prototype.

The change of tailwater elevation is the controlling factor in the formation of the vacuum. When tailwater is low, there is sufficient room above the water surface in the tunnel for air to flow into the space around the high-velocity jets and replace that being carried away. For this condition there would be very little demand for air through the vents. As the water reaches an elevation in the tunnel where the space above is considerably diminished, either one of two things may occur. If no air vent is provided, the amount of the vacuum may be rapidly increased and the velocity of the inbound air will be increased; or, if an air vent is provided, the demand for air will be supplied by it and the vacuum will not be increased. In the first case, as the air space in the tunnel decreases, the vacuum will increase because the necessary amount

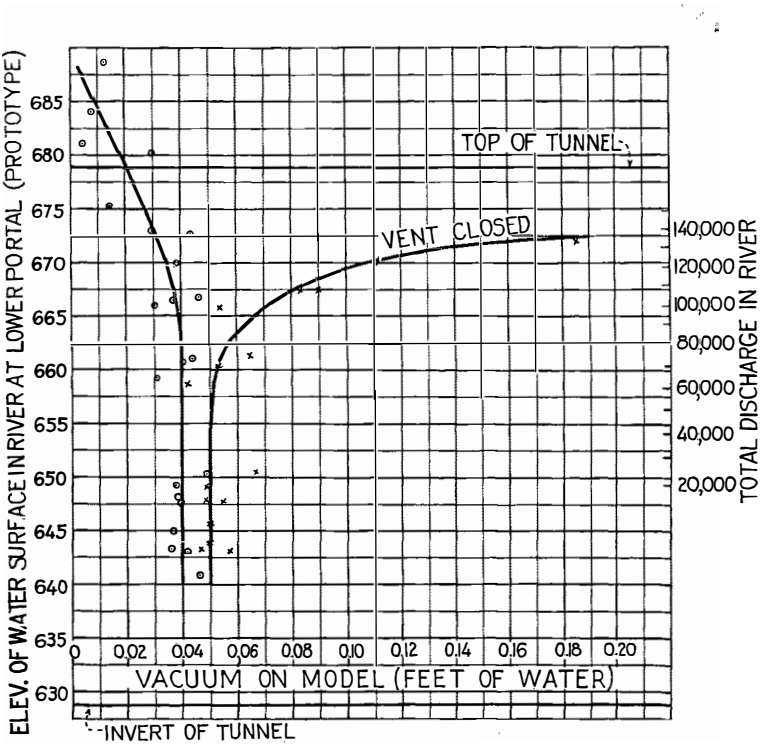

FIGURE 76—RELATION OF RIVER ELEVATION TO PRESSURE IN TUNNEL

of air cannot be supplied fast enough. This condition may continue until the tunnel is completely filled at the end.

As previously mentioned, there are two movements of air flow in the tunnel. The boundary layer, adjacent to the water surface, will be moving in the same direction as the water and at the same or slightly less velocity; while air near the roof of the tunnel will travel at a lower velocity in the opposite direction. The outward flow will be the last to disappear as the water surface approaches the tunnel roof at the portal, since the velocity of the water will be high and would tend to draw the air out rather than let it in.

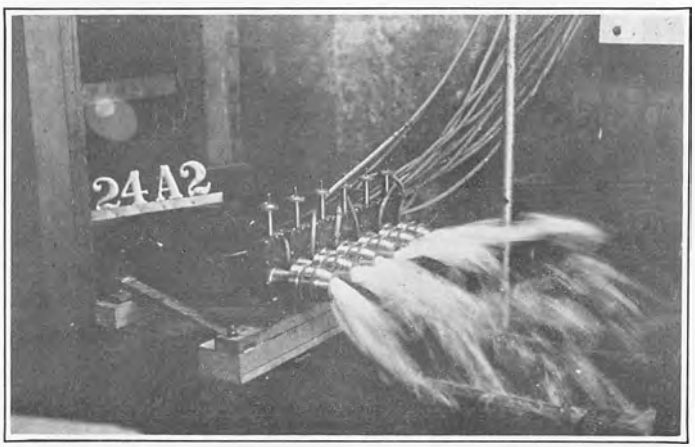

FIGURE 77—SURGING OF JETS, NEEDLE VALVES OPEN AND EMERGENCY GATES NEARLY CLOSED, 1:60 MODEL

As a result, the air demand on the vents would reach a maximum just before the water reached the top of the tunnel. When the tunnel is completely filled, the velocity of the water will be decreased and there will be a resulting decrease in the vacuum. This theory was substantiated by model observations. The most dangerous point is when the tailwater is at or very near the top of the tunnel.

Inasmuch as the present state of knowledge of the behavior of models in connection with the development of a vacuum and its resultant effects are not yet sufficiently developed to be absolutely certain, it was decided to form the junctions of the air tunnels in the concrete lining, as shown on figure 69; so that, should a contingency arise that the air tunnels did prove to be necessary, they

could be constructed without difficulty in the future at no greater cost than the original installation.

56. Needle Valve and Emergency Gate Model.—During the course of experiments on the 1:60 model studies were made of the effect of closing the paradox emergency gates with the needle valves completely open. It was discovered that a surging of the jets from the needle valves occurred when the paradox gates were nearly closed, see figure 77.

To further study this phenomenon, one of the needle valves used on the 1:20 model of the tunnel-plug outlet was mounted in its relative position with a model of an emergency gate, together with sufficient length of approach pipe. The surging or pulsations on the 1:20 model, shown on figure 78, were very similar to those observed on the 1:60 model. These photographs disclose only instantaneous conditions. Actually, the jet oscillated with a fairly definite cycle in a vertical plane, and the results were best recorded by motion pictures.

Operation of the emergency gate without the needle valve in place showed that the stream of high-velocity water expanded and completely filled the end of the pipe. Critical examination disclosed low-velocity areas on each side and a high-velocity area in the center, such that, with the needle valve in place, a body of water collected in the low-velocity pockets and was carried out by the high-velocity jet, causing surges or pulsations. At an opening of the paradox gate of approximately 15 percent, this surging caused a vibration of the entire model which could be felt distinctly at the end of the 20-foot approach pipe.

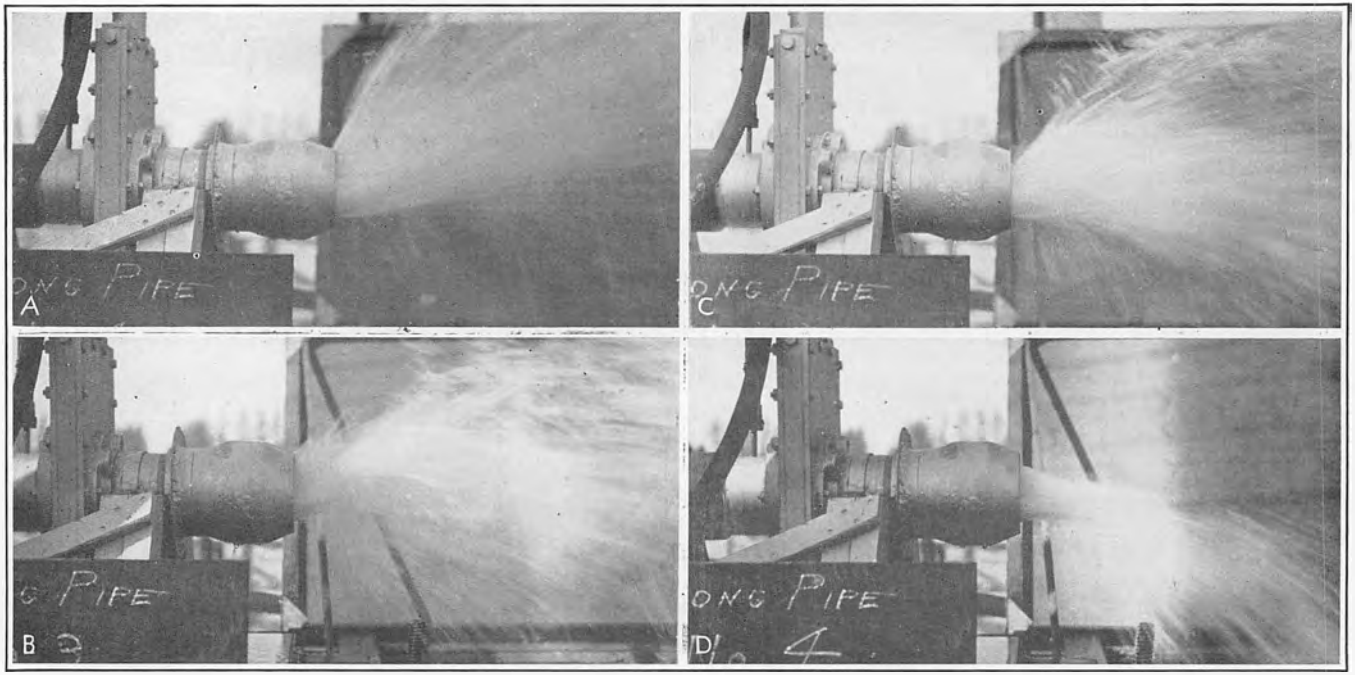

A. Emergency Gate Open 24.8 Percent
B. Emergency Gate Open 15.6 Percent
C. Emergency Gate Open 19.4 Percent
D. Emergency Gate Open 10.7 Percent

FIGURE 78—NEEDLE VALVE AND EMERGENCY GATE, 1:20 MODEL

CHAPTER V—CHANNEL CONDITIONS BELOW BOULDER DAM

RIVER MODEL

57. Introduction.—In the early stages of design of Boulder Dam, with its various appurtenant structures, it was considered that a scale model of the river channel below the proposed site would be of value in determining effects of discharges from the powerhouses, the canyon-wall outlets, the tunnel-plug outlets and the spillway tunnels on water surface elevations in front of the powerhouses and on the operating head of the turbines.

Unfortunately, urgency for other more detailed studies and lack of space in the hydraulic laboratory made it necessary to postpone the river studies until the design and construction of the dam had progressed to such an extent that major changes were no longer possible. It is believed, however, that sufficient information of value to the operating staff was gained to justify the expense of the studies. The results so obtained are presented with this in view.

58. Apparatus.—The model, shown in figure 79, with a scale ratio of 1:150, was constructed in the hydraulic laboratory of the Colorado Agricultural Experiment Station, Fort Collins, Colorado. The outlet works were constructed in detail, except that the discharge from the powerhouse was introduced through a 90-degree V-notch weir placed between the upstream wings of the powerhouses. Diaphragm orifices were installed in the conduits leading to the canyon-wall and tunnel-plug outlets, for measuring flow through those structures; while 90-degree V-notch weirs were so placed as to discharge into the models of the side-channel spillways, thereby introducing correct quantities at correct heads. Diaphragm orifices and V-notch weirs were calibrated in place by comparison with the master 90-degree, V-notch weir in the measuring channel.

The topography of the river bed, see figures 83-A and B, was constructed in detail by the use of galvanized iron guides, cut to conform to cross sections of the river and fastened in the wooden tank holding the model. Spaces between guides were filled with

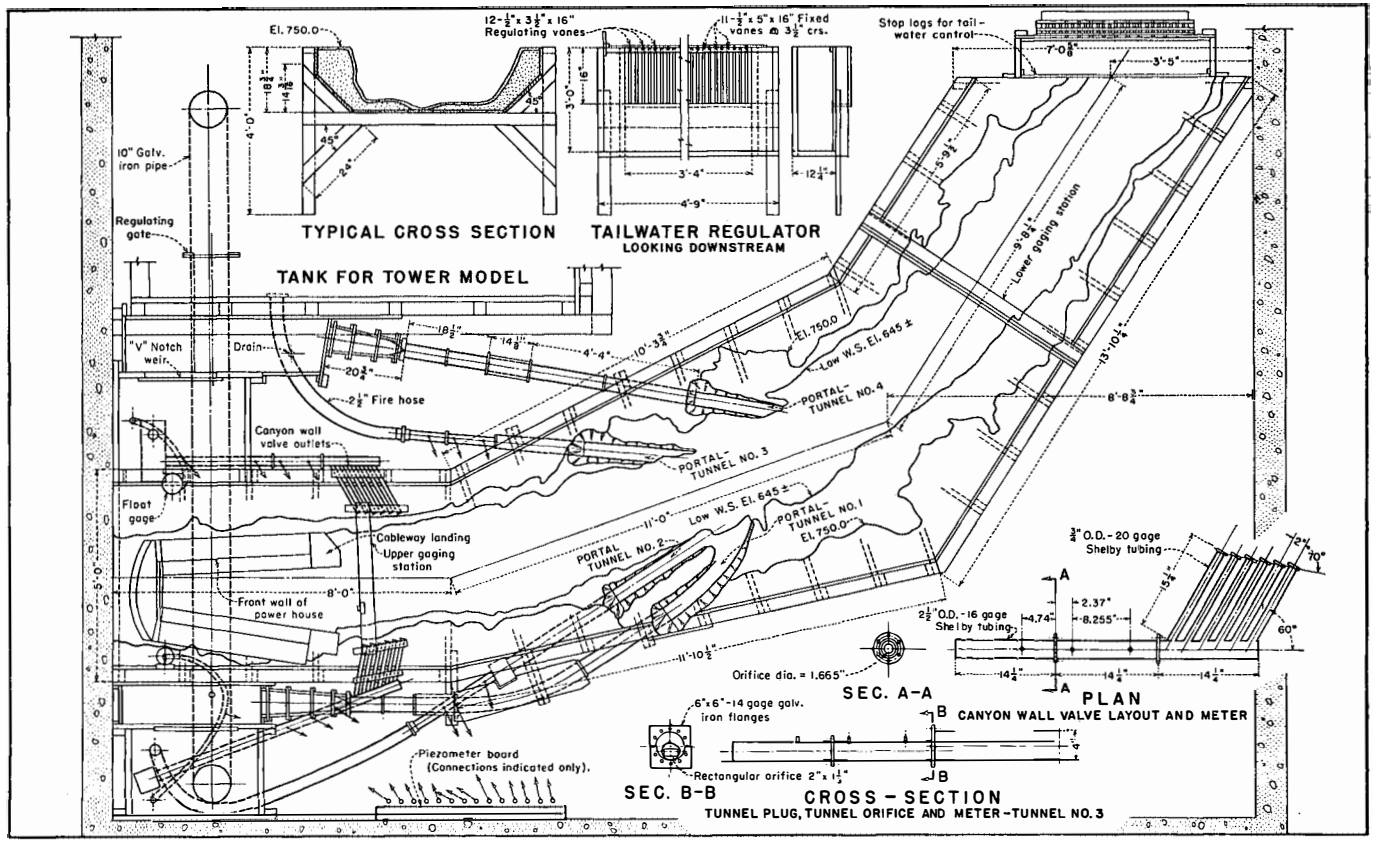

FIGURE 79—PLAN AND DETAILS OF RIVER MODEL, SCALE 1:150

damp sand to within an inch or two of the top of the metal and the remainder of the space was filled with concrete. The configuration of the river bed was detailed by hand, utilizing the metal guides and detail topography sheets as references. The bottom of the channel was filled with sand to conform to the movable material in the river bed. Stoplogs, adjustable in height, were placed at the lower end of the channel to hold the bed material to any given elevation; and a regulator, consisting of fixed and movable vanes, was used to control the elevation of the water surface. A sand box was built between the stoplogs and the regulator to trap the sand eroded from the river bed and prevent its being carried into the laboratory recirculating system.

Two gaging stations, for measuring river flow and determining the slope of the water surface, were installed on the model. One, known as the upper station, was installed to measure the elevation of the water surface directly upstream from the point at which the jets from the canyon-wall outlets impinged on the river banks. The other, located sufficiently far below the portals of the spillway tunnels to avoid interference from tunnel flow, was used to adjust the tailwater in proper relation to discharge.

59. River Conditions for Flow Combinations.—During the course of the experiments, flow data and conditions of river bed were recorded by three different methods:

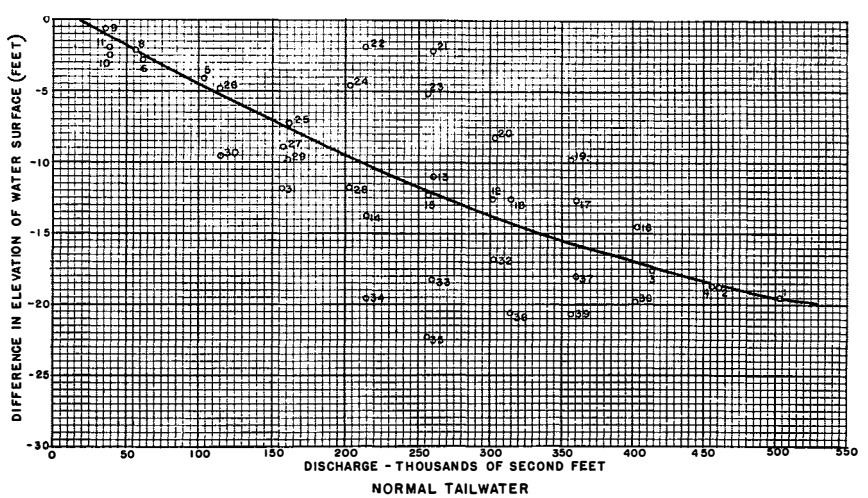

FIGURE 80—EFFECT OF OUTLET WORKS ON RIVER ELEVATION

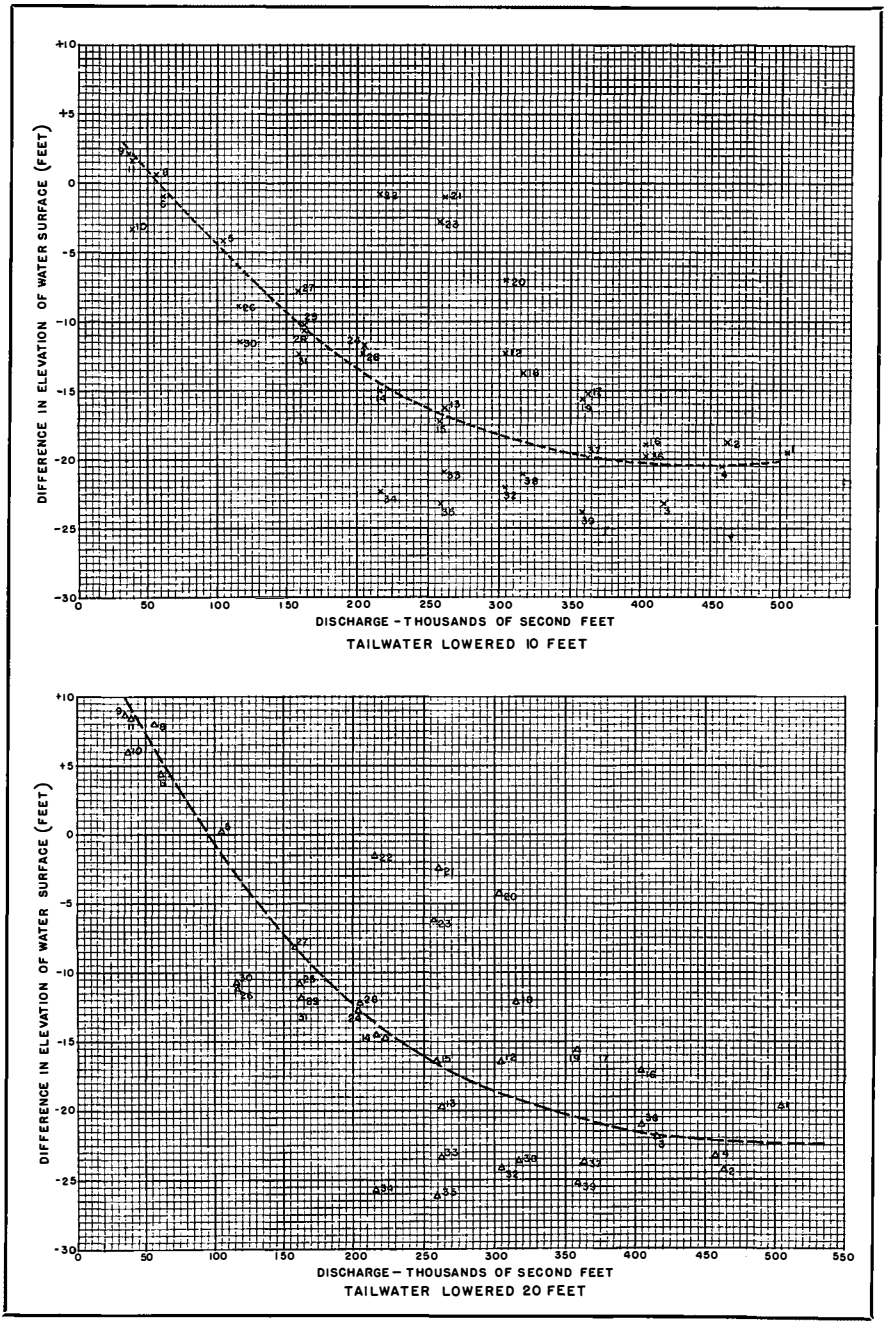

FIGURE 81—EFFECT OF OUTLET WORKS ON RIVER ELEVATION

1. Point gage readings were made at the stations above and below the outlet works, to record the effect of the anticipated "ejector" action produced by the outlet works discharging into the river at an angle. These data have been consolidated and tabulated in table 5, where practically any flow combination and its action can be determined at a glance. The data in the columns entitled "Rise" and "Drop" have been plotted on figures 80 and 81 against the total flow in the river for any specific run. Three tailwater elevations were used, namely: normal, 10 feet below normal, and 20 feet below normal. In all tests, the lower gaging station was used as a control, and the gage height for any given discharge was obtained from the rating curve on figure 82, constructed from gagings made prior to the start of construction. This discharge-elevation relationship is referred to as "normal."

2. Pictorial observations, using both still and motion-picture equipment, were made of conditions for each typical flow combination. A number of the still pictures have been included as figures 83 to 88, inclusive, to better illustrate the results.

3. Visual observations were made by the observer and record-

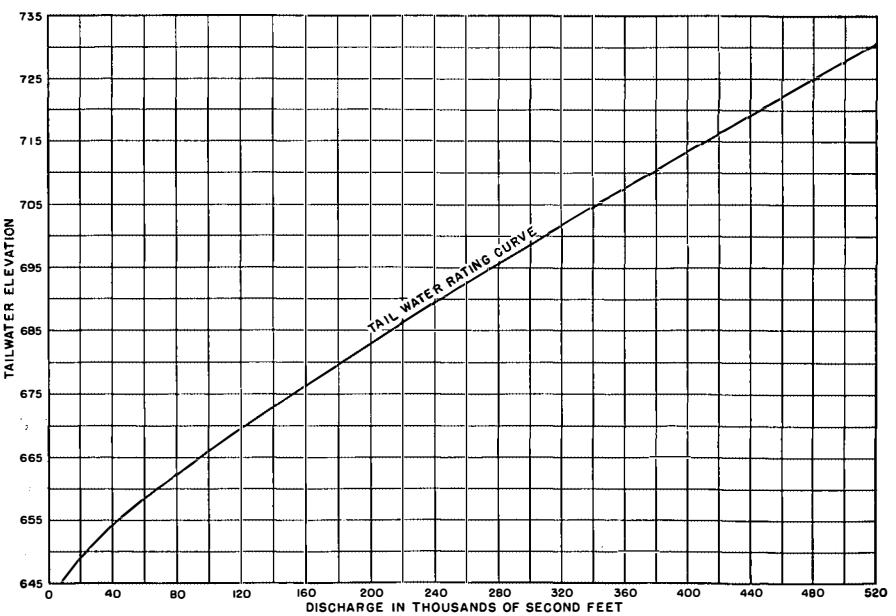

FIGURE 82—TAILWATER RATING CURVE

A. Method of Constructing River Bed

B. Completed River Model

Boulder Dam River Model, Scale 1:150

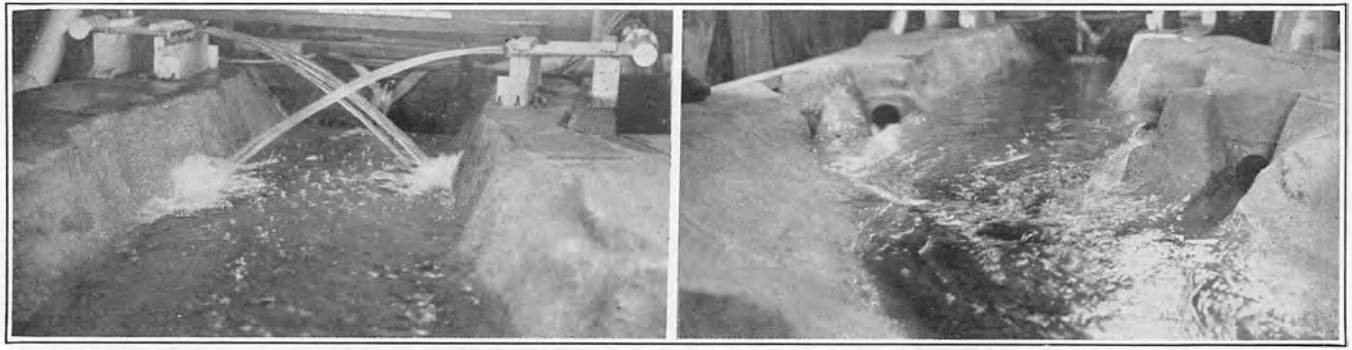

C. Normal Tailwater, Powerhouse 15,000 Second-Feet, Canyon Wall Outlets 21,000 Second-Feet

D. Normal Tailwater, Powerhouse 15,000 Second-Feet, Tunnel Plug Outlets 46,000 Second-Feet

FIGURE 83—CHANNEL CONDITIONS IN RIVER BELOW BOULDER DAM

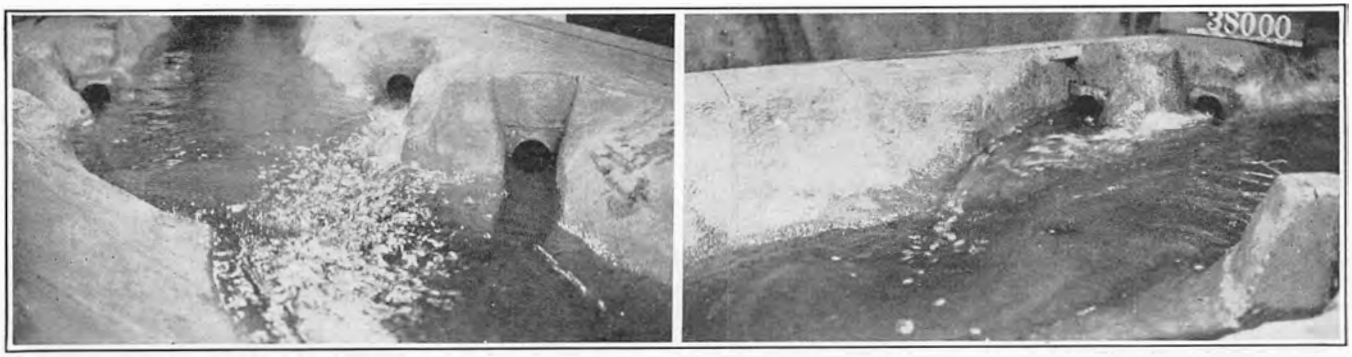

A. Powerhouse 15,000 Second-Feet, Arizona Tunnel Plug Outlet 23,000 Second-Feet, Normal Tailwater

B. Powerhouse 15,000 Second-Feet, Nevada Tunnel Plug Outlet 23,000 Second-Feet, Normal Tailwater

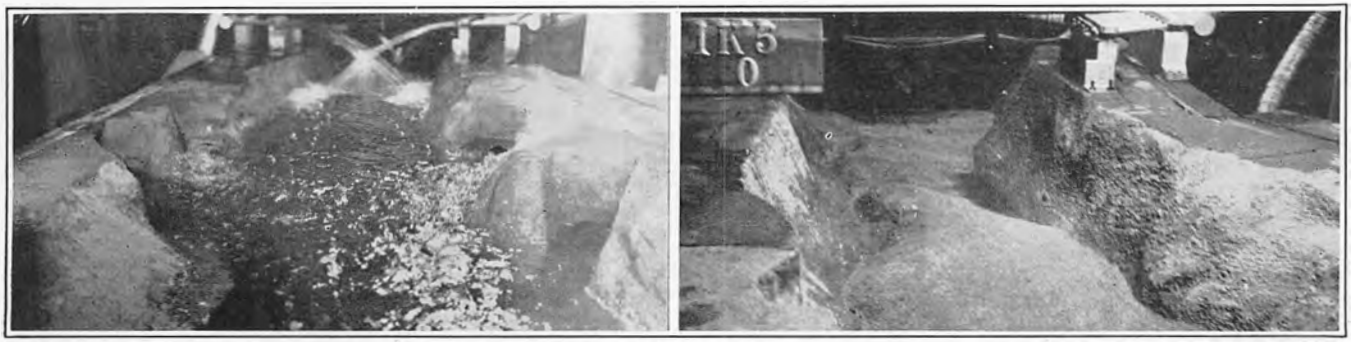

C. Normal Tailwater

D. Erosion of River Bed

Powerhouse 16,000 Second-Feet, Canyon Wall Outlets 42,000 Second-Feet, Tunnel Plug Outlets 46,000 Second- Feet

FIGURE 84—CHANNEL CONDITIONS IN RIVER BELOW BOULDER DAM

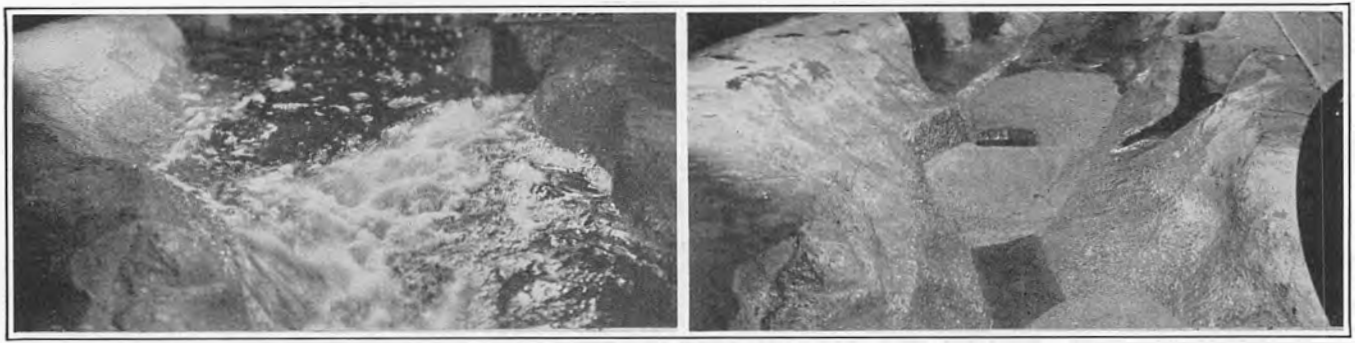

A. Normal Tailwater

B. Erosion of River Bed

Powerhouse 15,000 Second-Feet, Tunnel Plug Outlets 46,000 Second-Feet, Arizona Spillway 100,000 Second-Feet, Canyon Wall Outlets 42,000 Second-Feet

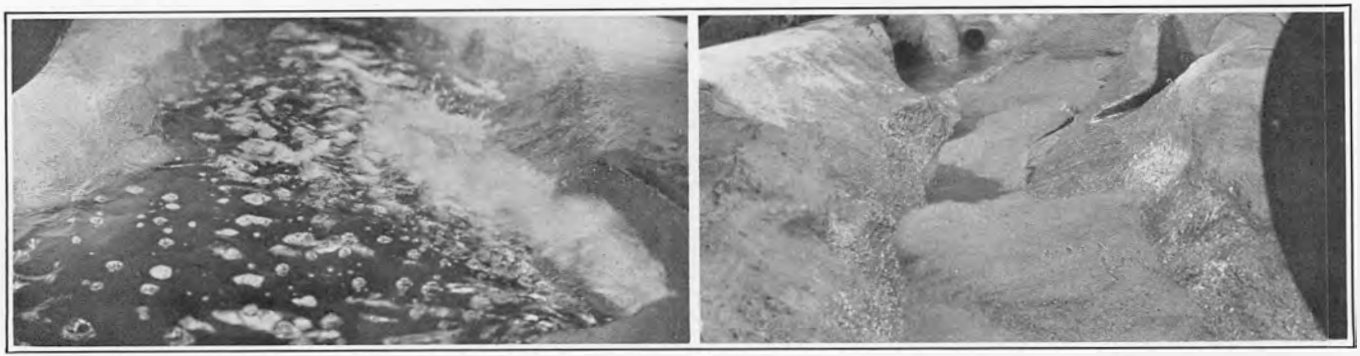

C. Normal Tailwater

D. Erosion of River Bed

Powerhouse 15,000 Second-Feet, Tunnel Plug Outlets 46,000 Second-Feet, Nevada Spillway 100,000 Second-Feet, Canyon Wall Outlets 42,000 Second-Feet

FIGURE 85—CHANNEL CONDITIONS IN RIVER BELOW BOULDER DAM

A. Normal Tailwater
Spillways 200,000 Second-Feet, Canyon Wall Outlets 42,000 Second-Feet, Tunnel Plug Outlets 46,000 Second-Feet, Powerhouse 15,000 Second-Feet

B. Erosion of River Bed

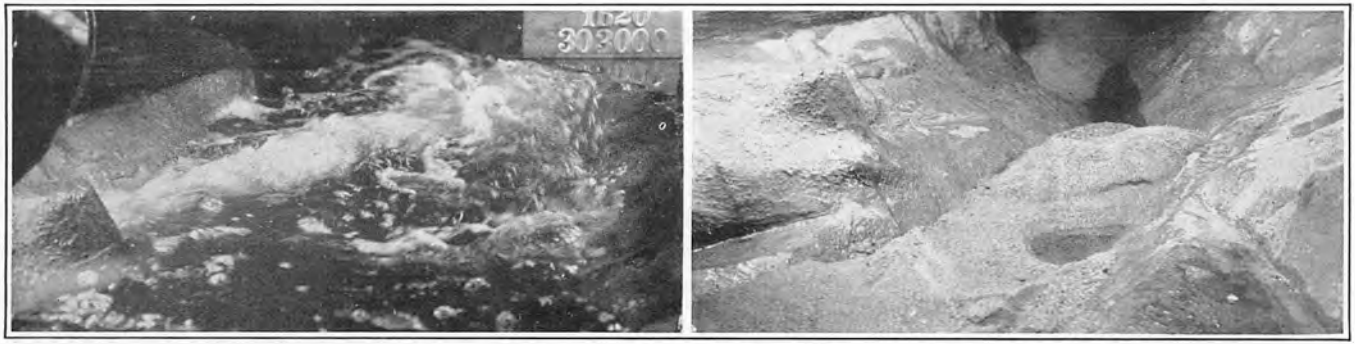

C. Normal Tailwater
Arizona Spillway 200,000 Second-Feet, Canyon Wall Outlets 42,000 Second-Feet, Tunnel Plug Outlets 46,000 Second-Feet, Powerhouse 15,000 Second-Feet

D. Erosion of River Bed

FIGURE 86—CHANNEL CONDITIONS IN RIVER BELOW BOULDER DAM

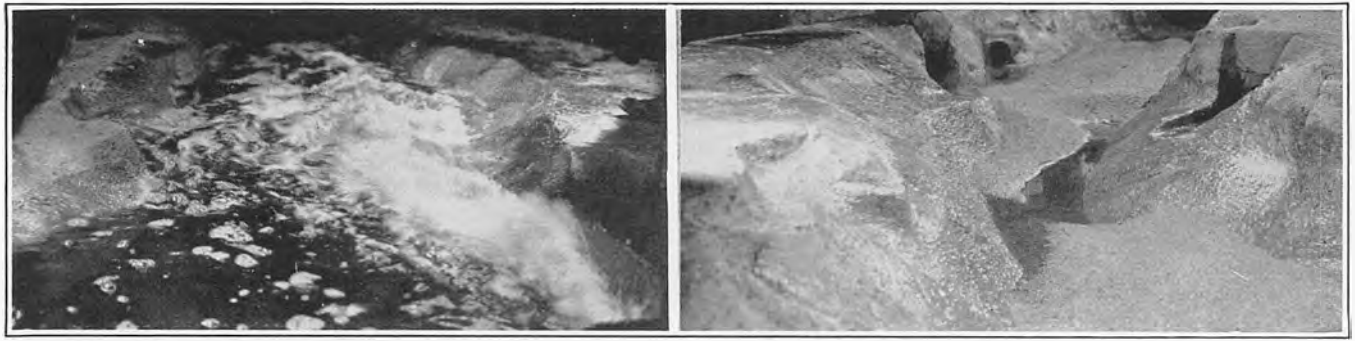

A. Normal Tailwater

B. Erosion of River Bed

Nevada Spillway 200,000 Second-Feet, Canyon Wall Outlets 42,000 Second-Feet, Tunnel Plug Outlets 46,000 Second-Feet, Powerhouse 15,000 Second-Feet

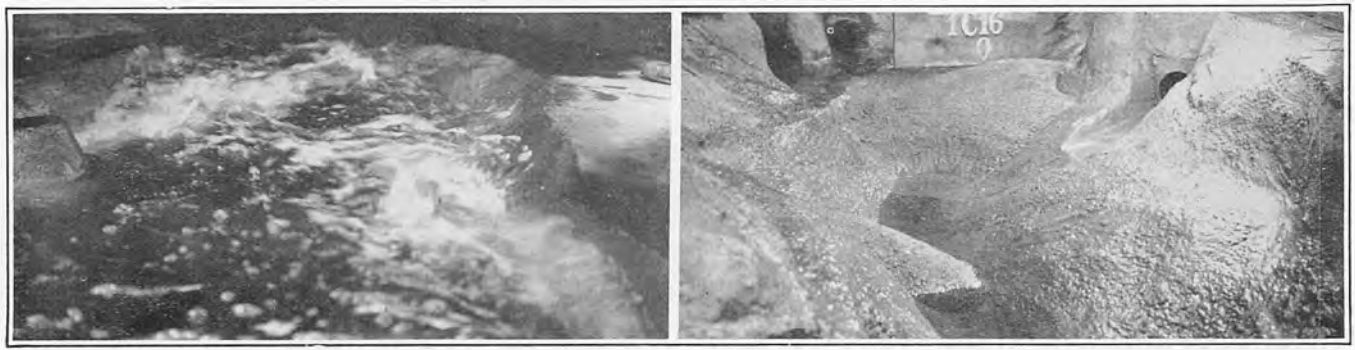

C. Normal Tailwater

D. Erosion of River Bed

Arizona Spillway 200,000 Second-Feet, Canyon Wall Outlets 42,000 Second-Feet, Nevada Spillway 200,000 Second-Feet, Tunnel Plug Outlets 46,000 Second-Feet

FIGURE 87—CHANNEL CONDITIONS IN RIVER BELOW BOULDER DAM

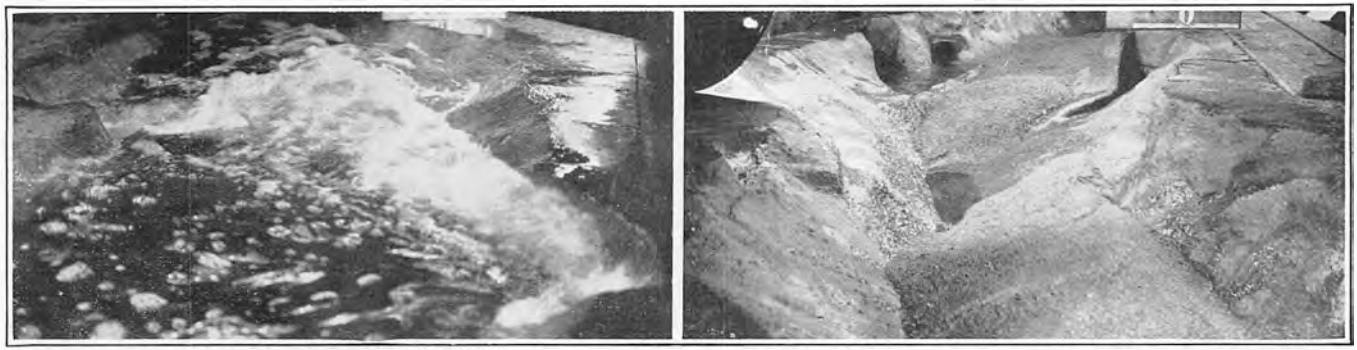

A. Normal Tailwater

B. Erosion of River Bed

Nevada Spillway 200,000 Second-Feet, Canyon Wall Outlets 42,000 Second-Feet, Arizona Spillway 100,000 Second-Feet, Tunnel Plug Outlets 46,000 Second-Feet

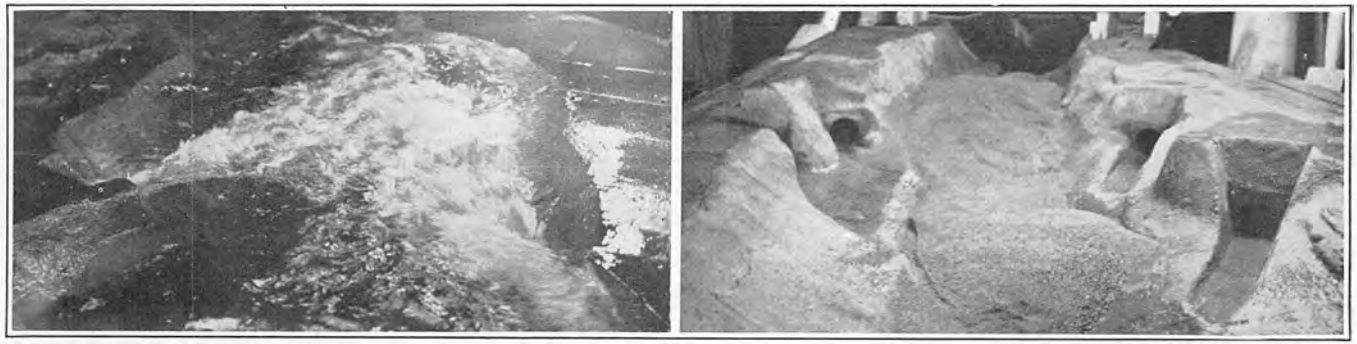

C. Normal Tailwater

D. Erosion of River Bed

Spillways 400,000 Second-Feet, Canyon Wall Outlets 42,000 Second-Feet, Tunnel Plug Outlets 46,000 Second-Feet, Powerhouse 15,000 Second-Feet

FIGURE 88—CHANNEL CONDITIONS IN RIVER BELOW BOULDER DAM

ed in the form of notes for each run. These deal primarily with erosion of the river bed and flow conditions in the river. They have been digested and condensed for the sake of brevity and are included herein as table 6. These data are self-explanatory and are cross-referenced to the photographs.

In analyzing point gage observations, shown in table 5, the results were divided into three classes:

1. Equal inflow from both sides of river, runs 1 to 9, and 12 to 15, inclusive.
2. Larger quantity of water from the Arizona side of the river, run 10 and runs 16 to 27, inclusive.
3. Larger quantity of water from the Nevada side of the river, run 11 and runs 28 to 39, inclusive.

Data from the first class were plotted on figures 80 and 81, for all three conditions of tailwater, namely: normal, 10 feet below normal, and 20 feet below normal. Curves were drawn through each group. Data from the other classes were also added for comparative purposes. In table 5, the data are presented in the order in which they were actually taken; while in table 6, they have been rearranged in the order of increasing total flow in the river below the outlet works, to allow comparison of effects of a similar flow from either or both sides of the river.

60. Conclusions.—It was expected, and the expectation has since been justified, that retrogression would occur; the movable material of the river bed would be transported downstream; and a new discharge-elevation relationship would result. In studying the effect of this retrogression, as indicated on the 1:150 model, it was possible, with the information available, only to move the rating curve down as a unit 10 and 20 feet, respectively, preserving its original shape. Actually, the rating curve for a condition of retrogression of 20 feet may have a slightly different characteristic shape, depending on the cross section of nonerodible material in the river bed. Furthermore, there are two variables at work which have a tendency to counteract each other and affect the tailwater relationship curve. As the river retrogresses, the slope will decrease and the velocity in the cross sections will decrease for a given quantity. On the other hand, as the river retrogresses, the cross-sectional area will increase with a resultant influence on the relationship.

As a result of these studies, which can only be considered as qualitative or indicative trends, it was shown that there are operating combinations of the various outlet works which are far superior to those originally planned, from the viewpoints of increasing the effective head on the turbines and of flow conditions in the channel, particularly below the portals of the spillway tunnels.

Since the results obtained from the studies can only be considered as relative or indicative, and since the retrogression of the river bed as a variable makes reliable results on models extremely difficult to secure, it is believed desirable that sufficient gaging stations be established downstream from the powerhouse and the spillway outlets to permit the collection of data. An analysis of such data would undoubtedly be a definite aid to the power-plant operating engineer in determining the most effective operating combination.

TABLE 5—RELATIONSHIP OF ELEVATION OF WATER SURFACE TO DISCHARGE WITH DIFFERENT OUTLET WORKS COMBINATIONS OPERATING

Run No.	Location of Outlets	DISCHARGE SECOND-FEET					ELEVATION OF WATER SURFACE IN RIVER							
							UPPER SECTION					LOWER SECTION		
		Power House	Canyon Wall Outlets	Tunnel Plugs	Spill-way	Total	Normal	10 Feet Below Normal	20 Feet Below Normal	Rise	Drop	Normal	10 Feet Below Normal	20 Feet Below Normal
1	Arizona	15,000	21,000	23,000	200,000	503,000	708.47	698.95	690.23	19.26		727.73	718.18	710.00
	Nevada		21,000	23,000	200,000					19.23				
										19.77				
2	Arizona	15,000	0	23,000	200,000	461,000	704.22	693.71	676.67	18.66		722.88	712.70	701.21
	Nevada		0	23,000	200,000					18.99				
										24.54				
3	Arizona	15,000	0	0	200,000	415,000	694.75	677.17	667.71	17.46		712.21	700.30	689.70
	Nevada		0	0	200,000					23.13				
										21.99				
4	Arizona	15,000	21,000	0	200,000	457,000	702.98	689.81	678.88	18.54		721.52	710.30	702.28
	Nevada		21,000	0	200,000					20.49				
										23.40				
5	Arizona	15,000	21,000	23,000	0	103,000	662.74	652.18	649.30	4.08		666.82	656.17	649.09
	Nevada		21,000	23,000	0					3.99	0.21			
6	Arizona	15,000	0	23,000	0	61,000	655.64	647.92	643.50	2.88		658.22	648.79	639.12
	Nevada		0	23,000	0					0.87	4.38			
8	Arizona	15,000	21,000	0	0	57,000	655.37	648.78	645.87	2.13		657.50	648.03	637.80
	Nevada		21,000	0	0						0.75			
											8.07			
9	Arizona	15,000	10,500	0	0	36,000	652.92	645.82	639.76	0.57		653.49	643.63	631.18
	Nevada		10,500	0	0						2.19			
											8.58			
10	Arizona	15,000	0	23,000	0	38,000	651.30	637.39	637.27	2.49		653.79	640.63	631.18
	Nevada		0	0	0					3.24	6.09			
11	Arizona	15,000	0	0	0	38,000	652.39	645.30	642.31	2.01		654.40	643.63	633.79
	Nevada		0	23,000	0						1.77			
											8.52			
12	Arizona	15,000	21,000	23,000	100,000	303,000	686.67	677.63	662.87	12.60		699.27	689.87	679.40
	Nevada		21,000	23,000	100,000					12.24				
										16.53				
13	Arizona	15,000	0	23,000	100,000	261,000	681.42	666.13	653.23	11.01		692.43	682.36	673.00
	Nevada		0	23,000	100,000					16.23				
										19.77				
14	Arizona	15,000	0	0	100,000	215,000	671.84	661.15	651.09	13.77		685.61	676.06	665.61
	Nevada		0	0	100,000					14.91				
										14.52				
15	Arizona	15,000	21,000	0	100,000	257,000	679.92	664.72	655.59	12.36		692.28	681.91	671.91
	Nevada		21,000	0	100,000					17.19				
										16.32				
16	Arizona	15,000	21,000	23,000	200,000	403,000	698.84	684.19	677.33	14.55		713.39	703.03	694.55
	Nevada		21,000	23,000	100,000					18.84				
										17.22				
17	Arizona	15,000	0	23,000	200,000	361,000	694.65	682.38	665.10	12.63		707.28	697.50	681.30
	Nevada		0	23,000	100,000					15.12				
										15.93				
18	Arizona	15,000	0	0	200,000	315,000	687.86	676.78	668.32	12.60		700.46	690.46	680.50
	Nevada		0	0	100,000					13.68				
										12.18				
19	Arizona	15,000	21,000	0	200,000	357,000	697.25	680.64	671.52	9.87		707.12	696.33	687.12
	Nevada		21,000	0	100,000					15.69				
										15.60				
20	Arizona	15,000	21,000	23,000	200,000	303,000	690.72	681.65	675.31	8.28		699.00	688.64	679.55
	Nevada		21,000	23,000	0					6.99				
										4.24				

TABLE 5—RELATIONSHIP OF ELEVATION OF WATER SURFACE TO DISCHARGE WITH DIFFERENT OUTLET WORKS COMBINATIONS OPERATING—CONTINUED

Run No.	Location of Outlets	DISCHARGE SECOND-FEET					ELEVATION OF WATER SURFACE IN RIVER							
							UPPER SECTION					LOWER SECTION		
		Power House	Canyon Wall Outlets	Tunnel Plugs	Spill-way	Total	Normal	10 Feet Below Normal	20 Feet Below Normal	Rise	Drop	Normal	10 Feet Below Normal	20 Feet Below Normal
21	Arizona	15,000	0	23,000	200,000	261,000	690.72	681.37	670.66	2.19		699.00	688.64	673.00
	Nevada		0	23,000	0					0.99				
										2.34				
22	Arizona	15,000	0	0	200,000	215,000	683.96	674.86	664.23	1.80		685.76	675.61	665.76
	Nevada		0	0	0					0.75				
										1.53				
23	Arizona	15,000	21,000	0	200,000	257,000	686.02	679.66	665.29	5.19		691.21	682.36	671.50
	Nevada		21,000	0	0					2.70				
										6.21				
24	Arizona	15,000	21,000	23,000	100,000	203,000	679.15	661.60	650.61	4.68		683.83	673.39	663.33
	Nevada		21,000	23,000	0					11.79				
										12.72				
25	Arizona	15,000	0	23,000	100,000	161,000	669.41	655.98	656.23	7.26		676.67	666.21	667.06
	Nevada		0	23,000	0					10.23				
										10.83				
26	Arizona	15,000	0	0	100,000	115,000	663.51	649.56	637.02	4.98		668.49	658.53	648.03
	Nevada		0	0	0					8.97				
										11.01				
27	Arizona	15,000	21,000	0	100,000	157,000	666.91	657.40	647.55	9.00		675.91	665.05	655.74
	Nevada		21,000	0	0					7.65				
										8.19				
28	Arizona	15,000	21,000	23,000	0	203,000	671.92	661.85	649.73	11.76		683.68	673.97	661.82
	Nevada		21,000	23,000	100,000					12.12				
										12.09				
29	Arizona	15,000	0	23,000	0	161,000	667.10	656.26	644.68	9.87		676.97	666.67	656.62
	Nevada		0	23,000	100,000					10.41				
										11.94				
30	Arizona	15,000	0	0	0	115,000	658.98	647.22	636.72	9.51		668.49	658.53	647.58
	Nevada		0	0	100,000					11.31				
										10.86				
31	Arizona	15,000	21,000	0	0	157,000	664.09	653.37	643.37	11.82		675.91	665.61	656.18
	Nevada		21,000	0	100.000					12.29				
										12.81				
32	Arizona	15,000	21,000	23,000	0	303,000	682.26	666.25	655.55	16.71		698.97	688.18	679.70
	Nevada		21,000	23,000	200,000					21.93				
										24.15				
33	Arizona	15,000	0	23,000	0	261,000	674.10	662.12	649.57	18.33		692.43	683.09	673.09
	Nevada		0	23.000	200,000					20.97				
										23.52				
34	Arizona	15,000	0	0	0	215,000	665.13	654.11	640.16	19.62		684.75	676.37	665.90
	Nevada		0	0	200,000					22.26				
										25.74				
35	Arizona	15,000	21,000	0	0	257,000	669.97	658.90	645.87	22.47		692.42	682.06	672.21
	Nevada		21,000	0	200,000					23.16				
										26.34				
36	Arizona	15,000	21,000	23,000	100,000	403,000	694.15	683.99	673.34	19.68		713.83	703.64	694.37
	Nevada		21,000	23,000	200,000					19.65				
										21.03				
37	Arizona	15,000	0	23,000	100,000	361,000	689.50	677.79	663.94	18.00		707.50	697.65	687.88
	Nevada		0	23,000	200,000					19.86				
										23.94				
38	Arizona	15,000	0	0	100,000	315,000	680.91	669.00	656.35	20.61		701.52	689.97	680.05
	Nevada		0	0	200,000					20.97				
										23.70				
39	Arizona	15,000	21,000	0	100,000	357,000	686.50	673.10	661.31	20.70		707.20	696.80	686.67
	Nevada		21,000	0	200,000					23.70				
										25.26				

TABLE 6—CHANNEL CONDITIONS IN RIVER BED BELOW BOULDER DAM

Run No.	Location of Outlets	DISCHARGE SECOND-FEET					FLOW CONDITIONS IN RIVER BED a. Normal Tail Water b. 10 Feet Below Normal c. 20 Feet Below Normal
		Power House	Canyon Wall Valves	Tunnel Plug Valves	Spillway	Total	
9	Arizona	15,000	10,500	0	0	36,000	(a) Flow in river was very quiet with three upstream valves on Nevada side and three downstream valves on Arizona side discharging. Sand was eroded where jets impinged. (b) The velocity was increased and sand bar flattened and washed farther downstream. (c) The velocity was further increased and sand washed farther downstream. Some sand was moving all along the river bed. More was moving at narrow point below the Arizona spillway exit.
	Nevada		10,500	0	0		
	FIGURE 83-C						
10	Arizona	15,000	0	23,000	0	38,000	(a) Flow in river was smooth. A slight return flow occurred upstream from the Arizona tunnel-plug stream and there was slight erosion where stream entered river bed. (b) The stream tended to flow along the Arizona bank and form a decided whirl along the Nevada bank. The sand was washed farther downstream and the erosion was greater. (c) The velocity and erosion increased and sand was washed along the river from tunnel plug downstream.
	Nevada		0	0	0		
	FIGURE 84-A AND B						
11	Arizona	15,000	0	0	0	38,000	(a) Flow in the river was smooth. Stream from tunnel plug met Nevada bank above the end of Nevada spillway tunnel cut. The water was deflected into the river and eroded considerably. A sand bar was formed below the Arizona spillway exit. (b) Velocity increased and more sand was piled across the river below the Arizona spillway exit. (c) Velocity increased and sand bar was flattened and washed downstream. Sand was washed from the Arizona spillway exit on down the river.
	Nevada		0	23,000	0		
	FIGURE 84-A AND B						
8	Arizona	15,000	21,000	0	0	57,000	(a) Flow conditions very smooth except where jets hit river. Slight erosion occurred and sand collected downstream from where jets impinged. (b) Sand was spread and washed farther downstream. (c) Sand was washed down to the spillway exit on the Arizona side.
	Nevada		21,000	0	0		

TABLE 6—CHANNEL CONDITIONS IN RIVER BED BELOW BOULDER DAM—Continued

Run No.	Location of Outlets	DISCHARGE SECOND-FEET					FLOW CONDITIONS IN RIVER BED a. Normal Tail Water b. 10 Feet Below Normal c. 20 Feet Below Normal
		Power House	Canyon Wall Valves	Tunnel Plug Valves	Spill-way	Total	
6	Arizona	15,000	0	23,000	0	61,000	(a) Flow in river was very smooth, a hydraulic jump formed at the exit of the Nevada tunnel and about 75 feet downstream from exit of Arizona tunnel. Sand erosion was slight below the tunnel-plug exits. Slight whirl formed upstream from junction of tunnel-plug streams. Erosion occurred opposite Arizona spillway exit.
	Nevada		0	23,000	0		(b) Sand erosion increased and a sand bar was formed across the stream below Arizona spill-way exit. Flow conditions were practically the same except the hydraulic jump had moved downstream slightly on the Nevada side and about 75 feet on the Arizona side.
	FIGURE 83-D						(c) The sand bar was washed downstream beyond the gaging station.
5	Arizona	15,000	21,000	23,000	0	103,000	(a) Flow in river was very smooth. The hydraulic jump from tunnel-plug was at the exit of the tunnels. The sand erosion by the tunnel plug streams was very slight. A bar of sand was thrown across the river downstream from the canyon wall jets. The sand bar started about 225 feet below the downstream valve on Arizona side and continued about 300 feet downstream.
	Nevada		21,000	23,000	0		(b) Flow conditions became a little rough and the sand bar below the canyou wall valves was flattened and moved downstream nearly to the tunnel-plug exits. The tunnel-plug streams eroded the river bed slightly. Hydraulic jump was just outside tunnels.
	FIGURE 84-C AND D						(c) The sand bar below the canyon wall valves was washed still farther downstream. The streams from the tunnel plugs eroded considerably and a sand bar was thrown across the stream about 750 feet downstream on the Nevada side and about 150 feet on the Arizona side.
26	Arizona	15,000	0	0	100,000	115,000	(a) Flow upstream from spillway exit was very smooth.
	Nevada		0	0	0		(b) Hydraulic jump was downstream from portal. Flow below spillway exits was a little rough. Sand bar was washed to a point below lower gaging station.
							(c) Velocity of powerhouse discharge increased. Spillway stream impinged on projecting point on Nevada side. The stream was split and two whirls were formed, one on the upstream side near the center of the stream and the other on the downstream side along the Arizona shore. The sand bar below the lower gaging station was washed completely downstream.

TABLE 6—CHANNEL CONDITIONS IN RIVER BED BELOW BOULDER DAM—Continued

Run No.	Location of Outlets	DISCHARGE SECOND-FEET					FLOW CONDITIONS IN RIVER BED a. Normal Tail Water b. 10 Feet Below Normal c. 20 Feet Below Normal
		Power House	Canyon Wall Valves	Tunnel Plug Valves	Spillway	Total	
30	Arizona	15,000	0	0	0	115,000	(a) Similar to conditions in Run 29-b. (b. Similar to conditions in Run 29-c. (c) Flow was fairly rapid, more erosion occurred and sand was washed full width of river bed downstream from spillway exits.
	Nevada		0	0	100,000		
27	Arizona	15,000	21,000	0	100,000	157,000	(a) Similar to conditions in Run 25-a. (b) Similar to conditions in Run 25-b. (c) Similar to conditions in Run 25-c.
	Nevada		21,000	0	0		
31	Arizona	15,000	21,000	0	0	157,000	(a) Similar to conditions in Run 29-a. (b) Similar to conditions in Run 29-b. (c) Sand washed downstream from the canyon wall valves and formed a bar across the Nevada tunnel-plug exit. The return flow on the Arizona side with the lower tail water washed sand into the Arizona spillway exit.
	Nevada		21,000	0	100,000		
25	Arizona	15,000	0	23,000	100,000	161,000	(a) Flow conditions were very quiet and similar to Run 24-a, except flow through the tunnel plugs was more noticeable. (b) Similar to conditions in Run 24-c. Hydraulic jump was outside of tunnel-plug portals. (c) Flow from Nevada tunnel plug hit wall of cut and deflected into river. Hydraulic jump was below the tunnel exit. Flow below the spillway exits was a little rough. Sand bar was washed mostly below the lower gaging station. The stream from the Arizona spillway slipped off into the river.
	Nevada		0	23,000	0		
29	Arizona	15,000	0	23,000	0	161,000	(a) Similar to conditions in Run 28-a, except the tunnel plug flow was a little more noticeable (b) Flow was nearly the same except more rapid. Spillway stream did not climb wall of cut as high as with normal tail water. Hydraulic jump moved out of the tunnel-plug exits. (c) Velocity was increased and spillway stream hit wall of cut and was deflected across the river, striking the Arizona side just below the spillway exit. Spillway stream climbed wall of cut very slightly and hydraulic jumps from tunnel plugs moved out into the stream. Sand bar was flattened and washed farther downstream.
	Nevada		0	23,000	100,000		

TABLE 6—CHANNEL CONDITIONS IN RIVER BED BELOW BOULDER DAM—Continued

Run No.	Location of Outlets	DISCHARGE SECOND-FEET					FLOW CONDITIONS IN RIVER BED a. Normal Tail Water b. 10 Feet Below Normal c. 20 Feet Below Normal
		Power House	Canyon Wall Valves	Tunnel Plug Valves	Spillway	Total	
24	Arizona	15,000	21,000	23,000	100,000	203.000	(a) Flow conditions were quiet above the spillway exits. Flow from the tunnel plugs was slightly noticeable. The stream from the Arizona spillway flowed across the river to the projecting point on the Nevada side. There was a return flow along the Nevada side above the stream and on the Arizona side below the stream. The sand bar near the lower gaging station was not quite so far downstream.
	Nevada		21,000	23,000	0		(b) Flow was a little more rough and very rapid through the tunnel plugs. Erosion was slightly more with the sand bar washed just a little more parallel with the Arizona bank.
	FIGURE 85-A AND B						(c) Hydraulic jumps were at the tunnel-plug portals. Impingement of spillway on projection very severe.
28	Arizona	15,000	21,000	23,000	0	203,000	(a) Flow conditions were the best obtained by any combination of spillways discharging. Flow from the tunnel plugs was noticeable. Stream from Nevada spillway was projected along cut and climbed wall almost to Elevation 750 then flowed into and down the center of the river. Erosion was very slight compared with other runs. There was a very slight return flow along each bank below the tunnel exits.
	Nevada		21,000	23,000	100,000		(b) Velocity and roughness was increased. Hydraulic jump was inside of the tunnel-plug portals. The stream from the Nevada spillway rose higher on the wall of the cut. Erosion slightly increased and a sand bar formed upstream from the lower gaging station.
	FIGURE 85-C AND D						(c) Hydraulic jump moved below tunnel-plug exits. Spillway stream did not climb wall as high. Erosion was slightly increased.
14	Arizona	15,000	0	0	100,000	215,000	(a) Similar to conditions in Run 12-a. The return flow along the Nevada bank was a little more noticeable and the hydraulic jump was at the exit of each spillway tunnel.
	Nevada		0	0	100,000		(b) The hydraulic jump moved about 75 feet from the exit of the Arizona spillway tunnel and slightly outside of the Nevada tunnel.
							(c) The hydraulic jump moved out into the stream on the Arizona side and about 150 feet downstream from the exit of the tunnel on the Nevada side.

TABLE 6—CHANNEL CONDITIONS IN RIVER BED BELOW BOULDER DAM—Continued

Run No.	Location of Outlets	DISCHARGE SECOND-FEET					FLOW CONDITIONS IN RIVER BED a. Normal Tail Water b. 10 Feet Below Normal c. 20 Feet Below Normal
		Power House	Canyon Wall Valves	Tunnel Plug Valves	Spillway	Total	
22	Arizona	15,000	0	0	200,000	215,000	(a) Similar to conditions in Run 20-b. (b) Similar to conditions in Run 20-c. (c) Arizona spillway stream extended across the river and climbed to Elevation 750. Whirl upstream became smaller. Flow downstream was very rapid.
	Nevada		0	0	0		
34	Arizona	15,000	0	0	0	215,000	(a) Similar to conditions in Run 33-b. (b) Similar to conditions in Run 33-c. (c) Flow from spillway hit wall of cut and was deflected across the river where it impinged on the Arizona bank near the spillway exit.
	Nevada		0	0	200,000		
15	Arizona	15,000	21,000	0	100,000	257,000	(a) Similar to conditions in Run 12-a. Hydraulic jump was slightly inside of the spillway tunnels. Nevada tunnel plug submerged occasionally. Arizona tunnel-plug exit was never completely submerged. (b) Hydraulic jump moved 75 feet downstream on the Arizona side and slightly below the tunnel exit on the Nevada side. (c) Hydraulic jump moved about 150 feet from the end of the Arizona spillway tunnel and about 75 feet downstream on the Nevada side.
	Nevada		21,000	0	100,000		
23	Arizona	15.000	21,000	0	200.000	257,000	(a) Similar to conditions in Run 20-b. (b) Similar to conditions in Run 20-c. (c) Similar to conditions in Run 22-c.
	Nevada		21,000	0	0		
35	Arizona	15,000	21,000	0	0	257,000	(a) Similar to conditions in Run 32-a. (b) Similar to conditions in Run 33-b. (c) Similar to conditions in Run 33-c, except the canyon wall valves washed sand along each bank and a sand bar was formed below the exit to the Nevada tunnel plug. Sand was not washed so far downstream on the Arizona side. Flow from the canyon wall valves was slightly faster on the Nevada side due to the unbalanced flow from the spillways.
	Nevada		21,000	0	200,000		

TABLE 6—CHANNEL CONDITIONS IN RIVER BED BELOW BOULDER DAM—Continued

Run No.	Location of Outlets	DISCHARGE SECOND-FEET					FLOW CONDITIONS IN RIVER BED a. Normal Tail Water b. 10 Feet Below Normal c. 20 Feet Below Normal
		Power House	Canyon Wall Valves	Tunnel Plug Valves	Spill-way	Total	
21	Arizona	15,000	0	23,000	200,000	261,000	(a) Similar to conditions in Run 20-a. (b) Similar to conditions in Run 20-b. (c) Similar conditions in Run 20-c, except flow through the tunnel plugs was more noticeable.
	Nevada		0	23,000	0		
13	Arizona	15,000	0	23,000	100,000	261,000	(a) Similar to conditions in Run 12-a. Flow from tunnel-plug exits was noticeable. (b) Similar to conditions in Run 12-b. Hydraulic jump was slightly outside of the Nevada spillway tunnel and about 50 feet below the Arizona spillway exit. (c) Hydraulic jumps moved out of all the tunnels. Flow was quite rapid from spillway exits on down the river. The hydraulic jump from the Arizona spillway moved out into the river.
	Nevada		0	23,000	100,000		
33	Arizona	15,000	0	23,000	0	261,000	(a) Similar to conditions in Run 32-a, except the flow from the tunnel plugs was more noticeable because of slightly lower tail water. (b) Hydraulic jump was at the exit of the Arizona tunnel plug and slightly inside the tunnel on the Nevada tunnel-plug portal. (c) Hydraulic jump from tunnel plug moved almost into the river. Stream from Nevada spillway did not climb as high on the wall of the cut. Sand was washed the entire width of the river and downstream into the tail-water regulator box. A more decided whirl was formed on the upstream side of the spillway jet.
	Nevada		0	23,000	200,000		
12	Arizona	15,000	21,000	23,000	100,000	303,000	(a) Flow above spillway streams was very quiet. Spillway streams meet in center of river and directly out from Arizona exit. Streams from Nevada side climb wall of cut to about Elevation 750. Whirl was noticeable on Nevada side above the point where Arizona stream hits Nevada wall. A sand bar was thrown across the river. There was considerable erosion where streams met, more so along the Nevada wall. Tunnel plugs were completely submerged. (b) Sand was washed farther downstream and more parallel to Arizona bank. Hydraulic jump was inside Nevada tunnel and just outside Arizona tunnel. Tunnel plugs still submerged. (c) Sand bar was washed farther downstream. Flow from tunnel plugs was noticeable. Upper end of sand bar remained about the same.
	Nevada		21,000	23,000	100,000		

FIGURE 86-A AND B

TABLE 6—CHANNEL CONDITIONS IN RIVER BED BELOW BOULDER DAM—Continued

Run No.	Location of Outlets	DISCHARGE SECOND-FEET					FLOW CONDITIONS IN RIVER BED a. Normal Tail Water b. 10 Feet Below Normal c. 20 Feet Below Normal
		Power House	Canyon Wall Valves	Tunnel Plug Valves	Spill-way	Total	
20	Arizona	15,000	21,000	23,000	200,000	303,000	(a) Flow above spillway exits was very smooth. The stream from the Arizona spillway shot across the river, impinged on the projecting point on the Nevada side and a large return flow formed which eroded at the lower end of the Nevada spillway cut. Considerable erosion occurred under the spillway stream. A bar of sand was thrown across to the Nevada side about 600 feet downstream. There was a return flow downstream from the spillway stream and on the Arizona side. (b) Flow from tunnel plugs was slightly noticeable. (c) Erosion was greater and the sand bar near the lower gaging station was flattened. Tunnel plug flows were slightly noticeable.
	Nevada		21,000	23,000	0		
	FIGURE 86-C AND D						
32	Arizona	15,000	21,000	23,000	0	303,000	(a) Flow conditions were as satisfactory as in Run 28-a, being very smooth above the spillway stream. Flow from the tunnel plugs was slightly noticeable. Stream from spillway climbed wall to Elevation 750 and was deflected into the river but flowed more along the Nevada bank than in Run 28-a. A whirl was formed on the upstream side of the spillway stream opposite the Arizona spillway exit. There was considerable erosion and a sand bar was formed clear across, starting directly opposite the Arizona spillway exit and continuing downstream and across to the Nevada side about 300 feet below the gaging station. A small amount of sand was washed in the exit of the Arizona spillway tunnel. (b) Little change in flow conditions, except for being more rapid and rough. Flow from the tunnel plugs was not noticeable. Sand was washed farther downstream. (c) Hydraulic jump was in the exit of the tunnel plugs. Spillway stream did not climb so high on the wall of the cut. Flow was much more rapid and rough. Sand was washed the entire width of the river and almost into the tail-water control box.
	Nevada		21,000	23,000	200,000		
	FIGURE 87-A AND B						
18	Arizona	15,000	0	0	200,000	315,000	(a) Flow above the spillway exits was very quiet. A whirl upstream from spillway streams piled sand in front of the tunnel-plug exit. (b) Arizona spillway stream tended to shoot across on river water surface and climb the projecting point on the Nevada side. The sand bar above the spillway streams was washed a little farther upstream. (c) Stream from Nevada spillway climbed wall of cut higher than at normal tail water or 10 feet below. Sand bar above streams was washed nearly to exit of Arizona tunnel-plug outlet.
	Nevada		0	0	100,000		

TABLE 6—CHANNEL CONDITIONS IN RIVER BED BELOW BOULDER DAM—Continued

Run No.	Location of Outlets	DISCHARGE SECOND-FEET					FLOW CONDITIONS IN RIVER BED a. Normal Tail Water b. 10 Feet Below Normal c. 20 Feet Below Normal
		Power House	Canyon Wall Valves	Tunnel Plug Valves	Spillway	Total	
38	Arizona	15,000	0	0	100,000	315,000	(a) Similar to conditions in Run 37-b. (b) Similar to conditions in Run 37-c. (c) Nevada spillway stream hit wall of cut and was deflected into the river. It extended into the river under the Arizona stream and allowed the Arizona stream to shoot across and climb the projecting point on the Nevada side. Flow was more rapid along the Nevada bank. The erosion was increased and sand was carried downstream.
	Nevada		0	0	200,000		
19	Arizona	15,000	21,000	0	200,000	357,000	(a) Similar to conditions in Run 16-a. (b) Similar to conditions in Run 16-b. (c) Similar to conditions in Run 16-c.
	Nevada		21,000	0	100,000		
39	Arizona	15,000	21,000	0	100,000	357,000	(a) Similar to conditions in Run 37-a. (b) Similar to conditions in Run 37-b. (c) Similar to conditions in Run 37-c.
	Nevada		21,000	0	200,000		
17	Arizona	15,000	0	23,000	200,000	361,000	(a) Similar to conditions in Run 16-a. (b) Similar to conditions in Run 16-b. (c) The flow was very rough and the hydraulic jump from the Arizona spillway was in midstream. The stream appeared to shoot across the river on top of the water surface. Hydraulic jump on the Nevada spillway was about 50 feet downstream from the exit. The flow from tunnel plugs was very noticeable and the jump was at the exit of the tunnels. Sand piled downstream from the Arizona tunnel-plug exit was washed nearer the center of the stream.
	Nevada		0	23,000	100,000		
37	Arizona	15,000	0	23,000	100,000	361,000	(a) Similar to conditions in Run 36-b. (b) Flow from tunnel plugs became noticeable. Spillway jumps were outside of tunnel exits. (c) The sand bar was washed farther downstream and flattened. Hydraulic jump was at the tunnel-plug portals.
	Nevada		0	23,000	200,000		

TABLE 6—CHANNEL CONDITIONS IN RIVER BED BELOW BOULDER DAM—Continued

Run No.	Location of Outlets	DISCHARGE SECOND-FEET					FLOW CONDITIONS IN RIVER BED a. Normal Tail Water b. 10 Feet Below Normal c. 20 Feet Below Normal
		Power House	Canyon Wall Valves	Tunnel Plug Valves	Spill-way	Total	
16	Arizona	15,000	21,000	23,000	200,000	403,000	(a) Flow above the spillway exits was very quiet. The velocity of the Nevada spillway stream was greatly reduced before it reached the stream from the Arizona spillway which allowed the Arizona stream to shoot across the river and climb the projection on the Nevada side. Part of the stream flowed upstream causing a whirl on the Nevada side. The flow was mostly along the Nevada side below the spillway exits. Tunnel plugs were completely submerged. Erosion at canyon wall valves was very slight. (b) Very little change in flow conditions or erosion. Hydraulic jump outside the Arizona tunnel and inside the Nevada tunnel. Tunnel plugs still submerged. (c) The tunnel-plug flow was noticeable. Erosion downstream was increased. Arizona spillway hydraulic jump was in the river. The Nevada spillway jump was at the tunnel exit.
	Nevada		21,000	23,000	100,000		
	FIGURE 87-C AND D						
36	Arizona	15,000	21,000	23,000	100,000	403,000	(a) Flow was fairly smooth. Arizona spillway stream did not shoot across the river and climb the projecting point on the Nevada side. Streams from the spillways met in the center of the river and continued down the river with the water along the Nevada bank having a slightly higher velocity. Tunnel plugs were completely submerged. The erosion was to rock in center of river bed opposite the Arizona spillway exit. Sand was piled upstream from junction of spillway streams. The sand bar below was nearly straight across the stream with the Nevada side extended a little farther downstream. (b) The junction of the spillway streams was such that the flow was more evenly distributed throughout the width of the river. More erosion occurred downstream and the sand bar was carried to about 300 feet below the gaging station where it extended the full width of the stream. (c) Flow from the tunnel plugs was noticeable. More erosion occurred downstream similar to (b).
	Nevada		21,000	23,000	200,000		
	FIGURE 88-A AND B						
3	Arizona	15,000	0	0	200,000	415,000	(a) Water above tunnel exits was smooth with exception of whirl immediately above spillway streams. Hydraulic jump was formed at exit of Arizona tunnel. Exit of the Nevada tunnel was covered and jump was inside tunnel. Streams met at a point in center of river directly opposite Arizona spillway exit. Some of the velocity of Nevada stream was dissipated before reaching the Arizona stream allowing the Arizona stream to climb point on Nevada side. (b) The hydraulic jump moved to the exit of the Nevada spillway tunnel and downstream from the Arizona tunnel. The return flow on the Nevada side and upstream from the spillway streams increased. (c) Velocity and flow increased.
	Nevada		0	0	200,000		

TABLE 6—CHANNEL CONDITIONS IN RIVER BED BELOW BOULDER DAM—Continued

Run No.	Location of Outlets	DISCHARGE SECOND-FEET					FLOW CONDITIONS IN RIVER BED a. Normal Tail Water b. 10 Feet Below Normal c. 20 Feet Below Normal
		Power House	Canyon Wall Valves	Tunnel Plug Valves	Spill-way	Total	
4	Arizona	15,000	21,000	0	200,000	457,000	(a) Tunnel-plug exits were completely submerged. Considerable disturbance occurred at the spillway tunnel exits caused by entrained air escaping. The stream from the Nevada spillway hit the canyon wall a short distance below the tunnel exit, climbed above Elevation 750 and followed the canyon wall. The stream from the Arizona spillway shot across the river, met the Nevada stream and impinged on the projection on the Nevada side. A decided whirl occurred on the Arizona side downstream from the streams and directly across from the projection. The flow from the canyon wall valves caused a slight disturbance above the tunnel-plug portals. (b) Roughness below spillway tunnels increased, and a decided whirl appeared upstream from point at which Arizona spillway stream struck Nevada bank. Streams met nearer center of river. Hydraulic jumps formed slightly above spillway tunnel portals. (c) Hydraulic jump in Nevada spillway tunnel was at portal and 75 feet below Arizona exit.
	Nevada		21,000	0	200,000		
2	Arizona	15,000	0	23,000	200,000	461,000	(a) Similar to conditions in Run 4-a. (b) Similar to conditions in Run 4-b. Flow from tunnel plugs was not noticeable. (c) Similar to conditions in Run 4-c. Flow from tunnel plugs was noticeable.
	Nevada		0	23,000	200,000		
1	Arizona	15,000	21,000	23,000	200,000	503,000	(a) Water upstream from spillway tunnels was fairly smooth except for slight disturbance from canyon wall outlet jets. A slight whirl formed upstream from spillway streams. Tunnel-plug outlets were completely submerged. Surging and bubbling occurred at exit of each spillway tunnel. Sand was washed completely away from cut on Nevada side to a point 900 feet downstream. A sand bar was formed across river bed above spillway tunnels and below tunnel plugs. A large bar of sand was formed across river starting above the gaging station on Arizona side and ending on Nevada side about 900 feet downstream. A small sand bar was formed across the river below the canyon wall valves. (b) Sand erosion occurred more quickly and flow spillway tunnels was rougher. Tunnel-plug exits were still submerged. (c) Flow condition still rougher.
	Nevada		21,000	23,000	200,000		

FIGURE 88-C AND D

BIBLIOGRAPHY

The following list of articles covers the theory of model testing and hydraulic problems related to penstocks:

1. ANGUS, R. W.
   Intakes for Power Plants, Bulletin No. 6, Section 11, University of Toronto, Faculty of Applied Science and Engineering, School of Engineering Research, 1936.

2. BALCH, LELAND R.
   Investigation of Flow Through Four-Inch Submerged Orifices and Tubes, Engineering Series, Vol. 8, No. 3, Engineering Experiment Station, University of Washington, Seattle.

3. BLAISDELL, F. W.
   Comparison of Sluice-Gate Discharge in Model and Prototype, Proc. Am. Soc. C. E., Jan., 1936, p. 65.

4. CARLSON, ROY W.
   Similitude Requirements in Model Design, Eng. News-Rec., Aug. 23, 1934, pp. 235-238.

5. CHICK, A. C.
   Dimensional Analysis and the Principle of Similitude as Applied to Hydraulic Experiments with Models. Hydraulic Laboratory Practice, Am. Soc. M. E., 1929, pp. 775-827.

6. FOSDICK, E. R.
   Tunnel and Penstock Tests at Chelan Station, Washington. Trans. Am. Soc. C. E., Vol. 101, 1936, p. 1409.

7. GIBSON, A. H.
   Hydraulics and Its Application, Pp. 136-146, 192-215, 368, 387.

8. GROAT, B. F.
   Theory of Similarity and Models, Trans. Am. Soc. C. E., Vol. 96, 1932, pp. 273-387.

9. HAMILTON, JAMES B.
   Suppression of Pipe Intake Losses by Various Degrees of Rounding, Bul. No. 57, Engineering Experiment Station, University of Washington, Seattle.

10. HARRIS, CHAS. W.
    The Influence of Pipe Thickness on Re-entrant Intake Losses, Bulletin No. 48, Engineering Experiment Station, University of Washington, Seattle.

11. ———
    Elimination of Hydraulic Eddy Current Loss at Intake, Agreement of Theory and Experiment. Bul. 54, Engineering Experiment Station, University of Washington, Seattle.

12. HODGSON, J. L.
    The Laws of Similarity for Orifice and Nozzle Flow, Trans. Am. Soc. M. E., Vol. 50, APM 50-3.

13. KUNZ, JACOB
Jets from Manifold Tubes, Trans. Am. Soc. M. E., APM 53-14, pp. 181, 186.

14. MONROE, R. A.
Tests of Friction Losses Made on Large Penstocks, Eng. News-Rec. Vol. 91, 1923, p. 598.

15. PIGOTT, R. J. S.
The Flow of Fluids in Closed Conduits. Trans. Am. Soc. M. E., August, 1933, pp. 497-515.

16. ROGERS, T. C., AND SMITH, T. L.
Experiments with Submerged Orifices and Tubes, Eng. News, Nov. 2, 1916, pp. 825-827.

17. SMITH, J. F. D.
Calibration of Rounded Approach Orifices. Trans. Am. Soc. M. E., Vol. 56, 1934, RP 56-10, p. 791.

18. SPITZGLASS, J. M.
Similarity Limitations and Its Application to Fluid Flow. Trans. Am. Soc. M. E., HYD 52-7c, pp. 111-122.

19. STEWART, C. B.
Investigation of Flow Through Large Submerged Orifices and Tubes, University of Wisconsin, Bul. No. 216.

LIST OF BULLETINS

The following list shows tentative titles of final reports on the Boulder Canyon Project now being prepared for publication. Titles and prices of printed reports now ready for distribution are also included. Appropriate announcements will be made in engineering periodicals as additional bulletins become available.

PART I—INTRODUCTORY

General Description of Project
History of Project
Legal and Financial Problems

PART II—HYDROLOGY

Stream Flow and Reservoir Operation
Lower Basin Utilization
Upper Basin Utilization

PART III—PREPARATORY EXAMINATIONS AND CONSTRUCTION

Geologic Investigations
Surveys and Preliminary Construction
(Topographic surveys, highways, railways, power lines, substations, and Boulder City).

PART IV—DESIGN AND CONSTRUCTION

General Features
Concrete Manufacture, Handling and Control
Boulder Dam
Diversion Structures and Spillways
Intake Towers and Outlet Works
Penstocks and Outlet Pipes
Hydraulic Valves and Gates
Handling Facilities
(Cableway, cranes, and other permanent handling facilities).
Power Plant Building
Generating, Transforming, and Switching Equipment
Turbines, Governors, and Mechanical Auxiliaries
Control, Communication, and Electrical Auxiliaries
Imperial Dam and Desilting Works
All-American Canal and Canal Structures

LIST OF BULLETINS—(Continued)

PART V—TECHNICAL INVESTIGATIONS

Trial Load Method of Analysing Concrete Dams
Model Tests of Boulder Dam
Slab Analogy Experiments
Stress Studies for Boulder Dam
Penstock Analysis and Stiffener Design
Model Tests of Arch and Cantilever Elements
Research Measurements at Dam

PART VI—HYDRAULIC INVESTIGATIONS

Model Studies of Spillways* (paper cover, $1.00) (cloth cover, $1.50)
Model Studies of Penstock and Outlet Works* (paper cover, $1.00) (cloth cover, $1.50)
Studies of Crests for Overfall Dams
Model Studies of Imperial Dam and Desilting Works
Model Studies of All-American Canal Structures
Silt Movement in Colorado River

PART VII—CEMENT AND CONCRETE INVESTIGATIONS

Thermal Properties of Concrete
Investigation of Portland Cements
Cooling of Concrete Dams
Mass Concrete Investigations
Contraction Joint Grouting
Volume Changes in Mass Concrete
(Largely Investigations at Owyhee Dam, Owyhee Project, Oregon).

*Available for distribution.

Peerless Printing Company, Denver, Colo. 2-14-38 3000.

For Sale at Offices of the U. S. Bureau of Reclamation in Denver, Colo., and Washington, D. C.